SELECTIVE DEHYDRATION OF HIGH PRESSURE NATURAL GAS USING SUPERSONIC NOZZLES

ANAHID KARIMI

Selective Dehydration of High Pressure Natural Gas Using Supersonic Nozzles

By
Anahid Karimi, B. Eng.

A Thesis
Submitted to the School of Graduate Studies
in Partial Fulfillment of the Requirements
for the Degree of

Masters of Engineering

Memorial University of Newfoundland

Your file Votre référence
ISBN: 978-0-494-31262-9
Our file Notre référence
ISBN: 978-0-494-31262-9

ABSTRACT

The dwindling high quality crude oil reserves and increasing demand for natural gas has encouraged energy industries further towards the discovery of remote offshore reservoirs. Consequently, new technologies have to be developed to efficiently produce and transport stranded natural gas to consuming markets. Compactness of production systems is the most challenging design criteria for offshore applications. From the gas quality perspective, water vapour is the most common impurity in natural gas mixtures. At very high gas pressures within the transportation systems hydrate can easily form even at relatively higher temperatures. Therefore, gas dehydration or hydrate inhibition systems for offshore gas production/processing facilities should meet these requirements. It should also be noted that at certain pressure and composition conditions, the presence of heavy hydrocarbons (C_2^+) in natural gas increases pipeline flow capacity and improves compression efficiencies. Supersonic separators are proposed in this thesis as a compact high-pressure processing system capable of selectively removing water from high-pressure natural gas streams without affecting the hydrocarbon content. A computer simulation linked to a thermodynamic property package is presented to predict the water removal efficiency and to compare the proposed system with conventional techniques. The simulation is first validated with a commercial computational fluid dynamics (CFD) software (Fluent) and then the effect of pressure, temperature, flow rate, friction and backpressure of the system in this method are analysed. Supersonic nozzles are also placed in different locations in a three-stage separation train on an offshore crude oil

production platform to test the efficiency for the recovery of Natural Gas Liquids (NGLs) from associated gas. The recovery of NGLs can significantly improve the economy of offshore crude oil production.

ACKNOWLEDGEMENTS

I sincerely thank my supervisor Dr. Majid Abedinzadegan Abdi for accepting me as a graduate student, for his patience and availability in discussing the cumbersome details of my thesis, for his constant encouragement in my hours of despair, and for supporting to attend and present my work in the 2006 SPE Gas Technology Symposium in Calgary.

I also acknowledge collaborations with Ph.D. student, Mr. Esam Jassim, in assisting to compare my results with those generated by commercial computational fluid dynamics (CFD) software (Fluent) simulations, and with Ph.D. student, Ms. Erika Beronich, in conducting NGL recovery case studies.

The financial support from the National Science and Engineering Research Council of Canada (NSERC) is also gratefully acknowledged.

I wish to thank Dr. Ramachadran Venkatesan, Associate Dean of Graduate Studies and Research, and Ms. Moya Crocker, Secretary to the Associate Dean of Graduate Studies and Research, for their superb administrative support.

Last but not least, I thank my family and friends for their love and support.

TABLE OF CONTENTS

LIST OF FIGURES

LIST OF TABLES

NOMENCLATURE

UNITS:

bbls/d: barrels/day
$STDm^3/d$: standard cubic meters per day
mol/s: mol per seconds
mg/std m^3: miligrams per standard cubic meter
Kmol gas/10^6 std. m^3: mole per standard cubic meter

LETTERS:

a, b: equations of state constants characterizing the molecular properties
c: speed of sound (m/s)
dL_c: Converging part incremental length
dL_d: diverging part incremental length
e: system energy
f: friction coefficient
h: mass enthalpy, KJ/Kg
h_o: stagnation enthalpy , KJ/Kg
k: specific heats ratio (C_p/C_v)
n: amount of substance in mole
u: constant of cubic equation of state
w: constant of cubic equation of state
A: cross section area, m^2
A_{ex}: exit cross section area
Cs: Control surface
Cv: Control volume
D: Diameter (m)
D_{in}: inlet diameter
D_{th}: throat diameter
D_{ex}: exit diameter
C_p: Specific heat capacity at constant pressure
C_v: Specific heat capacity at constant volume
G,F: Newton-Raphson functions
F_B: body forces
F_{Bx}: x-component of body forces
F_f: friction factor
F_s: surface forces
I: trust
L_c: length of the converging part

L_d: length of the diverging part
M: mach number
M_w: molecular weight
P: pressure, MPa
P_o: stagnation pressure
R: ideal gas constant
R_x: pressure force
Re_D: Reynolds number
S: mass entropy, KJ/Kg C
T: Temperature
T_o: stagnation temperature
V: velocity m/s
Z: compressibility
$\dot{m}$: mass flow, Kg/h
δQ : mount of heat transferred to the system
$\dot{Q}$: heat transfer rate
$\dot{W}_s$: shaft work
$\dot{W}_{shear}$: work done by shear stresses
$\dot{W}_{other}$: other work

GREEK:
α: onvergence half angle
β: ivergence half angle
ε: surface roughness
ρ: gas density (kg/m^3)
ρ_o: stagnation density
v: molar volume
$\overline{\xi}_c$: incremental properties
Φ : frictional loss term
τ : shear stress

CHAPTER 1: INTRODUCTION

The demand for natural gas has motivated the oil and gas industry to discover natural gas reservoirs even in remote and hard to reach locations. Natural gas is more abundant than estimated even just ten years ago. The global need for less-carbon and potentially no-carbon content fuels (such as hydrogen) is motivated by environmental concerns. Natural gas is, at present, the only hydrocarbon energy source that will lead to major reductions in green house gases and other pollutants. Natural gas, produced from the reservoir is not a single-component mixture, but a mixture of hydrocarbons which may include heavier than methane hydrocarbons constituents (C_2^+) or natural gas liquids (NGLs), reservoir water and various impurities such as inert gases, carbon dioxide, and hydrogen sulphide. Natural gas needs to be processed before being used in the supply network. The impurities such as nitrogen, carbon dioxide, hydrogen sulphide and heavy hydrocarbons can be removed in a central plant (Berger and Anderson 1980). However, some other impurities such as sand and free water should be removed near the wellhead.

Produced natural gas is in the dense phase. During natural gas processing it is likely that the water and the hydrocarbon components condense and form a liquid phase. This phase behaviour can be explained using the equilibrium phase diagrams known also as phase envelope of the stream. The condensation of water and hydrocarbons in natural gas decreases its heating value and causes operational problems such as corrosion, excessive pressure drop, hydrate formation and consequently slugging flow and reduction

in gas transmission efficiency. The possibility of obstruction due to the formation of hydrate within the flow lines is one of the most serious problems in the gas industry. The point at which gas hydrate forms and therefore becomes a source of trouble depends on the pressure, temperature, and gas composition. Within the transportation system and at very high pressure of the gas, hydrate can form even at relatively high temperatures (close or above 20^0C). Therefore, it is important to assure that hydrate does not form as the gas is transported from the wellhead to a processing facility. Line heating, injection of hydrate inhibitors, and dehydration are commonly practiced to meet this requirement (Hengwei et al., 2005).

In processes such as transmission of gas in high pressure pipelines and the gas storage in high pressure containers for land or marine transportation of gas in compressed form, in certain specific pressure and temperature conditions, the presence of heavier hydrocarbons in natural gas is favourable (Mohitpour et al., 2003). The mass flow capacity in pipelines is related to the gas gravity (directly proportional to molecular weight, M) and reversely proportional to the square root of the compressibility factor (Z). Light gases (with higher percentage of methane) have higher flow capacities because of the low gas gravity and the compressibility factor of close to unity. As the heavier hydrocarbons (C_2^+) are introduced in the gas stream, the gas gravity increases and the compressibility factor decreases. The overall effect of heavy hydrocarbons addition will be determined by reduction in gas compressibility, which not only depends on the gas composition but also on pressure and temperature (Mohitpour et al., 2003). Mohitpour et

al. reviewed the standard volume flow and the mass flow capacities at 1.66 °C (35 °F) and for pressures between 5.5-14.75 MPa (800-2,140 psia) for a mixture of methane and ethane. The results showed increases in the mass flow capacity with the increase of ethane content in the mixture which resulted in an increase in the amount of energy that could be transported with the mixture. The heating value of the mixture increased at the same rate. Therefore, higher hydrocarbon content of the gas improves the compressibility and transportability of the gas. Water however is a risk factor contributing to the plugging of the pipe and corrosion and therefore should be removed or dealt with in a proper way.

1.1 Objectives of study

The purpose of this thesis is to propose an alternative dehydration process. The proposed system should be capable of working at high-pressure conditions and be able to remove water selectively without affecting the hydrocarbon content of the gas. After evaluating different alternatives, a new approach in using supersonic dehydration systems is proposed to selectively remove water from the gas in supercritical conditions. This study provides a good understanding of the supersonic dehydration especially when water is removed selectively form high-pressure natural gas streams. In addition, the performance of such systems is also studied in the recovery of heavier hydrocarbons. For the NGL recovery studies, the supersonic separators are introduced within a typical crude surface separation facility on an offshore platform to determine the efficiency of the unit

for such applications.

1. 2 Scope of Study

Based on literature reviews, two companies have commercially implemented supersonic separators for gas treatment: Twister BV (Brouwer et al., 2004) and Translang TechnologiesLtd. (Alfyorov et al., 2005). Supersonic separators are used for different applications such as water and hydrocarbon dew pointing, natural gas liquids (NGL/LPG) extraction, heating value reduction, fuel gas treatment, CO_2 extraction, ethane recovery and Liquefied Natural Gas (LNG) applications (Brouwer et al., 2004 and Alfyorov et al., 2005).

Limited data and information is presented on the performance of supersonic separators in the previously mentioned applications. In this research a complete overview of water dew pointing applications using the supersonic separators are given.

1. 3 Thesis outline

The thesis is divided into seven chapters. Chapter 1 provides an introduction to the supersonic separators and their applications. In Chapter 2, several alternative processes to eliminate liquid phase from natural gas such as refrigeration, liquid desiccant dehydration, solid desiccant dehydration, and membrane separators are reviewed. The necessary background on the supersonic separators is also given Chapter 2. In Chapter 3, further introduction to the supersonic dehydration is given and the methodology to

simulate the system is discussed. In Chapter 4, the prediction of the behaviour of the supersonic dehydration unit based on the proposed model is presented. The nozzle is assumed to work in an isentropic (frictionless, reversible, and constant entropy) condition. A condition where friction exists is also presented. In Chapter 5, supersonic separators are introduced within a typical crude surface production system on an offshore platform to determine the efficiency of the unit to recover NGLs. Chapter 6 summarizes the thesis and the conclusions reached are presented. In addition, recommendations for future work are provided.

CHAPTER 2: LITERATURE REVIEW

In this chapter, various dehydration processes are reviewed and the introduction on a supersonic nozzle as the main part of the supersonic dehydration system is given.

2.1 NATURAL GAS DEHYDRATION AND HYDRATE INHIBITION

Natural gas dehydration is an important process for several reasons including the following:

1. Free water in natural gas can cause operational problems such as corrosion and excessive pressure drop due to the two-phase flow
2. Water decreases the heating value of the gas
3. Water can form hydrate and consequently plug the pipeline

Among all, hydrate formation is one of the most serious problems in natural gas industry and has been identified as a major hazard to the safe operation of natural gas transmission pipelines.

Gas hydrates are non-stoichiometric compounds that form when the host material, like water traps the guest molecules such as methane. The temperature and pressure of hydrate formation can be predicted on the gas composition basis. Hydrate crystals might not form even when hydrate formation is thermodynamically possible as the crystal growth process is random but to be safe, hydrate prevention is needed. There are several methods to prevent hydrate formation in natural gas pipelines:

2.1.1 Line heating

Line heating may keep the minimum line temperature above the hydrate formation point. The initial investment needed for this method is not very high as fuel is available to operate the heater. Line heaters are simple and do not need much maintenance however they do not remove the water vapour which causes hydrate formation. Line heating therefore is needed at any point where the risk of hydrate formation exists. This method is not very suitable for long distance pipeline transmission systems (Berger and Anderson, 1980).

2.1.2 Hydrate inhibitor injection

An alternative method to control hydrate formation is to use kinetic inhibitors, anti-agglomerates and thermodynamic hydrate inhibitors such as methanol, glycols (mainly ethylene and di-ethylene glycols). Injecting the inhibitors prevents hydrate formation by lowering the temperature at which hydrate might form at a given pressure. For an effective injection, inhibitor should be introduced at every point in the process where the wet gas is cooled down to its hydrate temperature. The injected inhibitor should preferably be recovered, regenerated, and re-injected in the process. The physical limitations and economics at certain conditions are factors to choose one inhibitor over the other (GPSA Data book 1998, and Covington et al., 1999). Anti-agglomerates prevent small hydrate particles from growing into larger sizes and kinetic inhibitors slow crystal formation. Kinetic inhibitors have some advantages as their required concentration is as low as 0.5-2.0 wt. % in the aqueous phase and they are non-volatile

but they are banned to be used in some areas due to environmental reasons and that too much inhibitor may even increase the hydrate formation rate (Iluhi, 2005 and Kidnay, Parrish, 2006). The principal thermodynamic inhibitors are methanol and ethylene glycols. Their required dosage is predictable but it can be as high as 50 wt. % of the aqueous phase. Ethylene glycol is usually preferred over di-ethylene glycol and tri-ethylene glycol due to its lower solubility and viscosity. The rate of harmful emissions (mainly aromatic hydrocarbons) from the glycol regenerators to the environment is the most common concern for glycol injection units. Methanol is usually not regenerated in the process so the disadvantage of damaging the environment might be omitted but it will be a costly process (Covington et al., 1999). Figure 2.1 shows a simple sketch of a glycol injection unit.

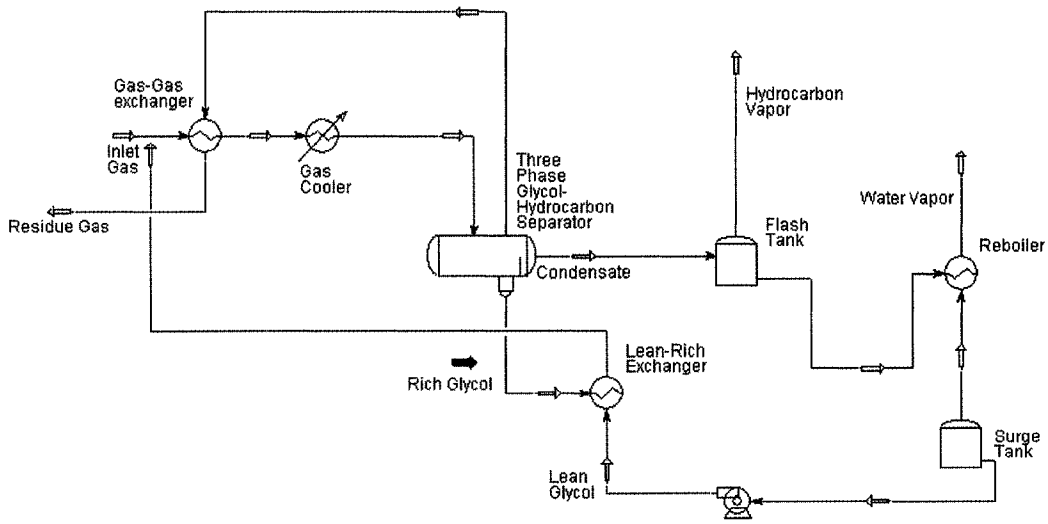

Figure 2.1: Typical glycol injection system

Hydrate formation can also be prevented by eliminating water using gas

dehydration processes. Dehydration may be performed with or without removal of other liquid phases and the condensable components of natural gas before delivery or consumption (GPSA Data book, 1998).

2.1.3 Absorption using liquid desiccants

Glycols are very good absorbers for water because the hydroxyl groups in glycols form similar associations with water molecules. Among different glycols such as di-ethylene glycol (DEG), tri-ethylene glycol (TEG) and tetra-ethylene glycol (TREG) which are used as liquid desiccants, Tri-ethylene glycol is the most common liquid desiccant for natural gas (GPSA Data book, 1998).

The intimate contact between a wet gas and glycol can be made in bubble cap or valve tray absorbers or other gas-liquid contact devices. The gas gives the water vapour to glycol as it passes through the absorber. Water-rich glycol leaves the bottom of the tower and is pumped through a regeneration system to boil off the absorbed water. It is then circulated back to the absorber to complete a closed loop process cycle (Ballard, 1979). Liquid desiccant systems are simple to operate and maintain and it is possible to automate them for unmanned operations (GPSA Data book, 1998). This technology needs a large facility and due to the need for glycol, there is a possibility for some operational problems and the way to prevent such problems should be recognized. Some of these problems and the way to avoid them are as follows (Ballard, 1979):

- Oxidation: air should be kept out of the system
- Thermal Decomposition: excessive heat should be avoided

- pH control: pH needs to be watched carefully by using glycol to lower the pH and increase the acidity and corrosion.
- Salt contamination: should be removed by an efficient scrubber before the glycol unit
- Liquid hydrocarbons: should be separated with the gas-glycol separator or activated carbon beds
- Sludge: solid particles suspended in glycol can be separated by good filtration
- Foaming: be prevented by effective gas cleaning ahead of the unit and filtration

Other glycol based gas dehydration technologies were developed to increase the glycol purity after regeneration and decrease the emission gas to the environment (GPSA, Data book, 1998). A process flow diagram for a typical glycol dehydration unit is shown in Figure 2.2.

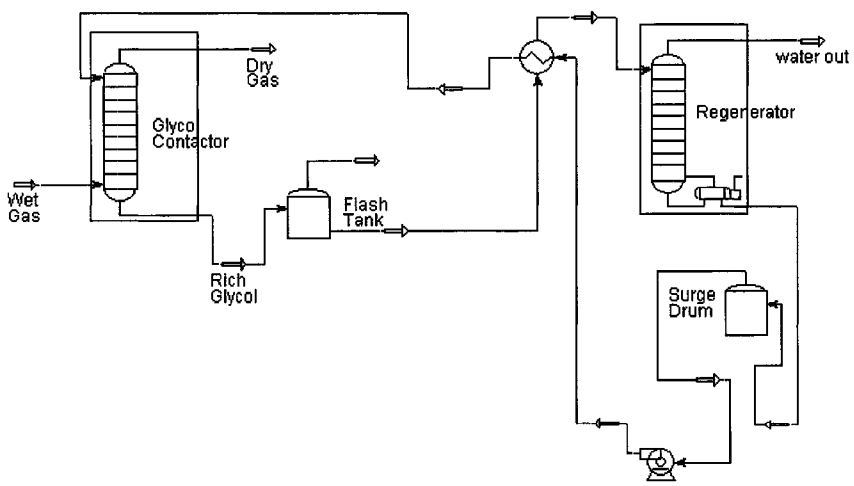

FiFigure2.2: Schematic diagram of a typical glycol dehydration system

2.1.4 Adsorption using solid desiccants

Solid desiccant dehydration is also known as dry-bed dehydration. It uses a solid reagent to remove water. Adsorbents also known as desiccants are high capacity material for water removal including alumina, silica gels, and molecular sieves. Molecular sieves produce the lowest water dew point and have the highest capacity for water removal but the heat required to regenerate them is more than alumina or silica gels. Molecular sieves are also more expensive compared to other desiccants. The solid desiccant dehydration system is consisted of two or more towers and the associated regeneration equipment. Before introducing the gas into a cylindrical bed containing the desiccant, the wet gas enters an inlet separator to remove contaminants and free water and hydrocarbon by gravity. Desiccants have limited capacity for water, become saturated soon, and therefore should be regenerated to restore its adsorptive capacity. The regeneration is usually accomplished by heating. Hot gas vaporizes the water from the adsorbent. Dry bed dehydration is a semi continuous process for which at least two parallel vessels filled with the adsorbent are required. In this arrangement, one vessel is adsorbing while other is regenerating (GPSA Data book, 1998, Ballard, 1979, and Manning and Thompson, 1991). Figure 2.3 outlines a schematic of this process.

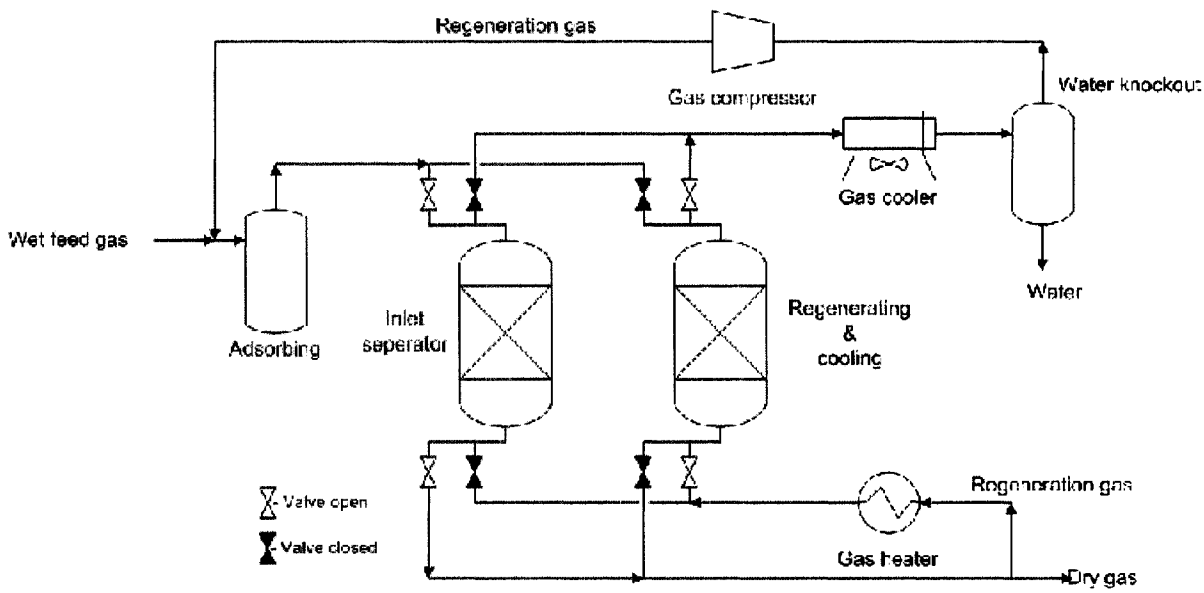

Figure2.3: Schematic of an example solid adsorbent dehydrator

2.1.5 Dehydration with calcium chloride

Solid anhydrous calcium chloride ($CaCl_2$) which forms various $CaCl_2$ hydrates when combined with water can be used as desiccant to dehydrate natural gas. As water absorption continues, brine solution will be formed. In this unit calcium chloride pellets are placed in a fixed bed. To increase the unit capacity three to four trays can be installed below the fixed bed to pre-contact the gas with the brine solution and remove a portion of water before the gas contacts the solid $CaCl_2$. The Unit might show poor performance under some conditions if $CaCl_2$ pellets bond together and form a solid bridge in the tower (GPSA Data book, 1998). Figure2.4 outlines a typical $CaCl_2$ dehydrator.

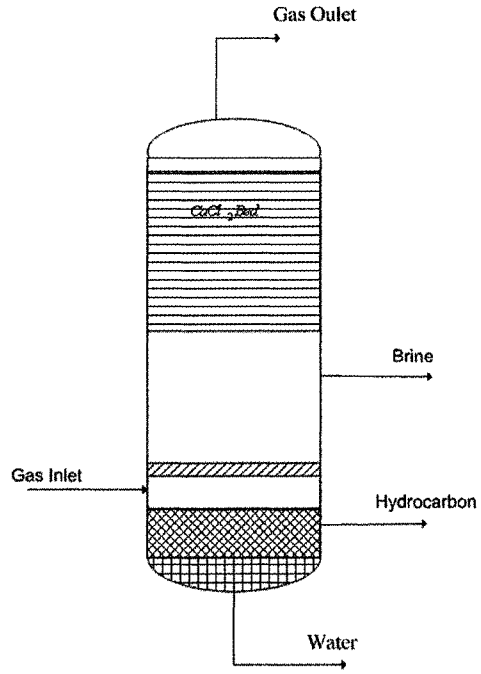

Figure2.4: Schematic of a typical CaCl2 dehydrator

2.1.6 Dehydration by refrigeration

Natural gas consists of many different components. Heavier-than-methane hydrocarbon constituents of natural gas that can liquefy in the field or processing plants are called natural gas liquids (NGL). Refrigeration through external vapour recompression is the simplest and most common process for dew point control of NGLs and water. In external or mechanical refrigeration systems the cooling is supplied by a vapour recompression cycles that typically use propane as the refrigerant or the working fluid. The refrigerant (often C_3 in natural gas industries) boils off and leaves the chillers as a saturated vapour (GPSA Data book, 1998 and Kidnay and Parrish, 2006). This

process is shown in Figure 2.5 (GPSA Data book 1998, Arnold and Stewart 1999, Manning and Thompson, 1991).

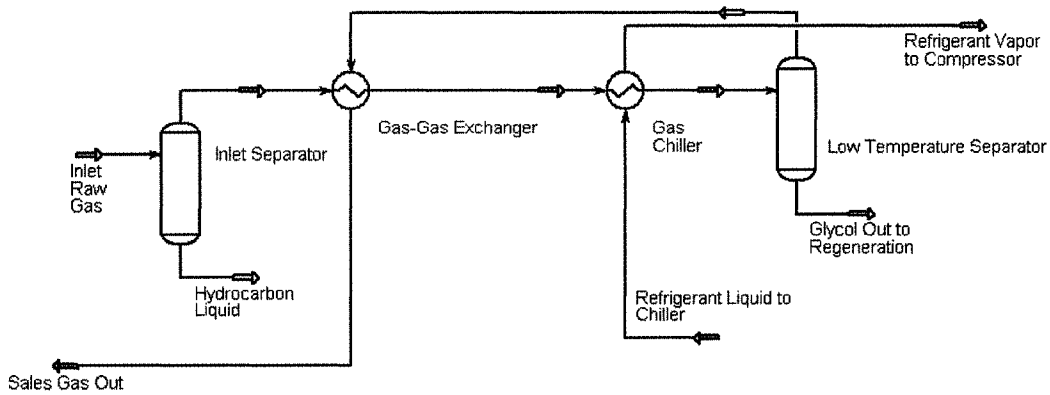

Figure2.5: External refrigeration systems

If the inlet pressure is high enough, there will not be a need for external cooling and the expansion refrigeration that is known as low temperature extraction (LTX) or low temperature separation (LTS) will be used. This process applies the Joule-Thompson (JT) effect to reduce the gas temperature upon expansion in order to condense water and hydrocarbon and recover condensate with or without hydrate inhibition. The Joule-Thompson (J-T) in this process induces "self-refrigeration" as apposed to "external refrigeration" (Manning and Thompson, 1991). To run LTS without using hydrate inhibitors, the temperature should be sufficient to prevent hydrate formation upstream of the valve where joule–Thompson expansion occurs. The expansion is essentially a

constant enthalpy process. The inlet gas passes through the gas-gas exchanger, then to an expansion or choke valve. Non-ideal behaviour of the inlet gas causes the temperature to fall with the pressure reduction (GPSA Data book, 1998, Manning and Thompson, 1991).This technique requires a large pressure drop so it is used when the main objective is to recover condensate. Figure2.6 shows an LTS that uses glycol injection and J-T expansion for cooling.

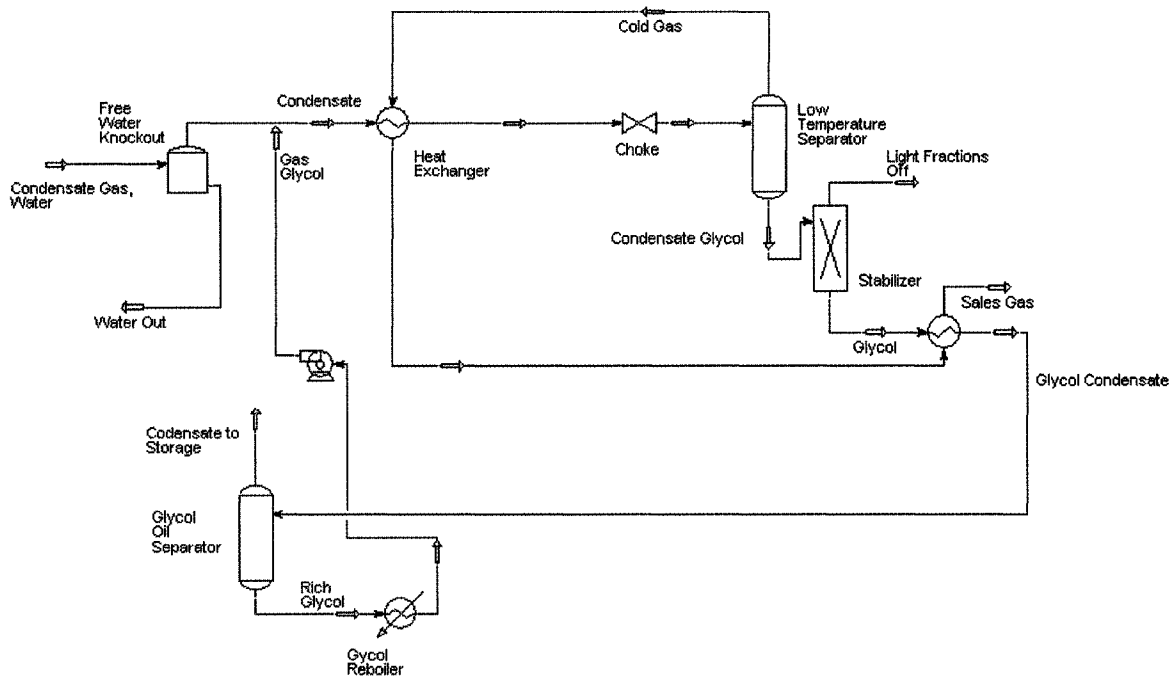

Figure2.6: Low-temperature separations with glycol injection

2.1.7 Dehydration by membrane permeation

Membranes have been successfully used to remove acid gases from natural gas. They are also being promoted by suppliers of membrane technology for water removal (Arnold and Stewart, 1999). They are relatively expensive (especially for large gas flow rates) and can be easily fouled by gas contaminants. They also need high pressure for efficient operation. However, they have a low-pressure drop through the process and do not need any chemical reagents. The installation and change of the membrane cartridge are relatively easy and the maintenance cost is low. The membranes' capability to remove water vapour is not selective and part of the gas is always wasted through co-permeation. Figure 2.7 shows the membrane dehydration process (Stookey et al. 1984).

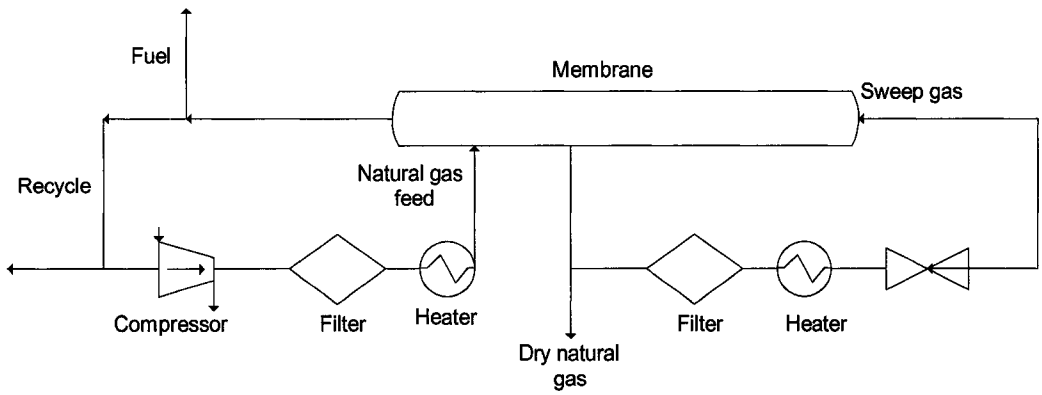

Figure2.7: Schematic diagram of a membrane dehydration process

2.1.8 Supersonic dehydration

Most of the previously mentioned methods have good dehydration performance but they have some disadvantages including the need for relatively large facilities, a considerable investment and complex mechanical work and the possibility of having a negative impact on the environment. Supersonic dehydration unit were introduced to overcome some of the disadvantages of the alternative processes for dehydration. Full scale supersonic separator units have been tested in five different gas plants with different gas compositions and operating conditions since 1998 (Brouwer et al., 2004). The first commercial gas conditioning technology using the supersonic separator in the offshore applications was started up in December 2003 (Brouwer et al., 2004). 3-S separator is another unit based on the same technology with different structure (Alfyorov et al., 2005). The idea of 3-S separators was proposed by a group of Russian specialists (Alfyorov et al., 2005). This group joined Translang Technologies Ltd., Calgary. 3-S separators performances have been studied and tested since 1996. An experimental test plant was constructed in Russia. Later another pilot plant for greater natural gas flow rate was built in Calgary. None of these facilities was capable of very high pressures. The first industrial 3-S separator was started operating in Western Siberia (Alfyorov et al., 2005). These cyclonic gas/liquid separators, which combine expansion and re-compression in a compact, tubular device, have very similar thermodynamic performance to that of turbo-expanders. A similar temperature drop as in turbo expanders, within which pressure transforms to shaft power can be achieved in both units by transforming

pressure to kinetic energy (Brouwer et al., 2004 and Schinkelshoek et al., 2006). The Twister supersonic separator and 3-S separators both include a supersonic nozzle to expand the saturated feed gas to supersonic velocities and therefore lower temperature and pressure which results in water and hydrocarbon condensation. Separation of the liquid droplets can be achieved by centrifugal forces using two different methods: a) using a wing or blade at the end of the nozzle and in the supersonic region, b) using a flow swirling device ahead of the nozzle. The former was used by the Twister's design at this stage and the latter was used in 3-S separators. In both cases after liquids are separated from the gas, dry gas in the exit becomes subsonic and some of the pressure can be recovered. Another unit with the same technology was tested experimentally with wet air as a working fluid and 1 MPa working pressure (Hengwei et al., 2005). The pressure recovery of this system was less than 75%.

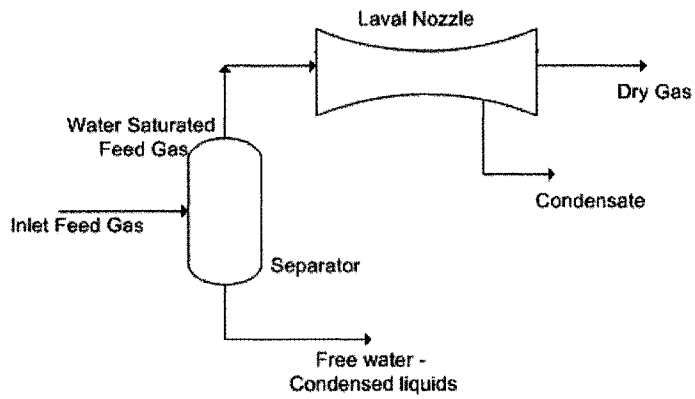

Figure2.8: Schematic diagram of a supersonic dehydration unit

The main part of the supersonic dehydration unit is a supersonic (converging – diverging) nozzle (see Figure 2.8). The supersonic nozzle is simple in design and does not include any moving parts. In the supersonic nozzle both condensation (or solidification of hydrate) and separation occur at supersonic velocities, which leaves hydrate no time to deposit on the wall surfaces due to the short residence time and the high velocity of the fluid. The simplicity of this device makes it suitable for unmanned operation (Brouwer et al., 2004 and Schinkelshoek, 2006) for underwater or remote gas production applications. As a result, the gas in this system can be dehydrated in a smaller, lighter, cheaper, more environmentally friendly, and less complex facility.

In the supersonic dehydration unit, the gas temperature is lowered based on gas expansion principles without the need of any refrigerant. The compactness of this design is a major advantage over traditional means of dehydration particularly for offshore applications. The gas velocity in this device is very high which prevents fouling or deposition of solids and ice. Refrigeration is self-induced therefore no heat is transferred through the walls and unlike external refrigeration systems, no inhibitor injection and inhibitor recovery system are necessary. Intensive water dew points down to -50 to -60 °C can be achieved without any external cooling or use of solid adsorption techniques. The major drawback of this system is the pressure loss due to the expansion in the nozzle. New designs are under development to overcome the loss of energy as the gas passes through the high speed nozzles. Most of the traditional means of dehydration remove water and hydrocarbon simultaneously and they are not selective to any one element

alone. At certain conditions of pressure and temperature, presence of heavy hydrocarbons (C_2^+) increases the gas gravity and reduces the compressibility factor, which results in an increase in the pipeline mass flow capacity (Mohitpour et al., 2003). Furthermore, the compactness and reliability of the process equipment are very important especially for offshore applications where the foot print area is at a premium. Therefore, for special applications development of a compact system that is capable of selectively removing water from high pressure natural gas streams without affecting the hydrocarbon content will be needed. To remove water selectively natural gas should be kept in a single phase and hydrocarbon condensation should be avoided.

2.2 Flow properties in a converging-diverging nozzle

In order to analyze the behaviour of fluid in supersonic nozzles a sound understanding of the basics of thermodynamics, phase equilibrium and dynamics of compressible fluid flow is required. These principles are briefly reviewed in the following sections.

2.2.1 Compressible flow

Natural gas is a highly compressible fluid. In compressible fluids the density changes as the fluid pass though flow passages. Two different kinds of processes can cause density to change. In a dynamic process the fluid density can change in association

with the fluid acceleration, whereas in a thermodynamic process in which density changes due to the\e addition of heat from an external source. Sometimes density changes are because of combination of both processes (Greitzer et al., 2004).

2.2.2 Equilibrium phase diagrams

Phase diagrams also called phase envelopes, are used to examine the phase or phases that may exist at any given conditions of pressure and temperature. The diagrams show the locus of points between the two equilibrating phases on a P-T plot (see Figure 2.9). Several terms are used to define different points on the phase envelope. Cricondenbar and cricondentherm are the respective maximum pressure and temperature at which liquid and vapour can coexist in equilibrium. If the pressure is kept above the cricondenbar (above the phase envelope), a single dense phase exists. Bubble point line is the locus at which vaporization begins and dew point line is the locus at which condensation begins. These two lines meet each other at the critical point. The system changes from all liquid to all vapour and vice-versa in the critical point. P_c and T_c on the following phase diagram show the critical pressure and temperature respectively.

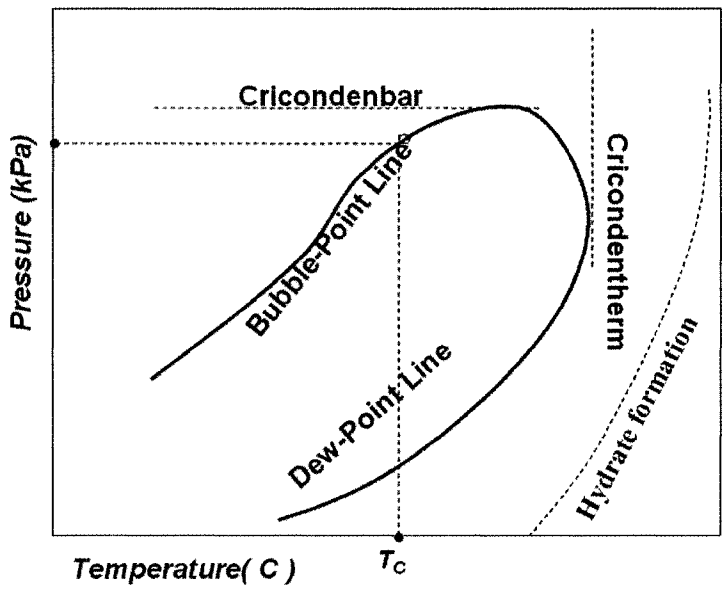

Figure 2.9: Phase envelope of a multi-component mixture

For a multi-component mixture, the gap between the dew point and bubble point lines can vary with composition. The gap becomes wider as heavier hydrocarbons are added to the mixture. As a result, the points indicating cricondenbar and cricondentherm can move upward or downward depending on the gas composition.

The fluid at a temperature and pressure conditions above its critical values is called *supercritical* as its expansion or compression at constant temperature does not result in any phase change.

Non-hydrocarbon impurities such as water, carbon dioxide, hydrogen sulphide and nitrogen also affect the shape of the phase envelope. Presence of carbon dioxide and hydrogen sulphide lower the cricondenbar but nitrogen increases cricondenbar. On the other hand, as water has a low vapour pressure it does not have a significant effect on the

shape of hydrocarbon phase envelope except in high temperature and low pressure regions (Campbell, 1992).

2.2.3 Equations of state

By using basic thermodynamic relations and the equations of state (EOS), the gas properties such as density, enthalpy, and entropy can be predicted. Equations of state describe the interconnection between the measurable thermodynamic properties of a fluid system. Many gases follow the ideal gas law very closely at high temperatures and low pressures usually up to 400 kPa (Campbell, 1992). The ideal gas equation becomes increasingly inaccurate at higher pressures and lower temperatures and fails to predict condensation from gas to liquid. Ideal gas law describes a gas whose molecules do not interact with each other and it is simply defined with the following formula:

$$pv = nRT \tag{2.1}$$

Many different equations have been developed to describe non ideal, real gas behaviour. Real gas laws predict the true behaviour of a gas by considering the terms to describe attractions between molecules. The van der Waals (VW) equation which was the first cubic equation to predict the real gas properties was developed in 1873 (Molleson and Stasenko, 2005). The van der Waals equation does predict the formation of liquid phase but its agreement with experimental data is limited for conditions where liquid forms. The Redlich-Kwong (RK) equation, a two-parameter equation, was

introduced in 1949 as an improvement to van der Waals equation. Although this equation is superior over the previous equations of state, it cannot be used to predict the vapour-liquid equilibrium properties. Later a third parameter was added to the cubic equations of state and an accurate prediction was taken using Soave-Redlich-Kwong (SRK) and Peng Robinson (PR) equations in year 1972 and 1976. SRK and PR are the most commonly used equations of state in natural gas processing industries. The cubic equations have the following general form (Jacobsen et al., 1997):

$$p = \frac{RT}{v-b} - \frac{a}{v^2 + ubv + wb^2} \tag{2.2}$$

Where b, u, and w are constants and a is a function of temperature and has dimensions of Pv^2. The quantities v and R may be expressed on either mass or molar basis.

2.2.4 Basic fluid flow equations

The basics equations of fluid flow can be derived from the principles of mass, energy and momentum conservation as well as laws of thermodynamics (Fox and McDonald, 1985). A fixed control volume can be used to develop the general governing equations between two points for the flow stream:

Continuity equation:

$$\frac{\partial}{\partial t}\int_{cv} \rho dV + \int_{cs} \rho \vec{V}.\vec{dA} = 0 \tag{2.3}$$

Momentum equation:

$$F_s + F_B = \frac{\partial}{\partial t}\int_{cv} V\,\rho dV + \int_{cs} V\,\rho \vec{V}.\vec{dA} \tag{2.4}$$

First law of thermodynamics:

$$\dot{Q} - \dot{W}_s - \dot{W}_{shear} - \dot{W}_{other} = \frac{\partial}{\partial t}\int_{cv} e\rho dV + \int_{cs}(e + pv)\rho \vec{V}.\vec{dA} \tag{2.5}$$

Second law of thermodynamics:

$$\int_{cs}\frac{1}{T}\frac{\dot{Q}}{A}dA \le \frac{\partial}{\partial t}\int_{cv} s\rho dV + \int_{cs} s\rho \vec{V}.\vec{dA} \tag{2.6}$$

Certain assumptions will be made to simplify the governing equations for each condition.

2.2.5 Quasi-one dimensional flows

In most of the high-speed gas flows within a duct as the cross sectional area varies along the duct, pressure, temperature, density and velocity changes downstream of the duct. But the flow direction will remain approximately the same. This is called *quasi one-dimensional flow*. This type of analysis is a useful estimate to study the response of the compressible flow to alternations in area, addition of mass, momentum, and energy. *The quasi one-dimensional* assumption can be applied to a duct or channels where the length along the flow direction is much larger than the width. Nozzles are one of the common examples of this geometry.

2.2.6 Stagnation properties

Stagnation state is a theoretical state in which the flow is brought to complete rest in an isentropic process. To specify the compressible flow stagnation properties the isentropic processes is considered. Stagnation properties are the reference properties of the fluid if it is decelerated to zero velocity. For ideal gas the equations for the stagnation properties have been specified and exist in literature (Fox and McDonald, 1985). The following equations show the calculations for stagnation pressure, temperature, and density respectively:

$$\frac{P_0}{P} = \left[1 + \frac{k-1}{2} M^2\right]^{k/k-1} \tag{2.7}$$

$$\frac{T_0}{T} = 1 + \frac{k-1}{2} M^2 \tag{2.8}$$

$$\frac{\rho_0}{\rho} = \left[1 + \frac{k-1}{2} M^2\right]^{1/k-1} \tag{2.9}$$

For real gas stagnation properties can be found by solving the basic equations along with a suitable equation of state for compressible, steady state, one dimensional isentropic flow where heating loss and system works and gravity forces are negligible. The basic equations will be simplified as follows (Fox and McDonald, 1985):

Continuity equation:

$$\rho_1 V_1 A_1 = \rho_2 V_2 A_2 = \rho V A = \dot{m} = cons\tan t$$

(2.10)

Momentum equation:

$$R_x + p_1 A_1 - p_2 A_2 = \dot{m} V_2 - \dot{m} V_1 \tag{2.11}$$

Where R_x is the surface force acting on the control volume.

First law of thermodynamics:

$$h_0 = h_1 + \frac{V_1^2}{2} = h_2 + \frac{V_2^2}{2} \tag{2.12}$$

h_0 is the stagnation enthalpy which is constant throughout an adiabatic flow field.

Second law of thermodynamics for an isentropic (constant entropy) flow can be written as follows (Fox and McDonald, 1985):

$$S_2 = S_1 = S \tag{2.13}$$

2.2.7 Speed of sound

The terms subsonic and supersonic refer to the conditions where the fluid velocities are less and greater than the speed of sound - an important characteristic for compressible flow systems. By solving the continuity and momentum equations for steady state and uniform flow conditions and assuming that the process is reversible and adiabatic, as there is very little time for heat transfer in sound wave propagation, the

speed of sound can be calculated using the following equation:

$$c = \sqrt{\left(\frac{\partial P}{\partial \rho}\right)_s} \tag{2.14}$$

To calculate the speed of sound for ideal gas a simplified equation based on the ideal gas law is available (Fox and McDonald, 1985). Mach number is defined as the ratio of the local fluid speed to the speed of sound.

2.2.8 Shockwave

Shockwave is an irreversible discontinuity that happens if the flow can not achieve the exit properties with the same conditions at upstream of the shock. During this process, large change in pressure, temperature, and other properties including entropy can occur in a small distance and the supersonic flow becomes subsonic. The thickness of a shock is about 0.2 μm (Fox and Mc Donald, 1985). As the shock thickness is small, the cross section areas at the upstream and downstream of the shock are equal and the energy and heat loss is negligible. For each upstream condition of a shock, there is a single unique downstream state. The basic equations can be simplified as shown below to calculate the properties on both sides of the normal shockwave:

Continuity equation:

The cross sectional area upstream and downstream of the shock is equal as the shock is very thin therefore:

$$\rho_1 V_1 = \rho_2 V_2 = \frac{\dot{m}}{A} \tag{2.15}$$

Momentum equation:

$$p_1 A_1 - p_2 A_2 = \dot{m} V_2 - \dot{m} V_1 \tag{2.16}$$

First law of thermodynamics:

$$h_0 = h_1 + \frac{V_1^2}{2} = h_2 + \frac{V_2^2}{2} \tag{2.17}$$

h_0 is the stagnation enthalpy which is constant throughout an adiabatic flow field.

Second law of thermodynamics:

Through the shockwave, the flow is irreversible as the discontinuous property change happens, as a result the entropy across the shock increases:

$$S_2 > S_1 \tag{2.18}$$

Shock strength can be determined by the pressure increase across the shock (Greitzer et al., 2004).

2.3 Supersonic nozzles

The supersonic nozzle, which is the main part of the proposed dehydration unit, is

a tube, which is pinched in the middle. The nozzle is composed of three sections: the converging section (subsonic zone), throat (critical zone), and diverging section (supersonic zone) (see figure 2.10) .

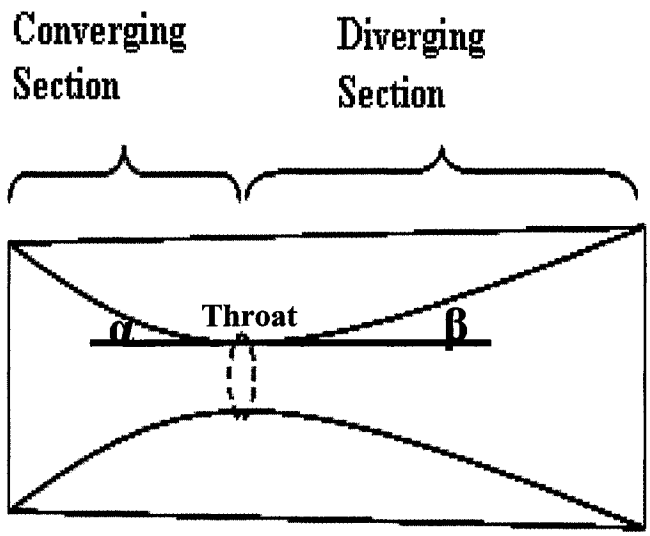

Figure 2.10: Different parts of a supersonic nozzle

Due to the constant flow rate, flow acceleration happens in the pipe carrying the flow as it narrows. Therefore, the function of the converging part is to accelerate the gas as well as keeping the flow uniform and parallel. In practical conditions, in order to get the sonic speed at the throat where the cross sectional area is minimum, usually the inlet diameter is kept larger than $\sqrt{5}$ of the throat diameter and the converging length is equal to or greater than the throat diameter (Man et al., 1997). Once the inlet thermodynamic conditions and the variation of the cross section area of the nozzle as a function of distance are defined, the outlet conditions will also be uniquely defined (Moraitis and

Akritidis, 1997). Figure 2.11 shows the different possibilities for the exit pressure of the nozzle and Figure 2.12 ouline the velocity distribution in the supersonic nozzle. If the mass flow rate is not sufficient to provide the desired pressure drop, the flow will be subsonic all the way through nozzle (see figure 2.11 and 2.12 line A). It accelerates in the nozzle and gets the minimum pressure and the maximum velocity in the minimum cross section of the nozzle, and decelerates in the diverging part of the nozzle. In this condition, the minimum area is not considered as the throat. The flow rate should increase until the flow velocity reaches the sonic velocity where the Mach number is close to unity in the minimum cross section of the nozzle. This smallest cross section is called the throat of the nozzle where the flow is called *choked flow.* The flow rate, in which choked flow happens, is the maximum possible flow for the specific nozzle geometry and the inlet condition (Fox and Mc Donald, 1985). If the *choked flow* never happens inside the nozzle because of insufficient mass flow rate, the flow will never accelerate to supersonic velocity. However, the sonic flow in the throat might become subsonic or supersonic as the cross sectional area increases in the diverging part of the nozzle. This depends on the ratio between the inlet stagnation pressure and the backpressure (ambient pressure at the exit of the nozzle). At a certain ratio between inlet and back pressure the exit flow is subsonic and most of the pressure will be recovered before any further compression happens (see line B, Figure 2.11 and 2.12). These exit properties will be called "*Nozzle recovery properties*" from now on in this thesis. If the flow is supersonic in the diverging part of the nozzle and no pressure recovery happens,

the outlet nozzle condition is called the "*design condition*" and the exit flow remains supersonic (line D, Figure 2.11 and 2.12). The properties in the *design condition* are called "*Nozzle design properties* "in this thesis. The nozzle subsonic pressure and the design pressure will be achieved if the backpressure is equal to the exit pressure of the nozzle. Line C indicates a case where a normal shockwave happens inside the diverging part of the nozzle. The normal shock happens if the backpressure falls between the nozzle's subsonic and design pressure. This nozzle is called *over-expanded* because the pressure at some point is less than backpressure. In an over expanded nozzle, a shockwave happens either inside or outside of the diverging part of the nozzle which results in pressure recovery. If the shock wave happens inside the diverging part of the nozzle, the back pressure and the exit pressure are equal. But in the conditions where the shock wave happens outside the diverging part but still between the subsonic and design pressure, the exit pressure is lower than the back pressure. Shockwave location is related to the inlet to back pressure ratio.

The nozzle with the backpressure less than the design pressure is called *under-expanded* as some of the expansion will occur outside of the nozzle.

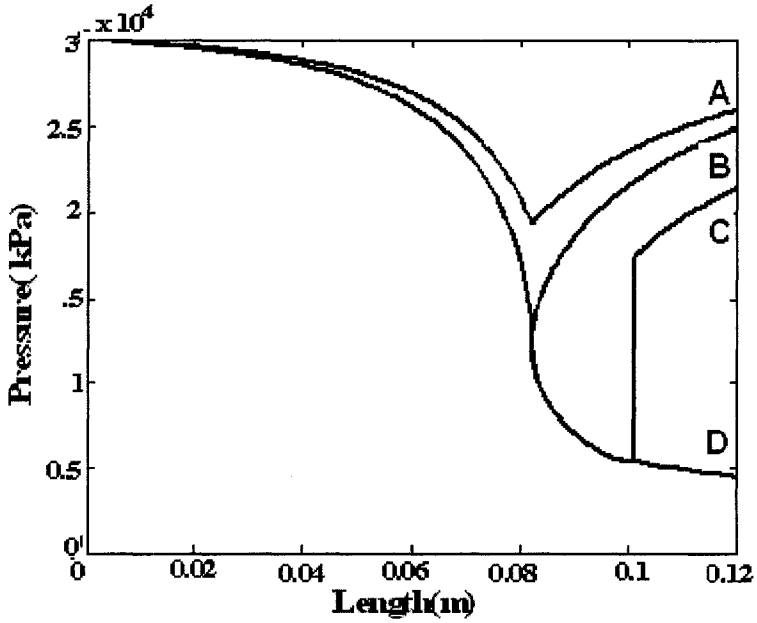

Figure 2.11: Different possible exit pressures in a Laval nozzle

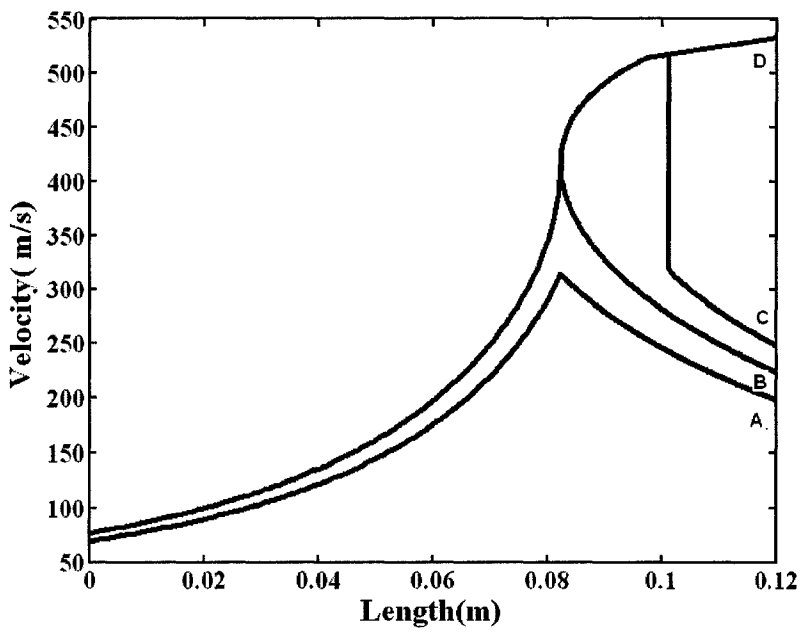

Figure 2.12: Velocity distribution in a Laval nozzle

Nozzle exit cross section area depends on not only the total length of the nozzle but also the throat location inside the nozzle. Throat location depends on the flow properties and needs to be determined as the first step to design a nozzle.

CHAPTER 3: MODELING OF SUPERSONIC NOZZLES

3.1 MODELLING APPROACH

This thesis focuses on modelling and designing the proposed supersonic dehydration system. The main part of the system is a converging-diverging nozzle, also known as the Laval nozzle. In the modelling approach two different software packages are linked: MATLAB, a numerical computing environment and programming language and HYSYS, a process modeling and simulation software. Connecting these two software packages leads to a powerful simulation tool to study new processes (Beronich et al., 2005) and helped this study to analyze various process alternatives.

As the stream pressure and temperature is reduced by gas expansion within the nozzle, the water vapour starts to condense to the aqueous phase. The condensed liquids (including possibly natural gas liquids in case the pressure is below the cricondenbar) should be removed from the gas stream before the nozzle diverges downstream of the shockwave (see Figure 3.1). Some gas leaves the nozzle together with the liquids, which should be separated and returned to the main gas leaving the nozzle at the exit. The nozzle should be designed such that the gas leaving at the exit contains the desired level of water and/or heavier hydrocarbons.

It is not the purpose of this work to focus on the ways by which these liquids could be separated within the nozzle; however, there are various techniques the liquid drop out could be separated (Alfyorov et al., 2005).

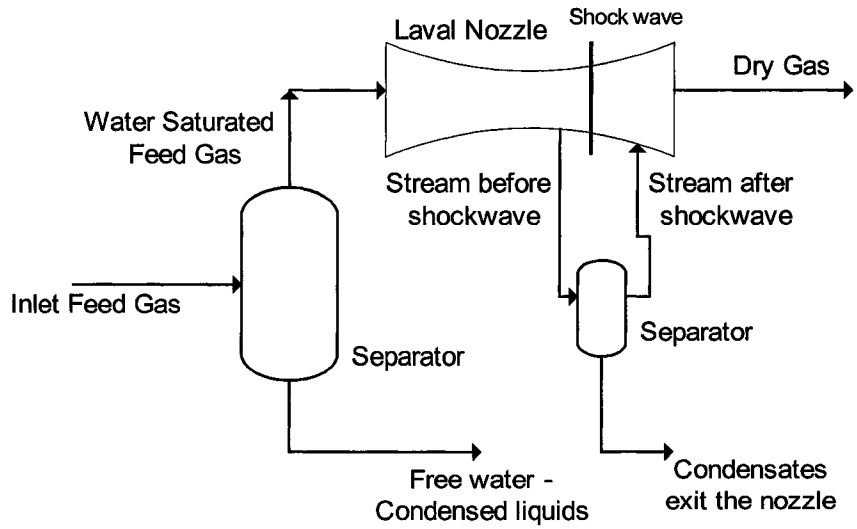

Figure3.1: Schematic diagram of a supersonic dehydration unit

The first step to solve a nozzle is predicting the behaviour of the stream which flows through the nozzle. Therefore, a MATLAB program was developed to solve the governing equations of the system such as the continuity and momentum equations as well as the first and second laws of thermodynamics. Besides, an equation of state is needed to calculate the thermodynamic properties of the gas stream such as density, viscosity, enthalpy, and entropy. The HYSYS process simulator was used to predict gas properties using commonly used thermodynamic models and fluid properties estimation techniques. The link between MATLAB and HYSYS gives simulation model the capability of working with different EOSs. Input parameters to HYSYS are gas composition, inlet temperature, pressure and the flow rate. Free water is almost always present at well head conditions and it is assumed that the produced gas is saturated before

entering the process (Kidnay and Parrish, 2006). The simulation was started with a dry gas composition. A mixer was introduced in the simulation to saturate the feed gas with water. Natural gas can hold different amounts of water at different conditions of pressure and temperature. Natural gas saturation capacity increases as temperature increases and pressure decreases. As the dry stream becomes saturated, there will be a change in composition, inlet temperature, and flow rate of the gas stream. Condensation of water causes a reduction in water dew point and a reduction in water content of the gas.

The flow through the nozzle is assumed to be supercritical, steady state, one dimensional and compressible with no heat exchange. Two different cases for this process were considered:

3.1.1 Isentropic, adiabatic, and frictionless modeling

The simplified conservation equations in the isentropic flow are as follows:

$$\rho_1 V_1 A_1 = \rho_2 V_2 A_2 = \rho V A = \dot{m} = \text{constant} \tag{3.1}$$

$$h_0 = h_1 + \frac{V_1^2}{2} = h_2 + \frac{V_2^2}{2} \tag{3.2}$$

$$S_2 = S_1 = S \tag{3.3}$$

By solving these equations, momentum equation will be satisfied automatically.

$$R_x + p_1 A_1 - p_2 A_2 = \dot{m} V_2 - \dot{m} V_1 \tag{3.4}$$

Where R_x is called the *thrust* and can be defined as $\left(\frac{P_1 + P_2}{2}\right)(A_1 - A_2)$.

A suitable equation of state is needed to predict the necessary properties. For the real gas assumption, the Peng-Robinson model was used here as the equation of state.

The ideal gas assumption was also made and the pertinent equations were included in the simulation program so that a comparison between real and ideal gas behaviour could be made. The only difference between the equations for real and ideal gas is the equation of state. Ideal gas law is used as the equation of state in ideal gas assumption. In this case, there will be no need to solve equations numerically as the simplified equations are already available in the literature (Fox and Mc Donald, 1985). In ideal gas flow, stagnation properties can be found by substituting the inlet properties in these analytically derived equations. Stagnation properties will be constant throughout the steady state flow and properties at each section can be found with respect to these properties.

3.1.2 Modeling with friction

In this case the flow is not isentropic and friction terms will be added to the equations (Ozalp, 2005). In frictional flow the mean incremental properties can be calculated using the following equation:

$$\bar{\xi}_c = \frac{\xi_{c,1} + \xi_{c,2}}{2} \tag{3.5}$$

The Reynolds number for each segment can be calculated using Equation 3.6:

$$\left(\mathrm{Re}_D\right)_c = \frac{\overline{U}_c \overline{D}_c}{\overline{\nu}_c} \tag{3.6}$$

It is known that the friction coefficient (f) is a function of the Reynolds number (Re_D) and the surface roughness (ε) and can be defined by the Colebrook (Ozalp, 2005) formula:

$$\frac{1}{\sqrt{\bar{f}_c}} = -3.6\log\left[\frac{6.9}{\left(\mathrm{Re}_D\right)_c} + \left(\frac{\varepsilon/\overline{D}_c}{3.7}\right)^{1.11}\right] \tag{3.7}$$

Having the friction coefficient in each segment, shear stress (Equation 3.8) and the friction factor (Equation 3.9) will be found as follows:

$$\overline{\tau}_c = \bar{f}_c \overline{\rho}_c \frac{\left(\overline{U}_c\right)^2}{2} \tag{3.8}$$

$$\left(\overline{F}_f\right)_c = \overline{\tau}_c \pi \overline{D}_c \Delta x_c \tag{3.9}$$

The frictional loss term can then be defined as:

$$\overline{\Phi}_c = \frac{\left(\overline{F}_f\right)_c U_c}{\dot{m}} \tag{3.10}$$

And the thrust is:

$$\bar{I}_c = \left(\frac{P_1 + P_2}{2}\right)(A_1 - A_2) \tag{3.11}$$

Therefore, the following equations together with an equation of state need to be solved simultaneously to predict the system.

$$\rho_1 V_1 A_1 = \rho_2 V_2 A_2 = \rho V A = \dot{m} = \text{constant} \tag{3.12}$$

$$h_1 + \frac{V_1^2}{2} = h_2 + \frac{V_2^2}{2} + \overline{\Phi}_c \tag{3.13}$$

$$\boxed{p_1 A_1 - p_2 A_2 = \dot{m} V_2 - \dot{m} V_1 + (\bar{F}_f)_c + \bar{I}_c} \tag{3.14}$$

Which will satisfy the entropy equation where:

$$\boxed{S_2 > S_1} \tag{3.15}$$

3.2 Numerical solution technique

Solving all the equations analytically, is a time consuming process if not practically impossible, therefore, a numerical technique was chosen to design the nozzle. The Newton- Raphson (NR) method was used in this study. By using this method the nonlinear equations can be solved simultaneously to predict the nozzle unknown variables. In design and analysis of the supersonic nozzle, the goal is almost always predicting two variables, pressure and temperature. These variables can be computed by the Newtonian iteration. A two variable NR method can be developed by preparing the following matrix (Hollis, 1996).

$$\vec{G}^{n+1} = \vec{G}^{n} - \left|\frac{\partial \vec{E}}{\partial G}\right|^{-1} \vec{F} \tag{3.16}$$

Where G shows the variables to be determined, F includes the equations that should be satisfied and n is the iteration level. All the derivatives in this simulation were computed numerically. The Newton-Raphson method was used in this simulation to solve the relevant equations for three different conditions. Equation 3.17 is the actual matrix used for each condition. Temperature and pressure are the variables to be determined and the general form of the Newton-Raphson method in this simulation is as described in Equation 3.16.

$$\begin{bmatrix} T \\ P \end{bmatrix}^{n+1} = \begin{bmatrix} T \\ P \end{bmatrix}^{n} - \begin{bmatrix} \frac{\partial F_1}{\partial T} & \frac{\partial F_1}{\partial P} \\ \frac{\partial F_2}{\partial T} & \frac{\partial F_2}{\partial P} \end{bmatrix}^{-1} \begin{bmatrix} F_1 \\ F_2 \end{bmatrix} \tag{3.17}$$

If the flow is assumed to be isentropic, energy and entropy equations should be satisfied so F_1 and F_2 are as follows:

$$F_1 = h_{i-1} + \frac{v_{i-1}^2}{2} - \left(h_i + \frac{v_i^2}{2}\right) = 0 \tag{3.18}$$

$$F_2 = S_{i-1} - S_i = 0 \tag{3.19}$$

In a non-isentropic flow when friction is present F_1 and F_2 are described as Equations 3.20 and 3.21, as entropy is not constant and the energy and momentum equations will be satisfied:

$$F_1 = h_{i-1} + \frac{v_{i-1}^2}{2} - \left(h_i + \frac{v_i^2}{2} + \overline{\Phi}_c \right) = 0 \tag{3.20}$$

$$\boxed{F_2 = P_{i-1}A_{i-1} + \dot{m}v_{i-1} - (P_i A_i + \dot{m}v_i + (\overline{F_f})_c + \overline{I_c}) = 0} \tag{3.21}$$

To predict the properties downstream of the shock F_1 and F_2 are defined as equations 3.22 and 3.23:

$$F_1 = h_{i-1} + \frac{v_{i-1}^2}{2} - \left(h_i + \frac{v_i^2}{2} \right) = 0 \tag{3.22}$$

$$F_2 = P_{i-1}A_{i-1} + \dot{m}v_{i-1} - (P_i A_i + \dot{m}v_i) = 0 \tag{3.23}$$

Where i denotes the properties in the section that properties are to be defined and $_{i-1}$ indicates the properties in the previous section.

In this method, an initial guess for pressure and temperature is made at each segment of known cross section area. The mixture density at the estimated pressure and temperature is then found using the EOS. As the flow rate is known, flow velocity can be predicted using the continuity equation. The actual properties are found by solving NR matrix.

3.3 Design of the Nozzle

In order to design a Laval nozzle, the following data should be predetermined:

- Nozzle inlet diameter
- Half convergent and divergence angle

- Inlet temperature of the dry gas stream
- Inlet pressure of the dry gas stream
- Inlet flow rate of the dry gas stream
- Nozzle total length

Nozzle is designed if its geometry, throat diameter, and the converging and diverging lengths, is known. The flowchart in Figure 3.2 describes the nozzle design procedure.

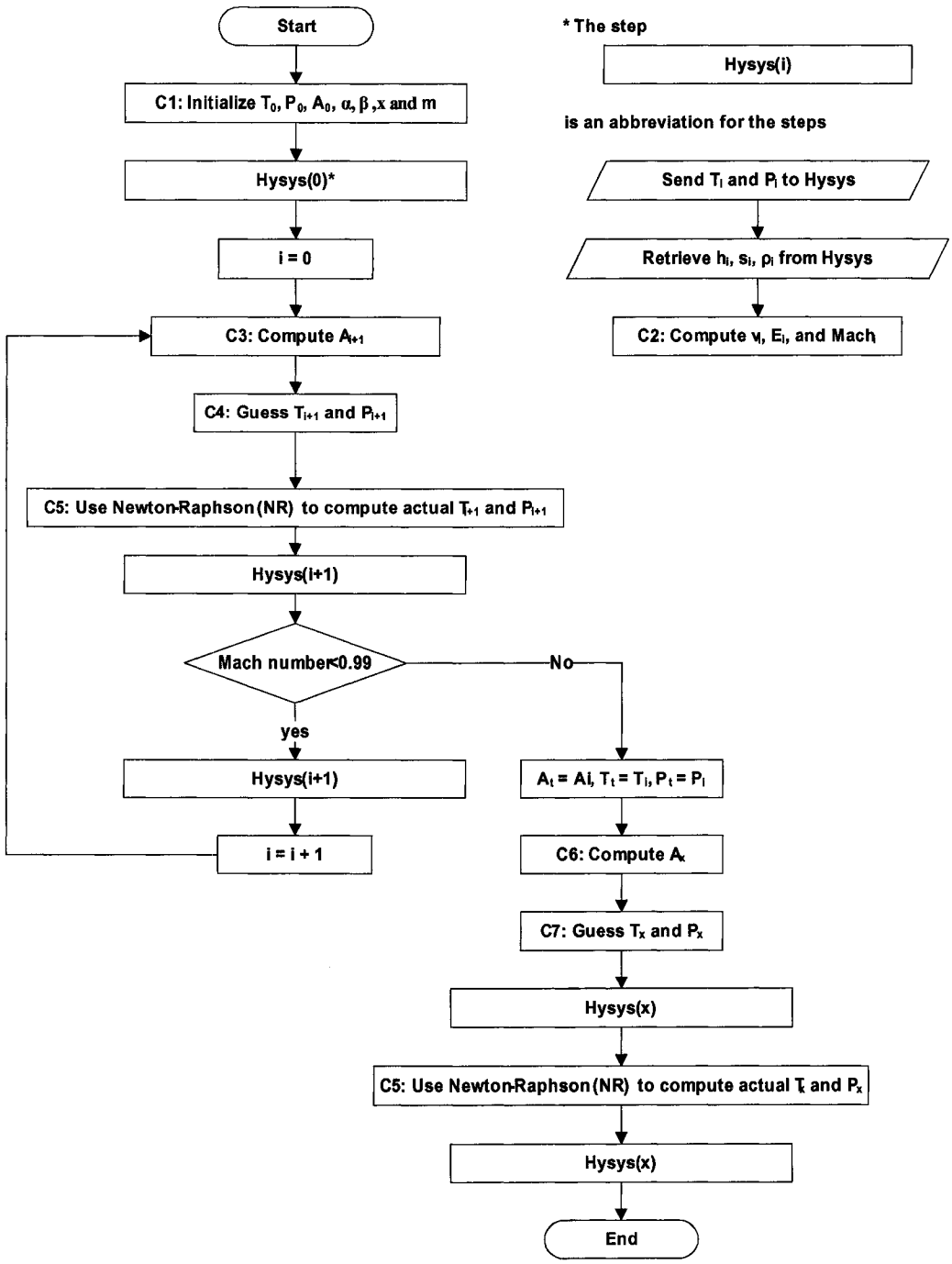

Figure 3.2: A flow chart for designing a nozzle

In this flowchart, Step C1 indicates that the program requires the user for the input of inlet flow conditions and the fixed parameters in the nozzle geometry. These parameters are inlet temperature, pressure, flow rate, inlet cross section area and the half convergence and divergence angles, and the length increments. The flow inlet conditions are given to the HYSYS simulator and by retrieving the density, enthalpy and entropy form HYSYS and using the continuity equation, flow velocity can be found as indicated in Step C2. Also in this step the speed of sound and Mach number are computed, and the set of the necessary equations to use in Newton-Raphson method will be formed. These set of equations are Equations 3.18 and 3.19 for the isentropic flow and Equations 3.20 and 3.21 for considering the presence of friction. To form and solve the friction equation kinematics' viscosity is retrieved from HYSYS, too. In Step C3, A_{i+1} is found having A_i as the previous cross section area (i is the incremental index). In this study, it is assumed that the nozzle cross section area changes linearly with length. Figure 3.3 shows the schematic diagram of a typical Laval nozzle where α and β are the convergence and divergence half angles respectively.

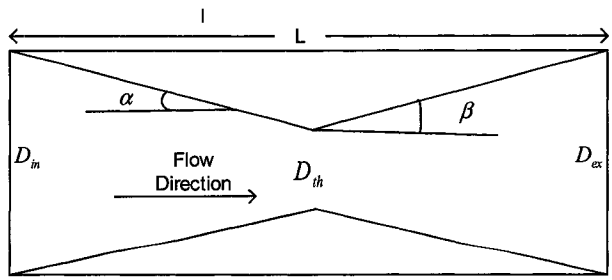

Figure3. 3: Schematic diagram of the supersonic nozzle

The nozzle is divided to smaller increments of length "x" and the flow properties at each incremental cross section area along the nozzle are calculated. In the assumed nozzle, the diameter at each increment will change with the following trend (Equation 3.18) in the converging part considering D_{in} as D_1 at the beginning.

$$A_{i+1} = \pi(D_i - 2x\tan\alpha)^2 / 4 \tag{3.18}$$

Step C4 asks the user for an initial guess for pressure and temperature to be used in the Newton-Raphson (NR) method. This initial guess is arbitrary; however, there might be an initial guess with which Newton-Raphson cannot converge. Using Newton-Raphson to calculate the actual pressure and temperature is done in Step C5. This process continues until the Mach number is greater than 0.99, which is really close to unity. This last cross section area will be the throat of the nozzle. As the total length and the throat of the nozzle are known, the converging (L_c) and diverging (L_d) lengths can be calculated. As shown in Step C6, the nozzle exit cross section area (A_x) will be found using Equation 3.19 and the throat diameter (D_{th}) and the half divergence angle of the nozzle.

$$A_{ex} = \pi(D_{th} + 2*(L\_d)\tan\beta)^2 / 4 \tag{3.19}$$

Knowing the exit cross section area, pressure and temperature and other flow properties can be known at the nozzle exit.

3.4 Rating of the Nozzle

In some situations the nozzle geometry is completely defined and the aim is to find the maximum possible flow rate and/or pressure and temperature distributions along the nozzle. If there is not enough flow rate in the system the overall pressure drop will be low, but at the same time the flow is not expanded to the sonic velocity and it will be subsonic everywhere in the nozzle. The flow in the system can be increased until the maximum flow rate can be found considering the sonic velocity and choked flow exist in the nozzle throat. Figure 3.4 illustrates the flow chart of rating a nozzle. As the first step (C1) to rate the nozzle, the user is asked for the initial inlet conditions such as pressure, temperature, the flow rate, and the complete nozzle geometry including the inlet, throat and outlet cross section areas. The necessary equations for the Newton-Raphson method will be formed in Step C2 by retrieving the enthalpy, entropy, density, and kinematics viscosity and by finding the velocity. In Step C3 an initial guess for pressure and temperature in the throat is made. The Newton-Raphson method is used to predict the actual pressure and temperature at the throat. If this method converges and the actual properties are found in the throat, Mach number at the throat will be computed and if the flow is choked (Mach number>0.99), the same procedure will be repeated (Steps C5 and C6) to find the exit pressure and temperature. If Mach number at the throat is less than 0.99, the flow rate should be adjusted and the flow capacity is higher. In case the Newton-Raphson method does not converge to find the pressure and temperature in Step C4, the flow rate is more than the maximum possible flow rate and it is needed to be

reduced. By dividing the converging and diverging length to smaller increments (defined as *dL_c* and *dL_d*), pressure and temperature distribution along the nozzle can be found. To find the properties distribution in the nozzle, a parameter for a diverging length increment (*dL_d*) is defined and the cross section areas are computed using Equation 3.20.

$$A_{i+1} = \pi(D_i + 2*(dL\_d)\tan\beta)^2 / 4 \qquad (3.20)$$

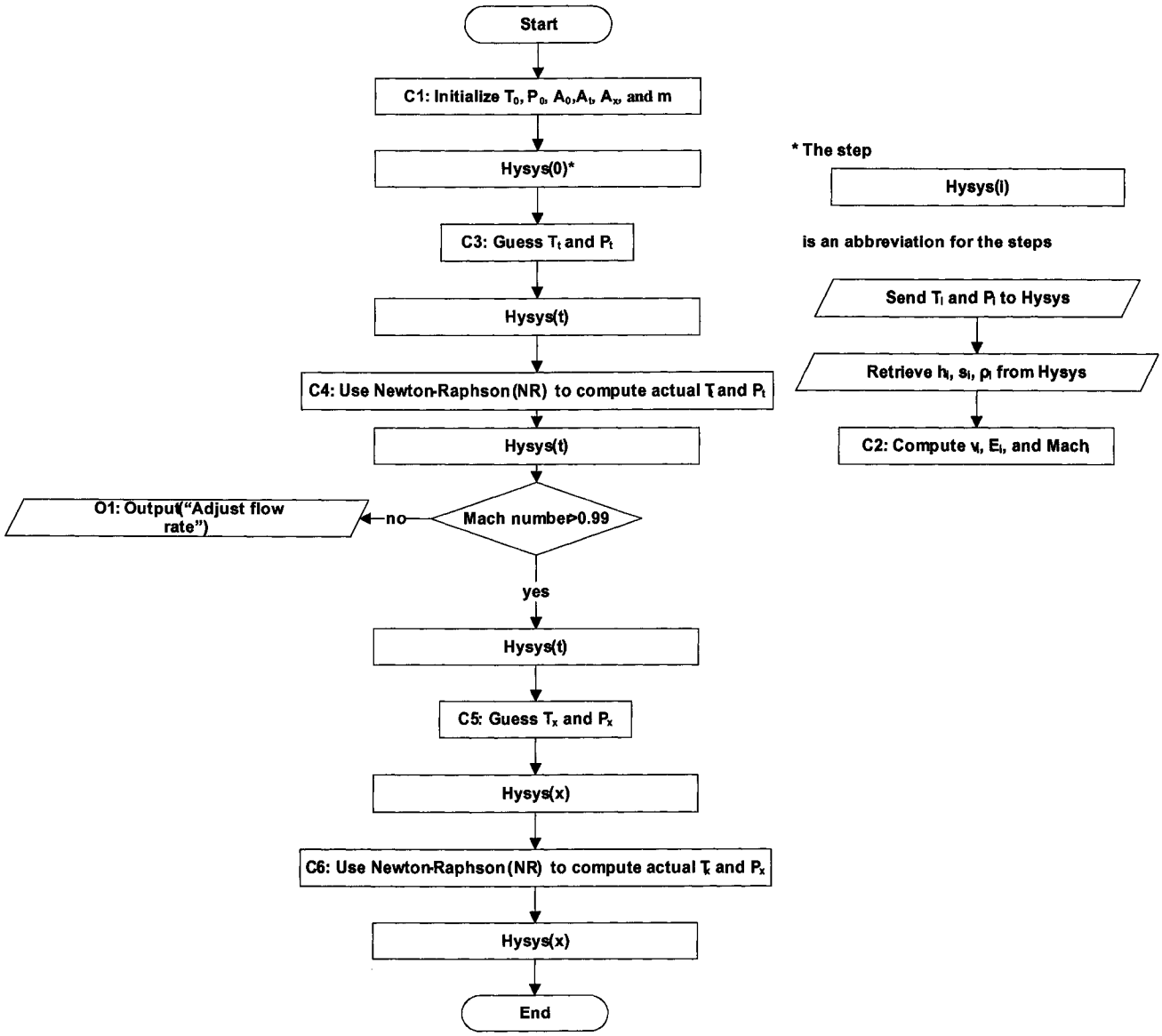

Figure 3.4: Flow chart for rating a nozzle

3.5 Shockwave prediction

After the nozzle is either designed or rated, it is time to find the properties such as pressure and temperature properties and predict the shockwave location (if happening). The flow expands as the nozzle converges and the flow pressure and temperature will be predicted using the Newton-Raphson method. The other properties such as density, velocity, and Mach number will be computed using the pressure and temperature. By reducing the pressure and temperature, the water in the flow starts condensing and the remaining water in the vapour phase is retrieved from the HYSYS. After the throat, depending on the backpressure of the nozzle, the pressure might recover without any further expansion or it might expand further down and become supersonic. Therefore, more liquid will be separated in the liquid phase. If the flow is supersonic in the diverging part of the nozzle, depending on the backpressure a shockwave may occur. The shockwave might happen inside or outside of the diverging part of the nozzle.

In this process a few shock locations were assumed at different lengths form the nozzle throat, in the diverging part of the nozzle. Since the pressure and temperature along the nozzle before the shock is predicted at each cross section area, the upstream properties of the shockwave are known. The condensed liquids should be separated before the shock. This process was simulated in HYSYS by using a separator (3.5). A vapour stream from the top of the separator enters the diverging part of the nozzle after the shock. A set of flow properties upstream of the shock are found. The flow properties

in the rest of the nozzle are found with respect to the shock's downstream properties. Finally the exit properties, including the pressure recovery percentage are predicted as the exit nozzle cross section area is already known.

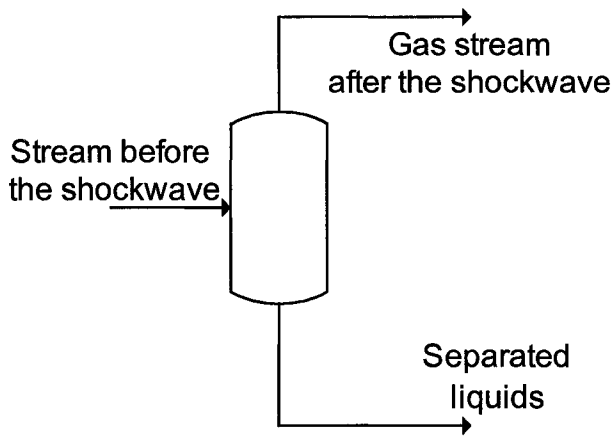

Figure 3.5: Process simulation to separate the condensed liquid.

If the selective water removal is required the pressure and temperature before the shock need to be kept above the cricondenbar and cricondentherm (Karimi and Abedinzadegan Abdi, 2006). There are several possibilities to keep the pressure and temperature such that the fluid remains in a single phase. The stream can be compressed to pressures well above critical pressure so the fluid remains in supercritical conditions all the way through the nozzle. The combination of high pressure with high temperature is another method of keeping the stream in a single phase. In a number of conditions of pressure and temperature (especially high pressures), the pressure recovery percentage

can be chosen in order to predict the shockwave before hydrocarbon condensation happens while near to complete water removal is achieved. In lower pressure conditions, selective water removal can still be achieved but a higher pressure-recovery will result in less expansion in the stream and a reduction in the water removal efficiency.

CHAPTER 4: ANALYSIS AND RESULTS

4.1 MODEL VALIDATION

The proposed model to simulate the flow behaviour in the supersonic nozzles was validated by the computational fluid dynamics (CFD) modeling using commercial CFD software (Fluent). Unlike HYSYS, Fluent is limited to a few EOS and can only use a pure gas as the working fluid rather than a gas mixture. Therefore, in the CFD modelling, pure methane was considered as the working fluid and the modified Benedict Webb Rubin (MBWR) used as the equation of state. In this equation of state, pressure is an explicit function of temperature and density as shown in Equation 4.1:

$$P = \rho RT + Y(\rho, T) \tag{4.1}$$

Where function Y includes 32 terms and 33 adjustable constants.

The nozzle geometry and other nozzle's parameters are shown in Table 4.1. The nozzle has a rectangular cross section area and the inlet and outlet cross section areas are 0.04 and 0.03 (m^2), respectively.

Table 4.1: Nozzle geometry for validation with Fluent

Nozzle inlet diameter (m)	0.0400
Nozzle throat diameter (m)	0.0163
Nozzle outlet diameter (m)	0.0300
Nozzle converging length (m)	0.0527
Nozzle diverging length (m)	0.1473
Nozzle total length (m)	0.2000

To predict the flow behaviour in the supersonic nozzle with the proposed model

in this thesis, pressure, temperature and the flow rate should be known as the inlet conditions. However, in CFD simulation, the inlet pressure and temperature are sufficient to predict the flow behaviour in the nozzle and the flow rate will be computed based on the inlet conditions. Fluent uses a rather complex k-e turbulent model and solves the governing partial differential equations using finite volume approach to predict the flow field behaviour. The proposed model in this thesis uses the simplified one-dimensional conservation laws and other related thermodynamic relations discussed before in Chapter 3 to predict the variation of various parameters along the nozzle. Table 4.2 lists the inlet pressure and temperature. For the model used in this work, the inlet flow rate is predefined at 67,330 kmole/h (300 kg/s) and the predicted flow rate with CFD modelling is the same.

Table 4.2: Nozzle inlet flow conditions for validation

Inlet temperature(°C)	18.5
Inlet pressure (kPa)	9,250

The flow behaviour in the absence and presence of friction is predicted in both models. The results of this comparison with 75.67% inlet pressure recovery (backpressure of 7 MPa) are shown in Figures 4.1 to 4.5.

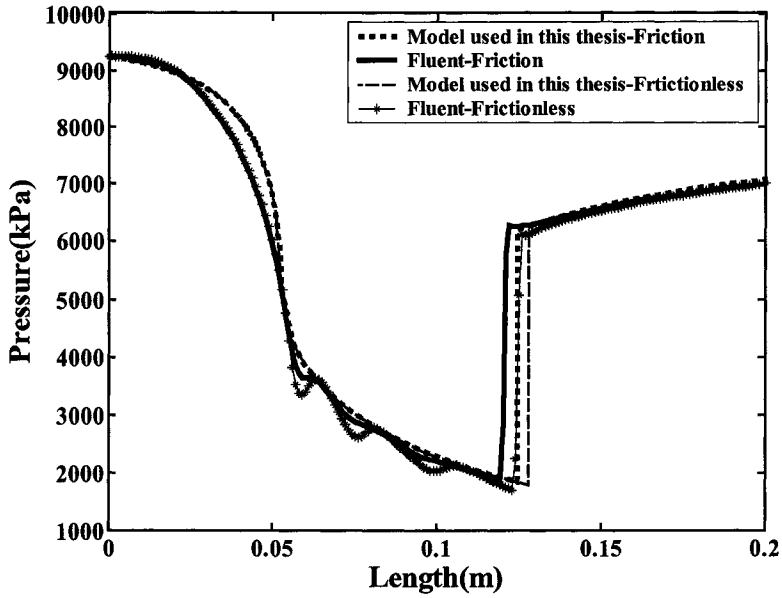

Figure 4.1: Pressure distributions and shockwave locations along the nozzle with 75.67% recovery of inlet pressure in the supersonic-CFD comparison study

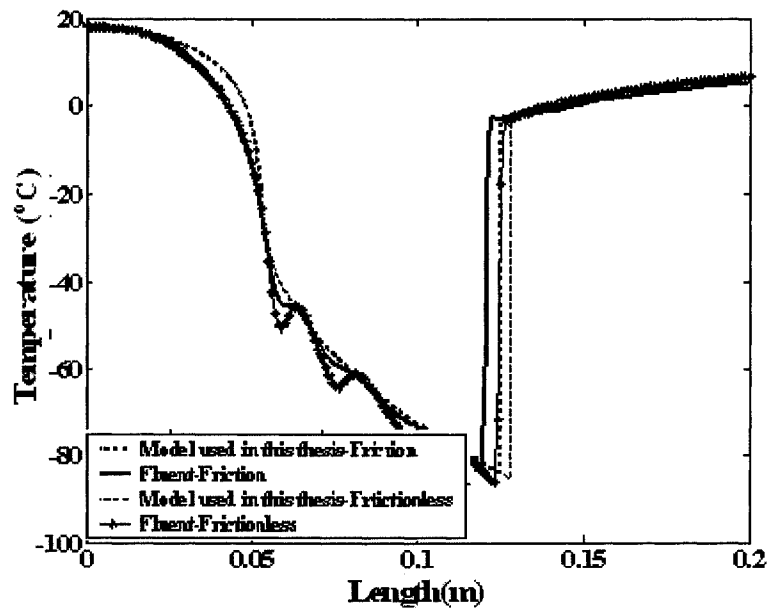

Figure 4.2: Temperature distributions and shock locations along the nozzle with 75.67% recovery of pressure inlet in the supersonic-CFD comparison study

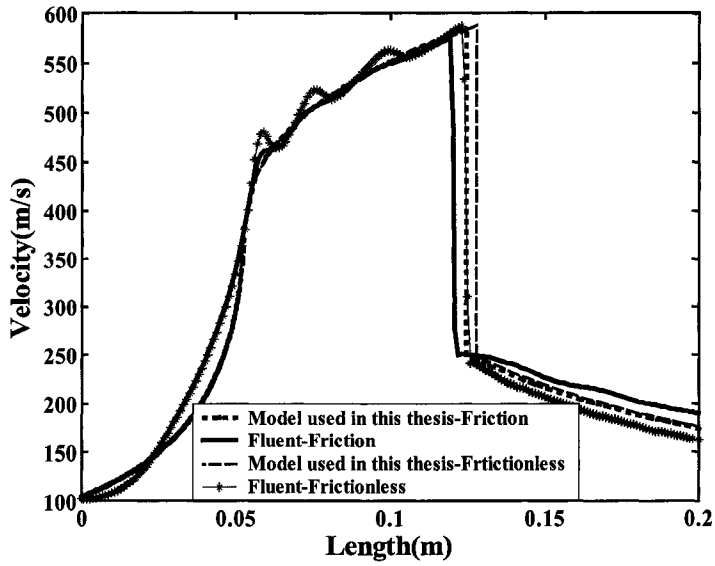

Figure 4.3: Velocity distributions and shock locations along the nozzle with 75.67% recovery of pressure inlet in the supersonic-CFD comparison study

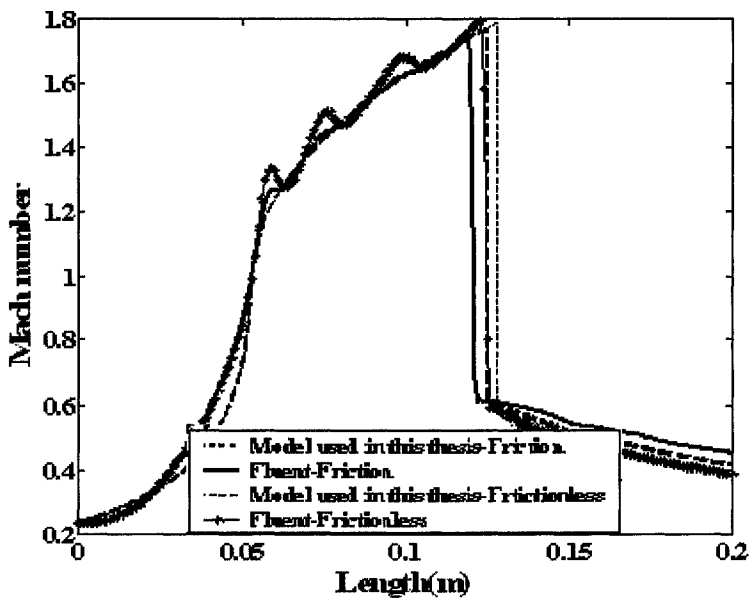

Figure 4.4: Mach number distributions and shock locations along the nozzle with 75.67% recovery of pressure inlet in the supersonic-CFD comparison study

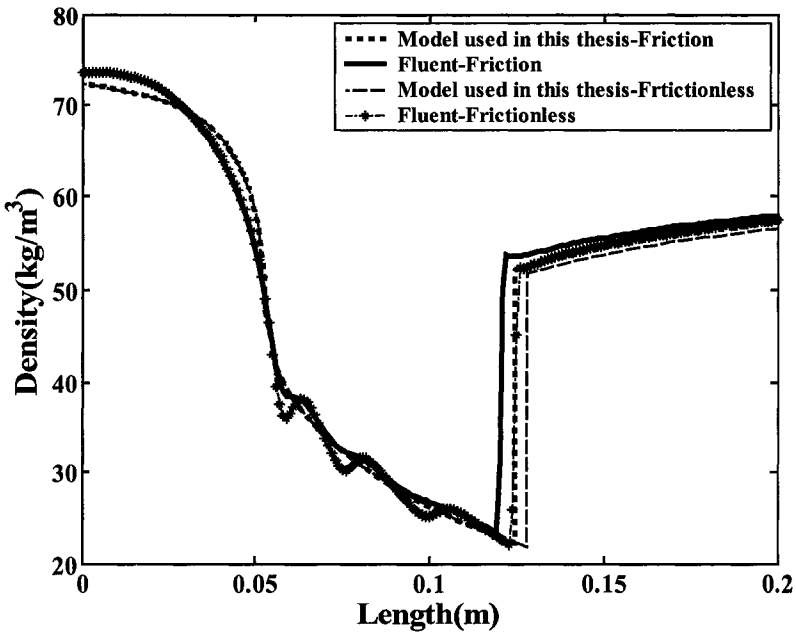

Figure 4.5: Density distributions and shock locations along the nozzle with 75.67% recovery of pressure inlet in the supersonic-CFD comparison study

Both simulations showed that the flow behaviour along the nozzle is not significantly affected by the presence of friction. The friction however changes the location of shockwave when it happens inside the nozzle. The shockwave location in the frictionless flow is ahead of the frictional flow and towards the nozzle exit. Table 4.3 shows the shock locations in both simulations, in the cases where friction is present, and in the frictionless case as a percentage of the total length.

Table 4.3: Shock location predicted with the two simulators (% of total length)

	Frictionless	**Friction**	**% Deviation**
CFD modeling	61.5	59.5	3.25
Model used in this thesis	64	62.25	2.73

The flow behaviour predicted by the proposed method for supersonic separator agrees extremely well with the behaviour predicted by a complex computational modelling software (Fluent), giving rise to the accuracy of computational modelling and analyses preformed in this thesis. We could not claim that the result would also agree well with the actual nozzle performance until experimental tests are conducted. Such tests are beyond the scope of the current research work.

4.2 Variables effects

A dry gas (a stream that does not contain water) with the composition shown in Table 4.4 is used in the simulation. It was assumed that the flow field is compressible, steady state, and one-dimensional.

Table 4.4: Dry gas composition for variable-effects studies

Gas Components	Mole fractions
Methane	0.95
Ethane	0.04
Propane	0.01

The natural gas water content depends on the stream conditions and the equation of state used. The dry gas stream was saturated with water in the HYSYS simulator to represent produced gas conditions. The gas is saturated in the HYSYS simulation using the appropriate equation of state assuming that natural gas is a real gas. In this simulation, the Peng-Robinson equation was used as the thermodynamic model to saturate the stream with water. In this process, a dry gas stream is mixed with free water

in a mixer, until the stream is saturated with water. Saturated gas is separated from free water in a separator as the vapour outlet and is used as the working fluid for the supersonic nozzle. The saturation results from HYSYS were compared with the data from the McKetta charts (GPSA Databook,1998) and the descripency between the two methods were less than ±3 .

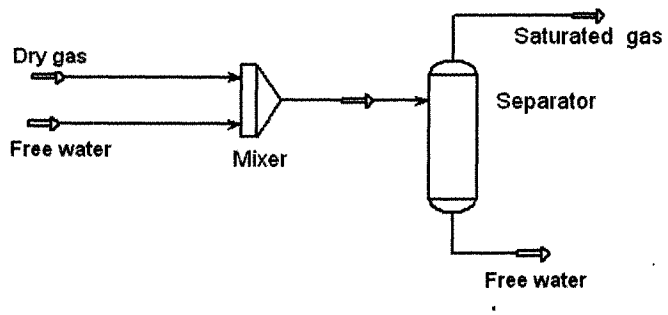

Figure4.6: Dry gas saturating in HYSYS simulator

In this study a dry stream with the inlet condition shown in Table 4.5 is defined as the base stream for all the simulations. This dry stream, after saturation, is called *"Test Stream"* in this thesis. Gas saturation will slightly change the stream temperature and flow rate. The inlet condition of the dry gas stream and the *"Test Stream"* are shown in Table 4.5. After the gas is saturated with water, the gas composition is changed. Table 4.6 shows the *"Test Stream"* composition.

Table 4.5: Gas inlet condition

Stream Parameters	Dry gas	Saturated gas
Temperature (°C)	20.00	19.85
Pressure (MPa)	30	30
Molar flow Rate (kmol/h)	5,000	5,001.14

Table 4.6: *"Test Stream"* gas composition

Gas Components	Mole fractions
Methane	0.94970
Ethane	0.39990
Propane	0.09997
Water	0.00023

"Test Stream" behaviour in the supersonic nozzle such as properties distribution along the nozzle, shockwave location, and water removal efficiency are studied as functions of different variables such as the nozzle length, equation of state, pressure, temperature and flow rate and backpressure in the nozzle.

To design a supersonic nozzle in this condition, the nozzle inlet diameter, and the convergence and divergence half angles are fixed as shown in Table 4.7. These parameters are chosen arbitrarily.

Table 4.7: Fixed parameters used in the study of variable effects

Nozzle inlet diameter (m)	0.04
Convergence half angle	6.85°
Divergence half angle	3.00°

In this design, the total length of the nozzle is also fixed. The nozzle length is chosen arbitrarily but within a range found using the following procedure. For each flow inlet condition and the nozzle geometry, there is a unique cross section area in which the

flow is choked (sonic velocity is reached). Therefore, the converging part in each nozzle is constant but the diverging part varies with the variation in the nozzle total length. The lower bound for the nozzle length is therefore where the nozzle turns to a mere converging nozzle and the total length is the distance from the nozzle inlet to the throat. The upper bound of the length is the longest length for which, at any flow rate smaller than the design flow rate, the exit pressure should not exceed the inlet pressure.

For the "*Test Stream*", the nozzle throat was designed and the converging part of the nozzle is found to be 0.082 *m*. A stream with the pressure and temperature equal to *"Test Stream"* but with the molar flow rate lower than the design flow rate of 5,000 *kmole/h* was introduced to nozzles with different lengths starting with the converging nozzle length. This molar flow rate is intentionally chosen very small to produce the lowest possible pressure drop in the longest possible nozzle where the exit pressure will be really close to inlet pressure. To simulate this situation, the nozzle length is increased gradually and the subsonic nozzle pressure is found for each condition. This process is continued until the longest nozzle length is found. The longest possible nozzle is when a tiny increase in the length will result in a subsonic nozzle pressure greater than the inlet pressure. The longest possible nozzle for the *"Test Stream"* is found to be 0.27 *m*. Therefore, the chosen nozzle length should be between 0.082 and 0.27 *m*. A short nozzle causes the high-pressure drop and long nozzle will result in a bigger nozzle. For this simulation, a nozzle of 0.12 *m* long is chosen.

A nozzle can be designed using the fixed parameters in the nozzle geometry and a

gas stream with known inlet pressure, temperature, and flow rate as a working fluid. Table 4.8 indicates the designed nozzle specifications considering the fixed length of 0.12 *m* for the nozzle.

Table 4.8: Nozzle specifications for *"Test Stream"*

Nozzle throat diameter(m)	0.021
Nozzle convergence length (m)	0.082
Nozzle divergence length(m)	0.038
Nozzle outlet diameter(m)	0.024

As the system of governing equations is solved, properties distribution along the nozzle will be known. For each designed nozzle, unique *"recovery properties"* and "*design properties*" exist. Different shockwave locations can be predicted by choosing different backpressures. Higher backpressure results in a higher pressure recovery. However, backpressure can not be higher than the nozzle *"recovery pressure"*. Higher pressure recovery causes the shockwave to happen earlier in the nozzle. It can therefore be chosen such that the stream conditions can be kept in the dense gas phase in the phase envelope and consequently a selective water removal can be achieved.

4.2.1 Influence of Equation of State

The *"Test Stream"* behaviour as a real gas, which follows the peng-Robinson equation of state, was compared with the results of simulation assuming that the stream is an ideal gas. In order to predict the property distributions along the nozzle for the ideal gas case, the stream properties such as molecular weight and k (C_p/C_v) for the ideal gas should be known. These properties can be extracted from standard physical properties

handbooks such as GPSA Data book or from the HYSYS physical properties library.

To compare the behaviour under real and ideal gas assumptions, two approaches were used:

4.2.1.1 Designing a new nozzle using ideal gas

As the first approach, a nozzle was designed using ideal gas law for the same stream conditions. Assuming a fixed nozzle length, the nozzle throat location was found considering the choked flow at the nozzle throat. Knowing the nozzle converging and diverging lengths, the outlet diameter will also be known (See Table 4.9).

Table 4.9: Designed nozzle specifications for an ideal gas

Nozzle throat diameter(m)	0.024
Nozzle converging length (m)	0.067
Nozzle diverging length(m)	0.054
Nozzle outlet diameter(m)	0.030

Figure 4.7 shows the geometry of the designed nozzle for the real gas and ideal gas assumptions. The nozzles geometry indicates that for the same inlet flow rate, the nozzle throat under ideal gas conditions is 18.34% larger than real gas which results in a 22% bigger outlet diameter. The length at which the ideal gas becomes choked is 18.8% shorter than the length for the real gas.

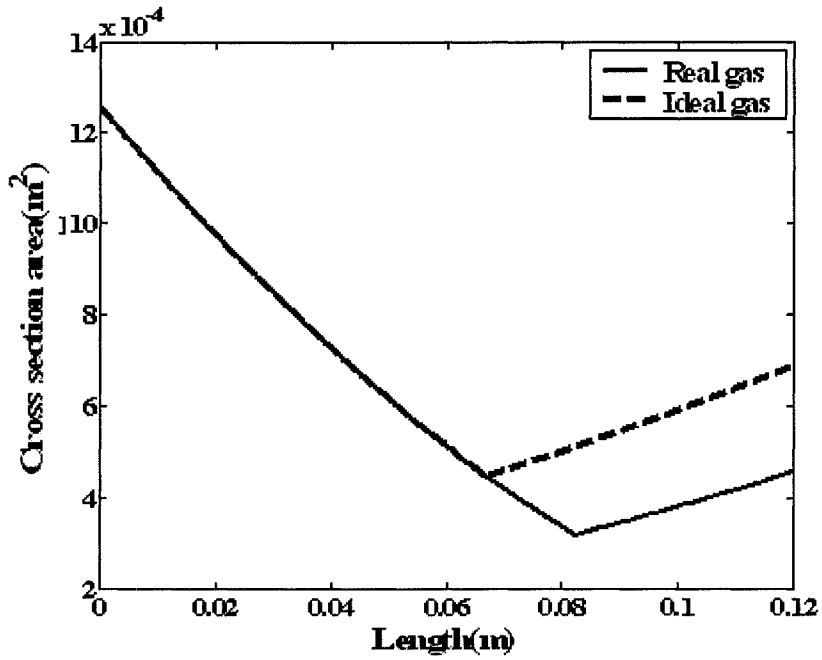

Figure 4.7: The geometry of the separated designed nozzle for ideal and real gas assumptions

In Figure 4.8, the nozzle subsonic pressures and nozzle design pressures for the two nozzles are presented and compared. The results show that ideal gas needs a longer nozzle to achieve the same pressure reduction as real gas. For the nozzle with the specified length in this example, the design pressure is 36.73 % and the subsonic pressure is 11.6% lower for the real gas. As a result, the highest possible inlet pressure recovery is 92.3% in an ideal gas situation and 82.7% for real gas.

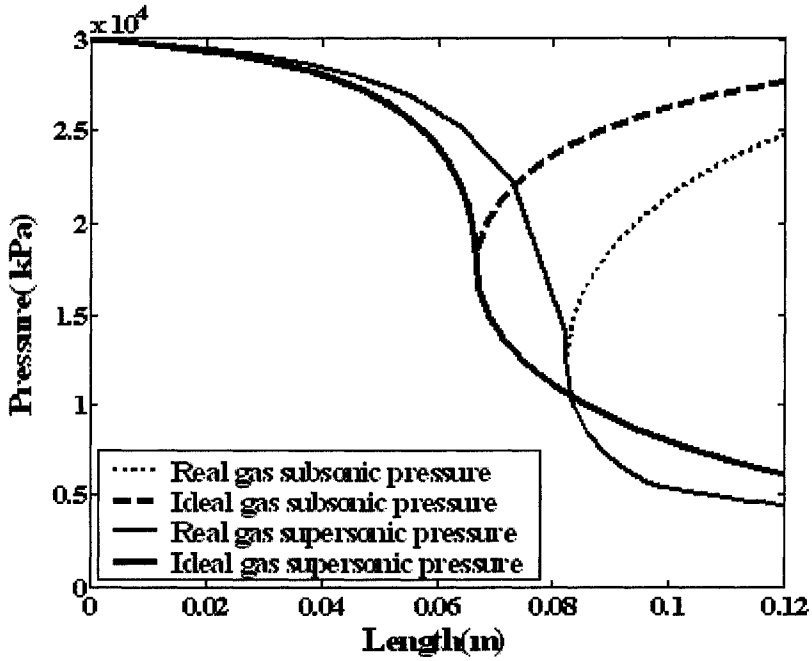

Figure 4.8: Pressure distributions along the separately designed nozzle for ideal and real gas assumptions

To be able to predict the shockwave location in the nozzle to partially recover the inlet pressure, backpressure should be chosen between the nozzle *"recovery pressure"* and *"design pressure"*. Figure 4.9 presents the pressure distribution along the nozzle when a normal shockwave occurs to recover 70% of the inlet pressure (exit pressure of 21 MPa). The shockwave in the real gas nozzle happens at 85% of the nozzle length and in ideal gas, it shifts 12% toward the nozzle exit. In the real gas case, the pressure reduction before the shockwave is 82.42% of the inlet pressure and it reduces to 78.22% of the inlet pressure for the ideal gas case.

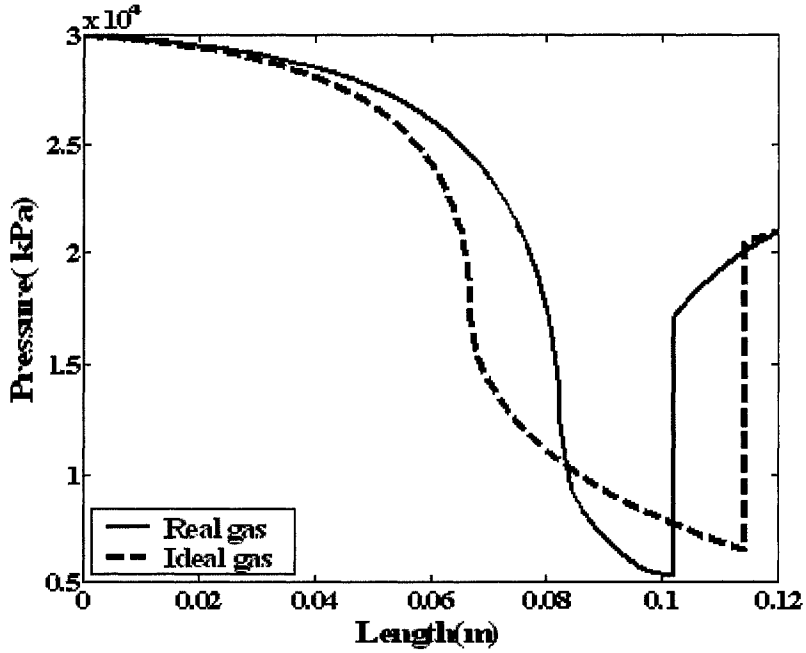

Figure 4.9: Pressure distribution and shockwave location along the designed nozzle for real and ideal gas assumptions with 70% inlet pressure recovery

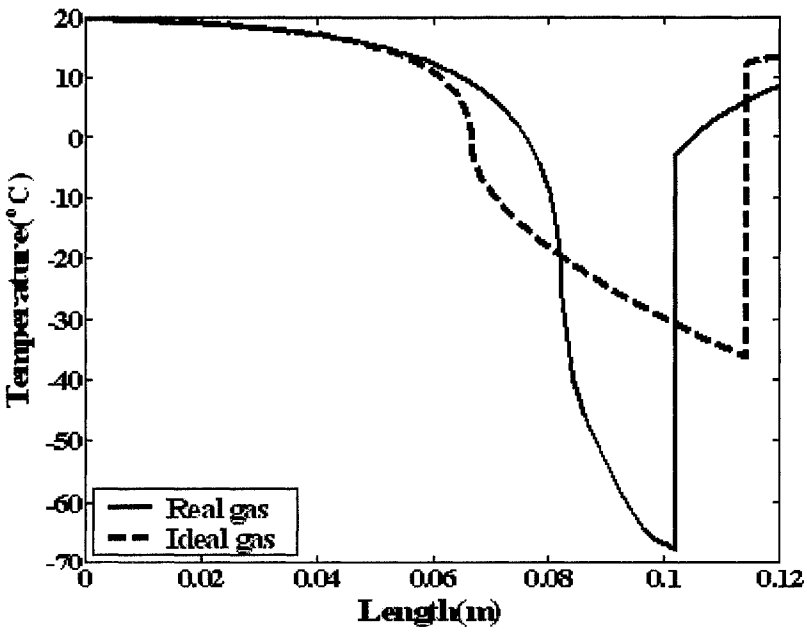

Figure 4.10: Temperature distribution and shockwave location along the designed nozzle for real and ideal gas assumptions with 70% inlet pressure recovery

Figures 4.10 and 4.11 show the temperature and velocity distributions in the designed nozzles under ideal and real gas conditions.

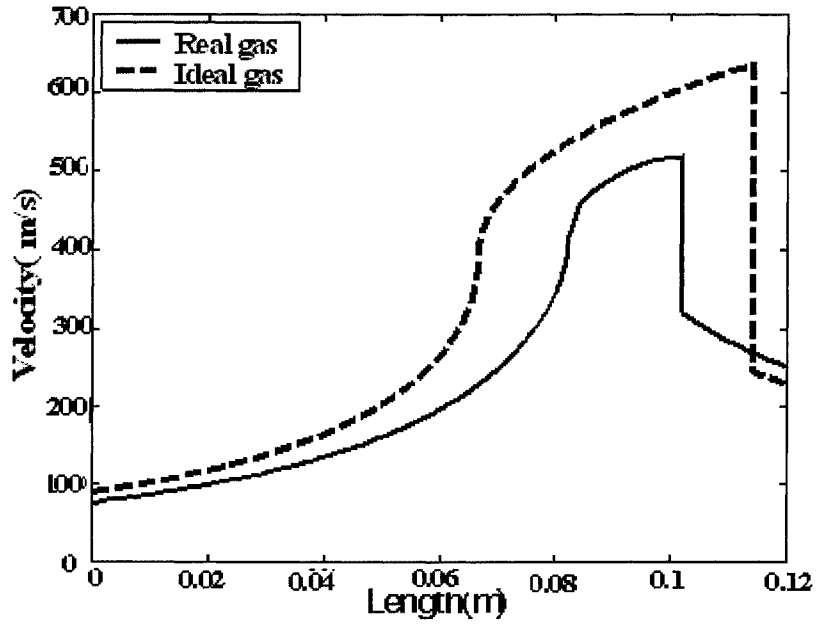

Figure 4.11: Velocity distribution and shockwave location along the designed nozzle for real and ideal gas assumptions with 70% inlet pressure recovery

The ideal gas assumption underestimates the water capacity of natural gas. Figure 4.12 shows water removal performance of the nozzle for a case where a 70 % of the inlet pressure recovery is considered as the design criteria. Both real and ideal gas can predict close to complete water removal, i.e., 99% for real gas and 95% for ideal gas (See Figure 4.12). As the pressure and temperature are lower in the ideal gas case, the only liquid phase will be the aqueous phase as the flow conditions stay within the gas phase region of the phase envelope. For the real gas case, just before the shockwave the

pressure and temperature fall into the two-phase region of the phase envelope and therefore a liquid hydrocarbon phase is formed. In Figure 4.13 , the pressure, temperature distribution along the nozzle as well as the phase diagram related to Peng-Robinson as the equation of state is shown. .

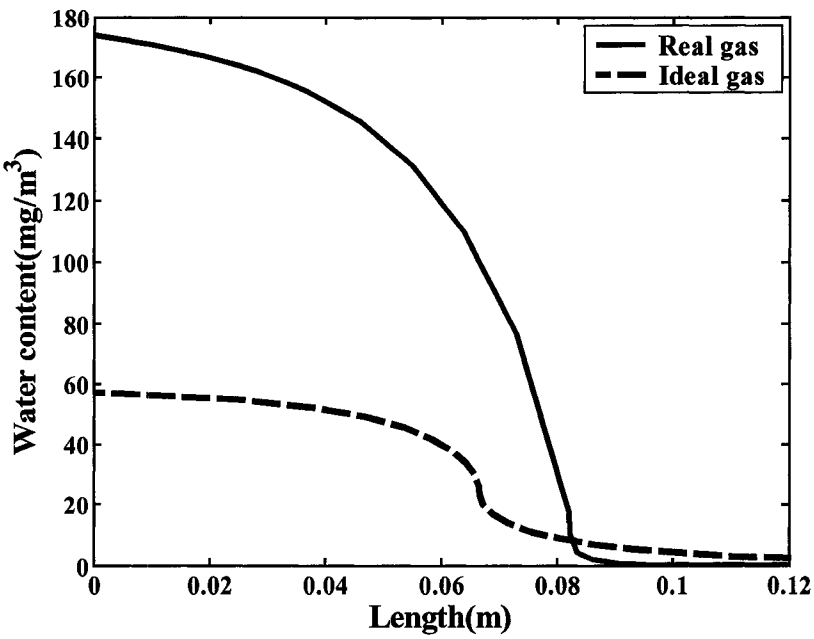

Figure 4.12: Theoretical water removal along the designed nozzle for real and ideal gas assumptions with 70% inlet pressure recovery

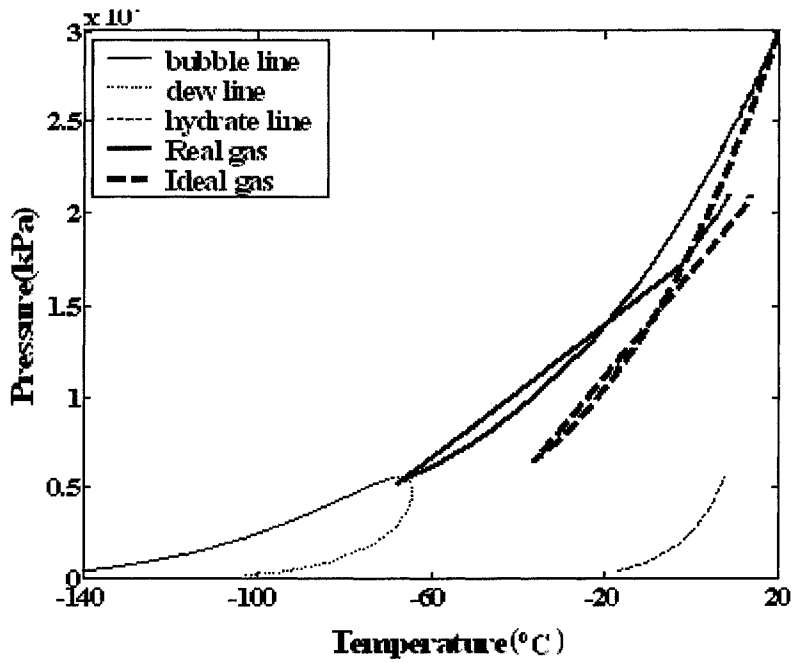

Figure 4.13: Phase envelope and Pressure-Temperature distributions along the designed nozzle for real and ideal gas assumptions with 70% inlet pressure recovery

4.2.1.2 Rating Nozzles Using Ideal Gas Assumption

Since the goal here is to use the same nozzle for both real and ideal gas cases, the nozzle needs to be rated under the two real and ideal gas conditions. Therefore, both real and ideal gas nozzles should have the same geometry. The nozzle flow capacity under ideal gas conditions is less than that of the real gas as the flow rate needs to be reduced to 3,524.7 from 5,001.14 *kmole/h* in order to get the Mach number close to unity at the throat. All the comparisons were made under constant nozzle specifications and inlet flow properties; the flow rate however could not be fixed. Figure 4.14 presents the comparison between the"*recovery pressure*" and the "*design pressure*" in each nozzle.

The ideal gas "*design pressure*" is 50 % and its"*recovery pressure*" is 8% higher than the real gas. Therefore, the inlet pressure can be recovered up to 8 % more in the ideal gas case. The maximum pressure recoveries for real and ideal gas situations are 82.7 and 89.3% of the inlet pressure, respectively.

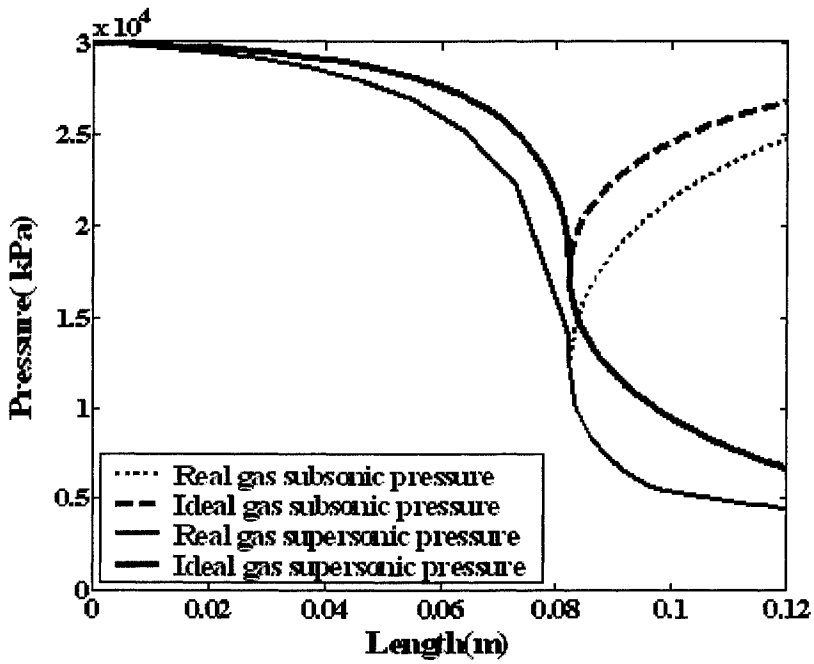

Figure 4.14: Pressure distributions along the rated nozzle for ideal and real gas assumptions

If the backpressure is fixed at 70% recovery of the inlet pressure (21 MPa at the nozzle exit), the shockwave location in the ideal and real gas cases will be different. Shockwave location for ideal gas will be at 97.33% of the total nozzle length while shock occurs at 82.83% of the total length in the real gas conditions. In the real gas case, the

pressure reduction before the shockwave is 82.42% of the inlet pressure and it drops to 76.6% for the ideal gas.

Figures 4.15, 4.16, and 4.17 present the pressure, temperature and velocity distributions along the nozzle for the same inlet pressure recovery (70%) condition.

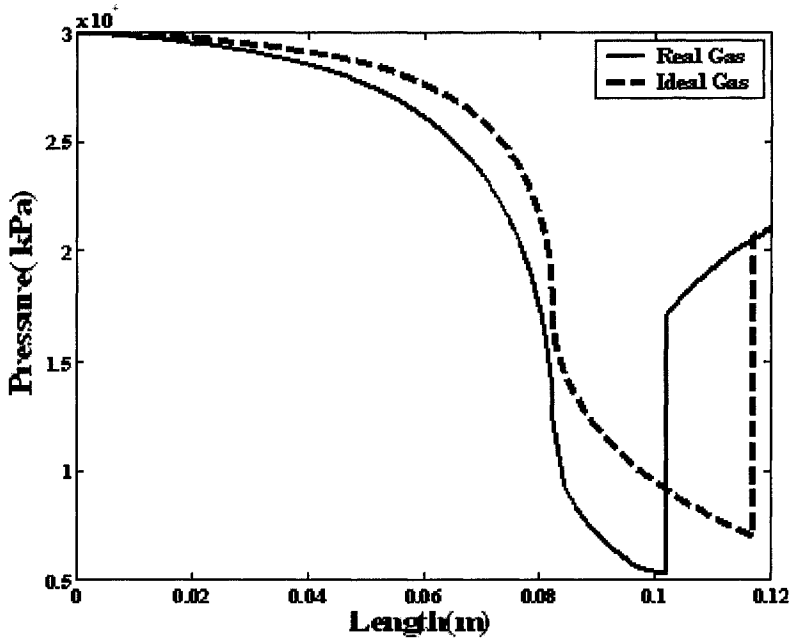

Figure 4.15: Pressure distributions and shockwave location along the rated nozzle for ideal and real gas assumptions with 70% inlet pressure recovery

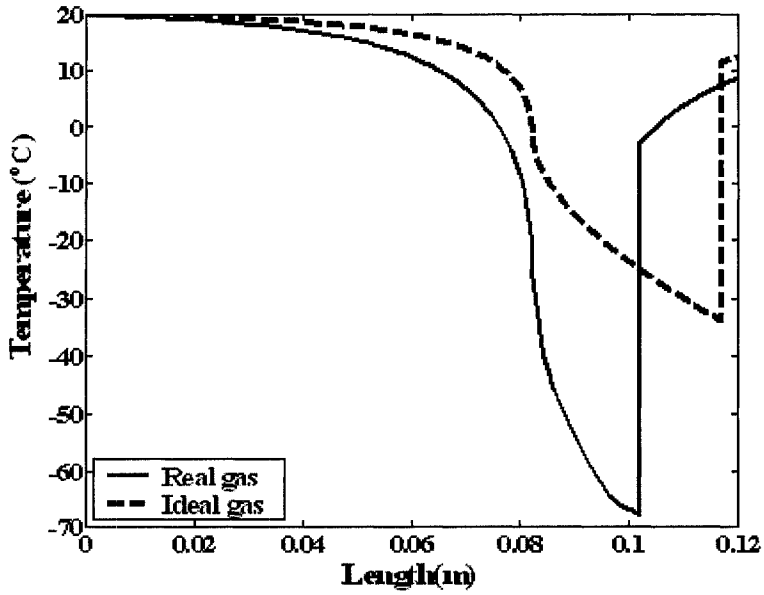

Figure 4.16: Temperature distributions and shockwave location along the rated nozzle for ideal and real gas assumptions with 70% inlet pressure recovery

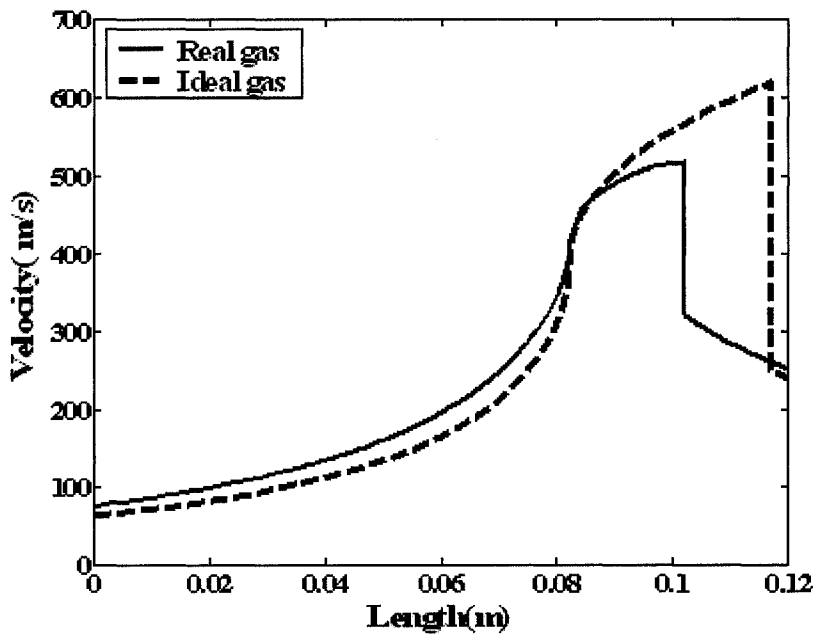

Figure 4.17: Velocity distributions and shock wave location along the rated nozzle for ideal and real gas assumptions with 70% inlet pressure recovery

The above discussions and analyses show the importance of choosing a suitable

equation of state. In a supersonic nozzle the ideal gas assumption, results in significant deviations in calculating the gas properties along the nozzle as well as predicting the nozzle performance when compared to the results obtained when the real gas assumption is made.

4.2.2 Effect Of Inlet Pressure

Four dry gas streams (streams with no water content) with equal temperatures and different pressures are introduced to the nozzle and saturated with water. As mentioned before water saturation slightly changes the temperature and the flow rate. The stream capacity to hold water will decrease by the increase in inlet pressure as shown in Table 4.10. The stream composition after saturation is shown in Table 4.11.

Table 4.10: Inlet streams conditions for inlet-pressure-effect studies

Stream Name	**1**	***Test stream***	**2**	**3**
Temperature(°C)	19.72	19.85	19.86	19.87
Pressure (MPa)	10	30	50	70
Molar flow Rate (kmol/h)	5,001.7	5,001.1	5,0010	5,000.9
Water content (mg/m^3)	264.5	174.1	150.3	109.7

Table 4.11: Streams gas composition (mole fractions) for inlet-pressure-effect studies

Methane	0.950	0.950	0.950	0.950
Ethane	0.040	0.400	0.040	0.040
Propane	0.010	0.100	0.010	0.010
Water	0.000	0.000	0.000	0.000

These streams were introduced to the nozzle designed using the *"Test Stream"* condition. For the streams with pressures above that of the *"Test Stream"* (Streams 3 and 4), the Mach numbers at the throat are lower than unity (0.333 and 0.231, respectively) which means the flow rate is not enough to reach supersonic conditions for the specified nozzle geometry. The Newton-Raphson component of the program diverges and fails to compute the Mach number at the throat for Stream 1. Therefore, either the flow rate should be adjusted in order to choke the flow at the throat or a suitable nozzle for each stream condition should be designed.

4.2.2.1 Designing nozzle for each gas streame in presssure-effect studies

The purpose of this study is to design a nozzle for each of the streams such that the flow becomes choked at the nozzle throat. The flow rate used for all different inlet conditions remains constant in this study. For each stream, the nozzle throat diameter should first be found. The throat distance from the inlet is the converging length of the nozzle and the lower bound for the nozzle total length. The upper bound for the nozzle length is predicted using the previously mentioned procedure (see Section 4.2). As shown in Table 4.12, the converging length of the nozzle increases with the inlet pressure while the throat diameter decreases. The nozzle designed for Stream 1 is a lot shorter than the nozzle for the other streams. A comparison was made between the pressure distributions in the nozzle designed for "*Test Stream*", and Streams 2 and 3 as the nozzle length for Stream 1 is different. Figure 4.18 shows the pressure distributions along the

nozzles designed using these three streams (*"Test Stream"*, Streams 2 and 3) as the working fluids. For this comparison, nozzle total length is considered to be 0.12 *m*. Figure 4.18 also shows the pressure distributions along the nozzle with the total length of 0.06 *m* for Stream1. The nozzle "*recovery pressure*" and "*design pressure*" are obtained in each case. These two pressures define the range of the nozzle exit pressure as a percentage of the inlet pressure. These ranges are shown in Table 4.13.

Table 4.12: Inlet condition of the streams in the pressure effect studies

Stream Name	**1**	***Test Stream***	**2**	**3**
Nozzle throat diameter(m)	0.035	0.020	0.016	0.014
Nozzle convergence length (m)	0.020	0.081	0.099	0.108
Length upper bound (m)	0.066	0.270	0.327	0.355

As shown in Table 4.13, for the same flow rate, a very shorter nozzle is designed for Stream 1 where the pressure is low. As the pressure increases, the nozzle's *recovery pressure* decreases which means that a longer nozzle should be designed to recover the same amount of pressure for streams with lower pressures. For Stream 3 and in a nozzle of 0.12 *m* long, the 70 % inlet pressure recovery never happens; therefore a longer nozzle should be designed.

Table 4.13: Inlet conditions for streams with different pressures

Stream Name	**1**	***Test Stream***	**2**	**3**
Nozzle length (*m*)	0.06	0.12	0.12	0.12
Exit pressure range (% of inlet pressure)	29.61 - 98.10	14.84 - 82.72	10.25 - 77.99	7.45 - 62.8

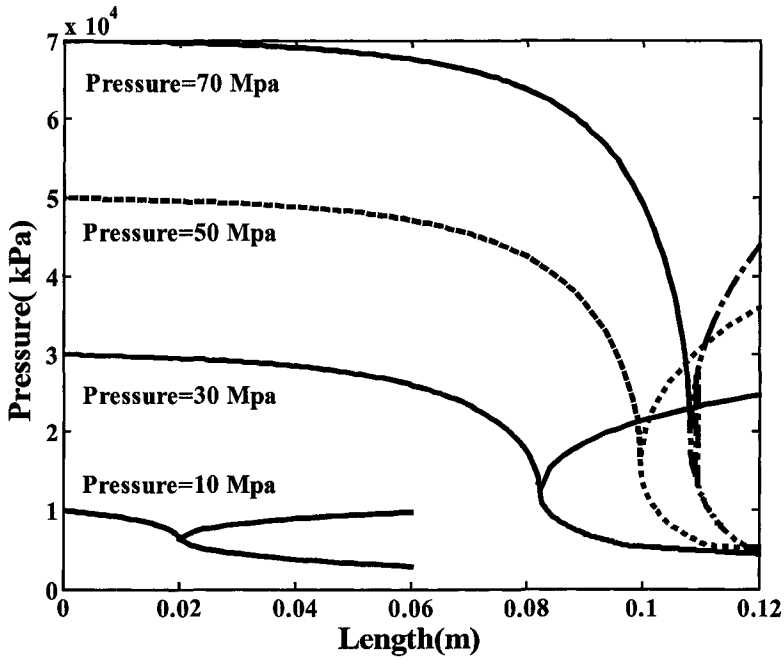

Figure 4.18: Pressure distributions along the designed nozzle for pressure-effect studies

A nozzle of 0.12 *m*, capable of recovering 70% of the inlet pressure could be designed for the *"Test Stream"* and Stream 2. Figures 4.19 to 4.21 show the pressure, temperature, and velocity distributions as well as shockwave locations along a nozzle with a length of 0.12 *m* with 70% inlet pressure recovery for the "*Test Stream*" and Stream 2 .

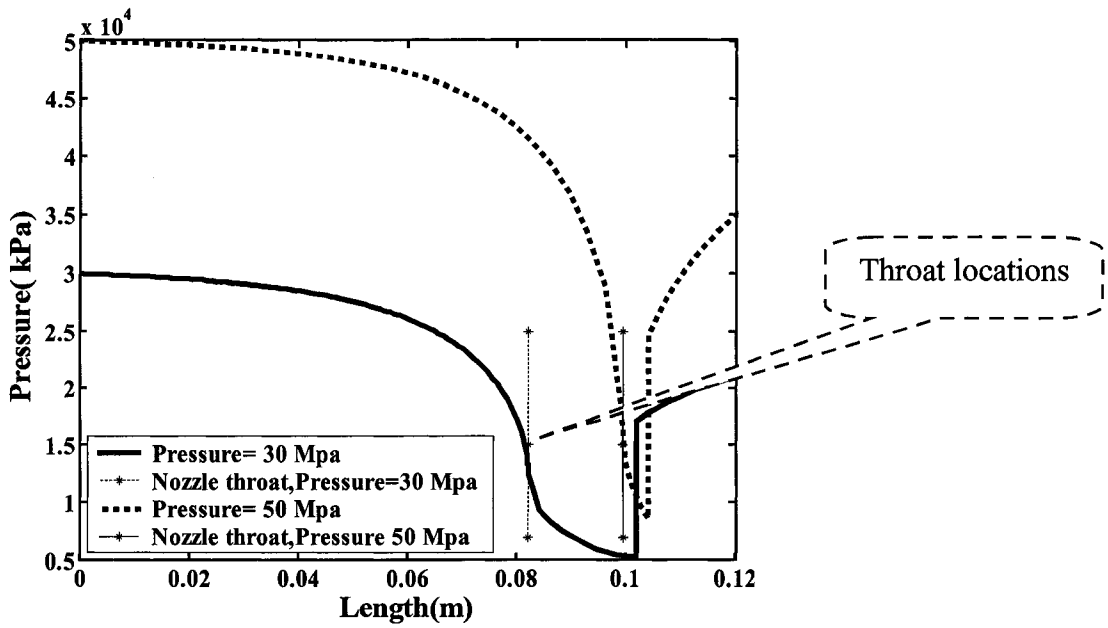

Figure 4.19: Pressure distributions and the shockwave location along the designed nozzle with 70% pressure recovery for pressure-effect studies

The increase in the inlet pressure causes the choked flow to happen later in the nozzle and therefore the throat for "*Test Stream* " is at 68.5 % of the total length and increases to 82.85% and 90% of the total length as the inlet pressure increases from 30 to 70 MPa. As mentioned 70% of the inlet pressure can not be recovered in the nozzle designed for Stream 3 but the shockwave happens inside the diverging part of the nozzle of 0.12 *m* long for the "*Test Stream* " and Stream 2 at 85.85 and 86.69% of the total nozzle length.

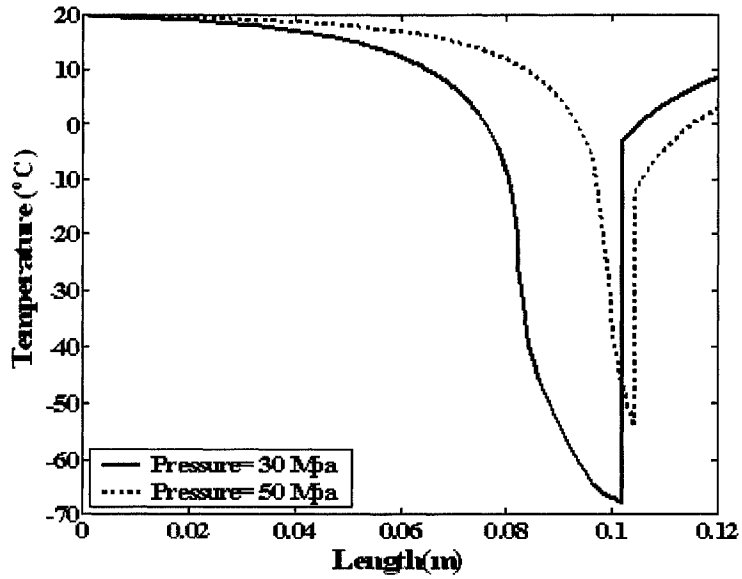

Figure 4.20: Temperature distributions and the shockwave location along the designed nozzle with 70% pressure recovery for pressure-effect studies

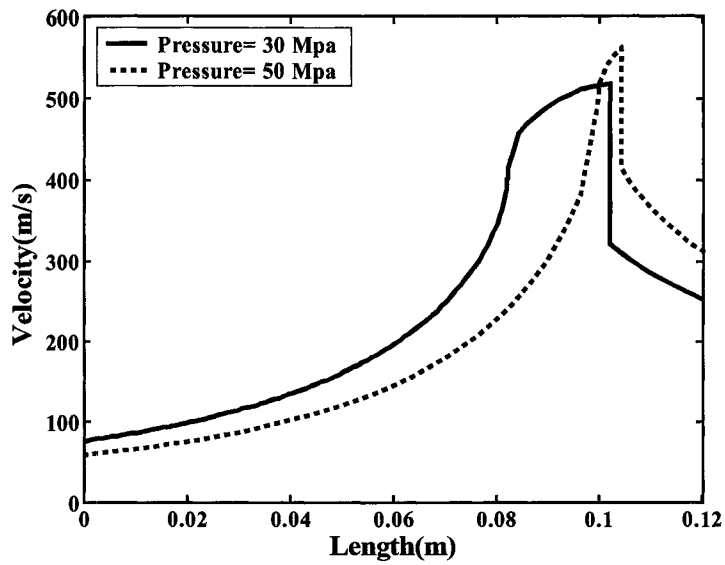

Figure 4.21: Velocity distributions and the shockwave location along the designed nozzle with 70% pressure recovery for pressure-effect studies

Figure 4.22 presents the phase envelope and the pressure-temperature distributions along the designed nozzle with 70% recovery of the inlet pressure. It can be seen that in Stream 2 (with an inlet pressure of 50 MPa), the selective water removal can be achieved as the pressure and temperature are kept above the phase envelope and in the single dense phase.

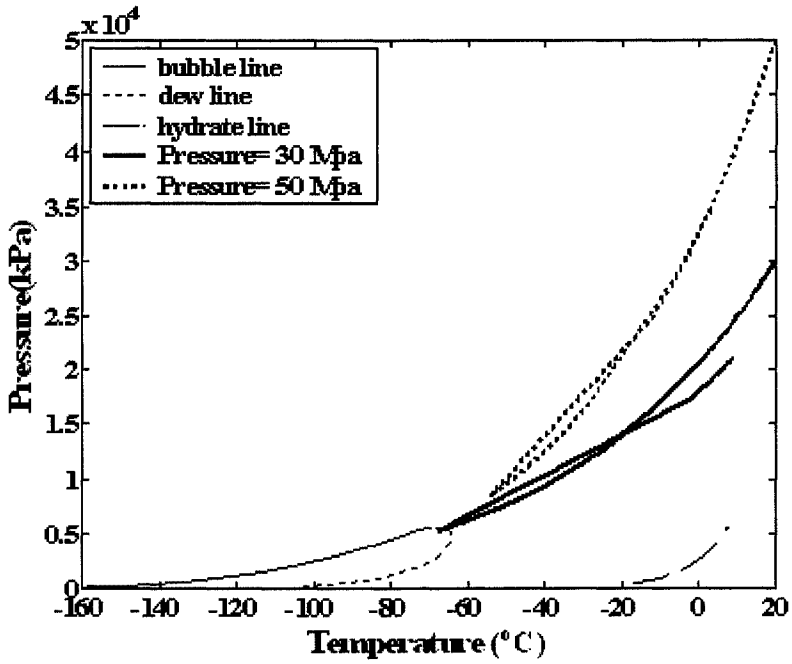

Figure 4.22: Phase envelope and Pressure-Temperature distributions for designed nozzle in pressure-effect studies with 70% inlet pressure recovery

4.2.2.2 RATING NOZZLES FOR EACH GAS STREAM IN PRESSURE- EFFECT STUDIES

Since the gas flow rates are either not enough or more than enough to achieve the sonic conditions at the throat, the inlet flow rates were adjusted for each stream condition. The flow capacity of the nozzle increases with pressure. Depending on the backpressure

of the nozzle, the exit pressure will fall in a range whose lower and upper bounds are given by a percentage of the inlet pressure as shown in Table 4.14. These results are shown in Figure 4.23.

Table 4.14: Adjusted flow rates and exit pressure range for pressure-effect studies

Stream Name	1	*Test Stream*	2	3
Molar flow Rate (kmole/h)	1,421	5.000	8,016	10,544
Exit pressure range (% of inlet pressure)	20.25 - 87.88	14.83 - 82.71	9.42 - 79.75	6.56 - 78.14

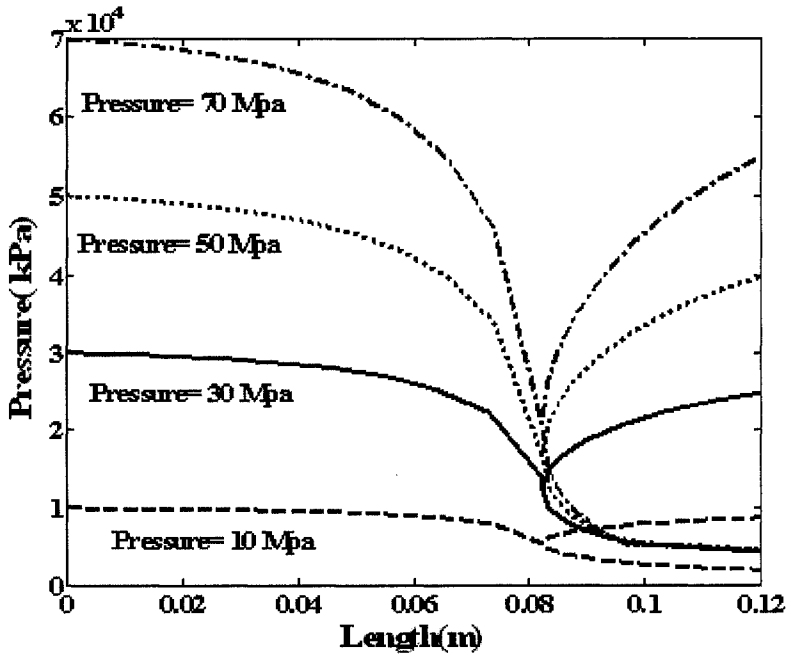

Figure 4.23: Pressure distributions along the rated nozzle for pressure-effect studies

As pressure increases from 10 to 70 MPa, the maximum pressure recovery of the nozzle will be reduced for nearly 10%. A shockwave occurs in the nozzle in all conditions of pressure and temperature, when 70% recovery of the inlet pressure is

desired. As Figure 4.24 shows, the decrease in inlet pressure will shift the shockwave location towards the nozzle exit.

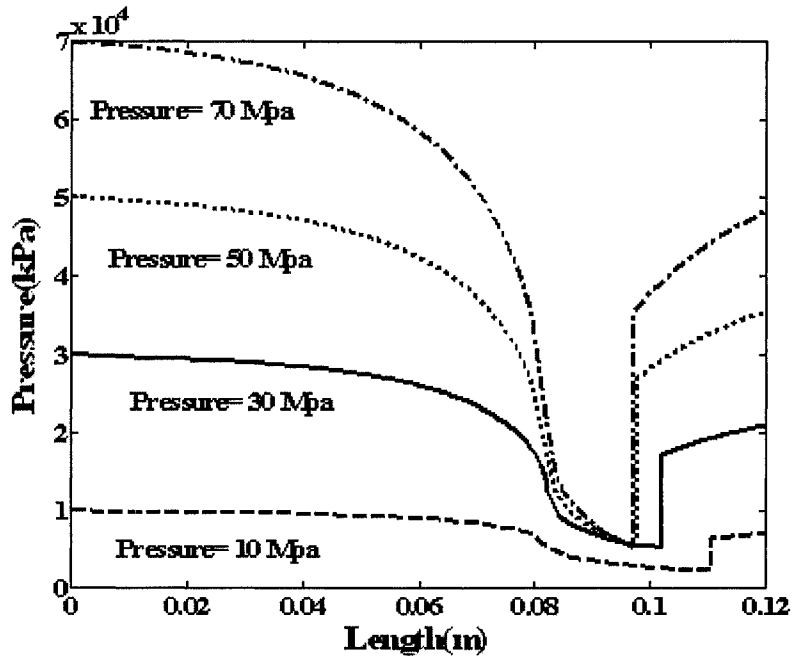

Figure 4.24: Pressure distribution for rated nozzle in pressure-effect studies with 70% inlet pressure recovery

Table 4.15 indicates that as the inlet pressure increases, the pressure along the nozzle will decrease further before the shockwave occurs. Since the location of shockwave is closer to the nozzle exit in lower inlet pressures, it can be concluded that pressure reduction will be steeper in higher pressures. As pressure decreases from 70 to 10 MPa, shockwave will shift 12.29 % towards the nozzle exit. Supersonic nozzles can therefore become shorter as inlet pressure increases and shockwave happens earlier in the nozzle.

Table 4.15: Shockwave location: comparison for pressure-effect studies

Stream Name	1	*Test Stream*	2	3
Pressure reduction (% of inlet pressure)	76.79	82.43	88.92	92.36
Shockwave location (% of total length)	92.25	85.03	81.41	80.92

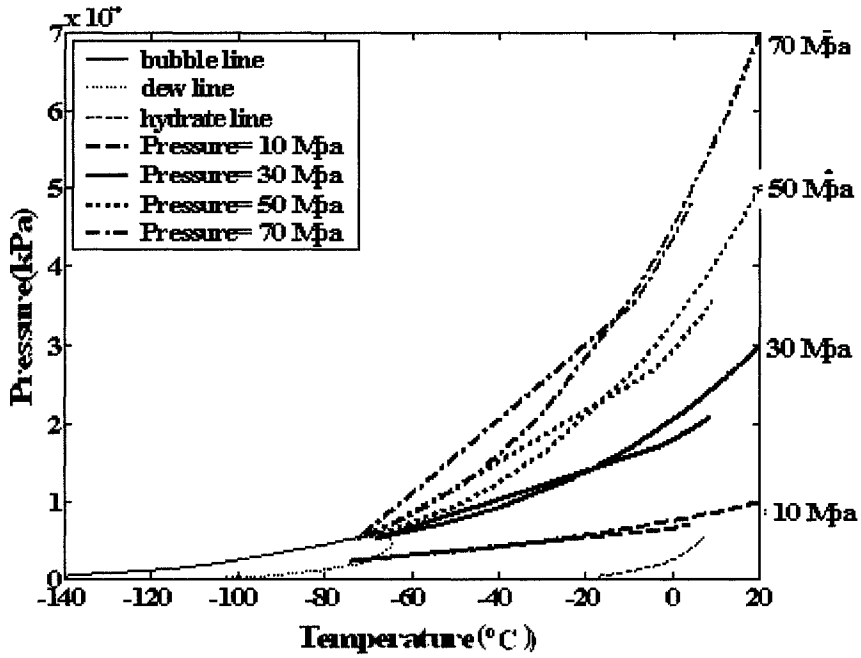

Figure 4.25: Phase envelope nd Pressure-Temperature distributions for pressure-effect studies with 70% inlet pressure recovery

Plotting the temperature variation with pressure for a nozzle in which 70% of the inlet pressure recovery is desired, illustrates in the four gas conditions, the lines remain in the dense phase region all the time and therefore, two liquid phases (water and hydrocarbon) will be present. However, as the inlet pressure increases the temperature-pressure variation is more likely to stay in the dense supercritical phase of the phase

envelope (see Figure 4.25). Figures 4.26 and 4.27 indicate the temperature and velocity distribution along the nozzle when 70 % recovery of the inlet pressure is the design criteria.

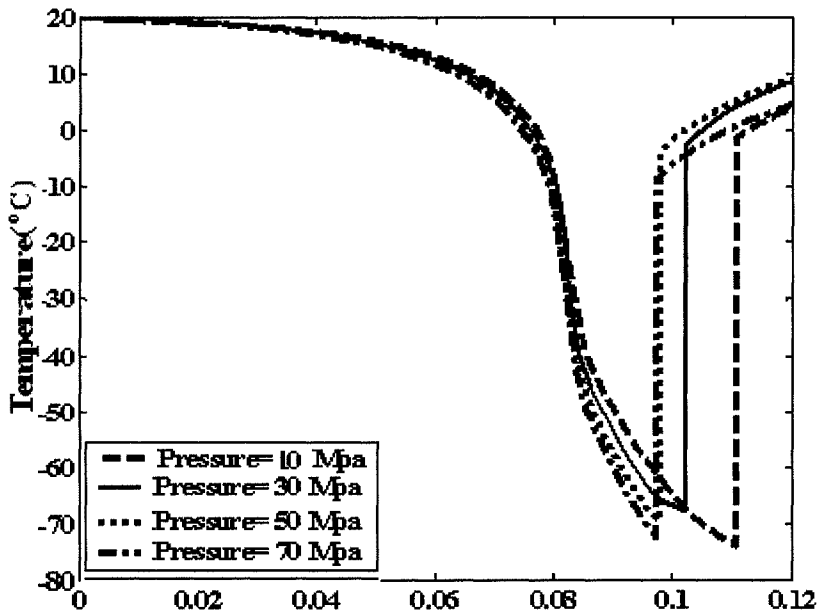

Figure 4.26: Temperature distributions and the shock wave location in the rated nozzle in pressure-effect studies with 70% inlet pressure recovery

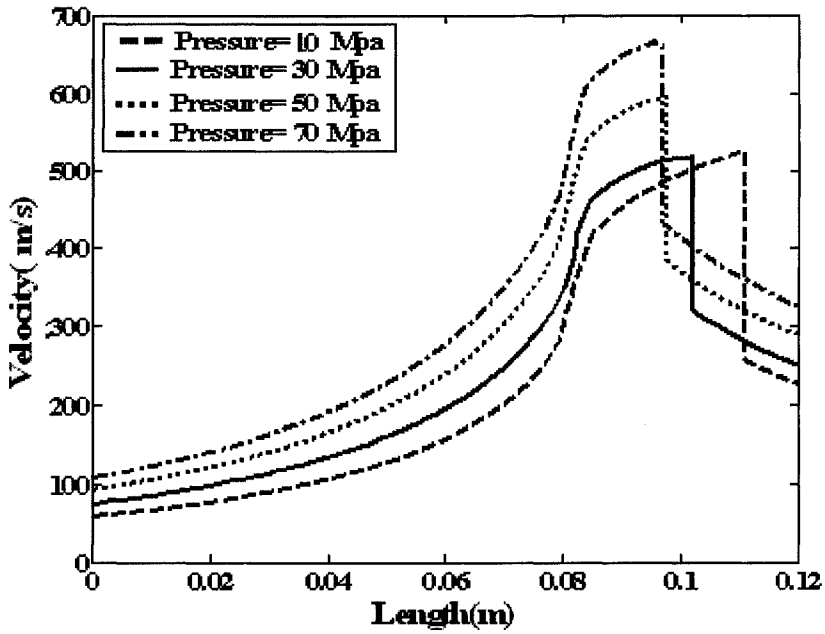

Figure 4.27: Velocity distributions and the shock wave location in the rated nozzle in pressure-effect studies with 70% inlet pressure recovery

4.2.3 Effect of inlet temperature

Four dry streams (streams with no water content) with equal pressures and different temperatures are introduced and saturated with water. As mentioned before water saturation slightly changes the temperature and the flow rate as shown in Table 4.16. It can be seen that the streams water content increases with the increase in temperature (see Tables 4.16 and 4.17).

Table 4.16: Inlet condition of the streams for inlet-temperature-effect studies

Stream name	1	*Test Stream*	2	3
Temperature(°C)	0.95	19.85	39.60	59.05
Pressure (MPa)	30	30	30	30
Molar flow Rate (kmol/h)	5,000.4	5,001.1	5,003.0	5,007.1
Water content (mg/m^3)	60.187	174.072	465.095	1,085.250

Table 4.17: Streams gas composition (mole fractions) for inlet-temperature-effect studies

Methane	9.4997E-01	9.4970E-01	9.4942 E-01	9.986E-01
Ethane	4.000E-02	3.9990E-01	3.997e-02	3.994E-02
Propane	9.999E-03	9.9970E-02	9.993e-03	9.986-03
Water	7011E-05	2.3000E-04	6.1042e-04	1.424E-05

These streams were introduced to the nozzle designed using the *"Test Stream"* as the working fluid. For the streams with the temperature lower than the *"Test Stream"* (Stream 1), the Mach number at the throat will be lower than unity (0.61414) which means the flow rate is not enough for this stream conditions and nozzle geometry. The Newton-Raphson component of the program (see section 3.4) does not converge to find the Mach number at the throat for Streams 2 and 3. Therefore, either the flow rate should be adjusted in order to choke the flow at the throat or a suitable nozzle for each stream condition should be designed.

4.2.2.1 Designing a new nozzle for each gas stream in tempersture –effect sudies

In order to have the choked flow at the nozzle throat in different inlet conditions and constant flow rates, a specific nozzle should be designed for each case. Designing a nozzle for each condition of inlet pressure and temperature with a constant inlet flow rate,

indicates that the length of the convergence part of the nozzle increases with inlet temperature Table 4.18 shows the throat diameter and the nozzle convergence length. Figure 4.28 presents the designed nozzle geometry for each condition.

Table 4.18: Nozzle geometry in temperature-effect studies

Stream name	1	*Test stream*	2	3
Nozzle throat diameter(m)	0.0192	0.0203	0.0212	0.0221
Nozzle convergence length (m)	0.0864	0.0813	0.0782	0.0746

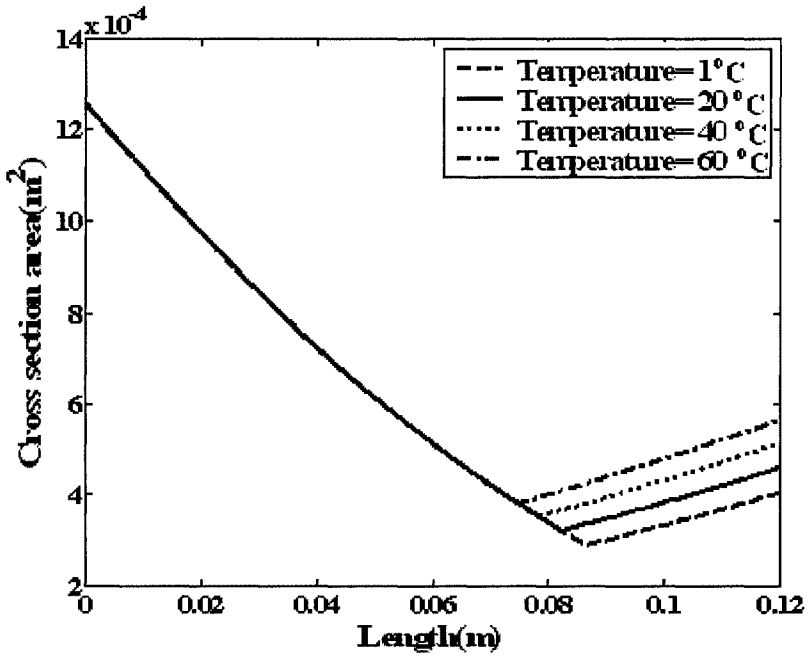

Figure 4.28: Designed nozzle geometry for temperature-effect studies

Figure 4.29 shows the nozzle *"recovery pressure"* and the *"design pressure"* in each nozzle. In all four cases the *"design pressure"* is about 15% of the inlet pressure. The highest possible pressure recovery in the nozzle, *"recovery pressure"*, increases with

the increase in temperature and falls between 79.26 and 87.13% of the inlet pressure for the nozzle with the defined length.

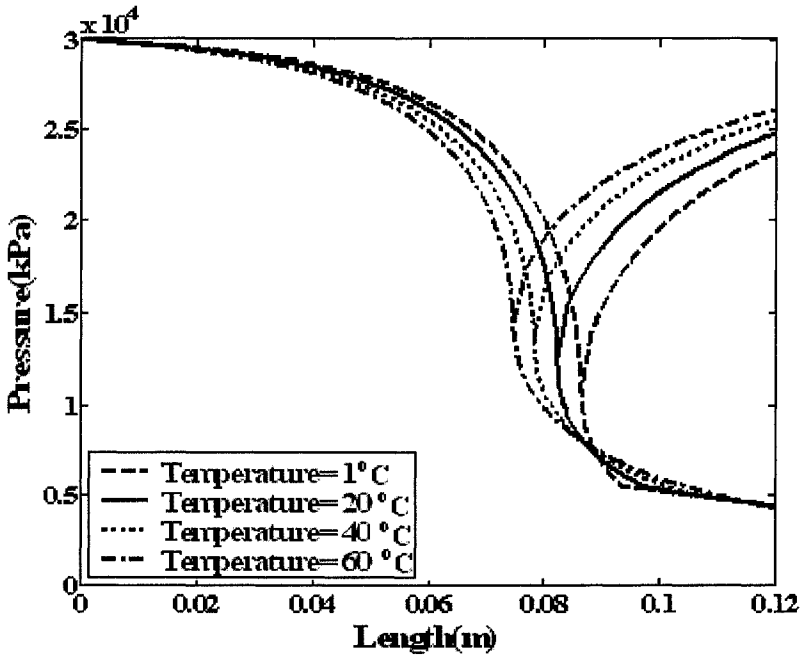

Figure 4.29: Pressure distributions along the designed nozzle for temperature-effect studies

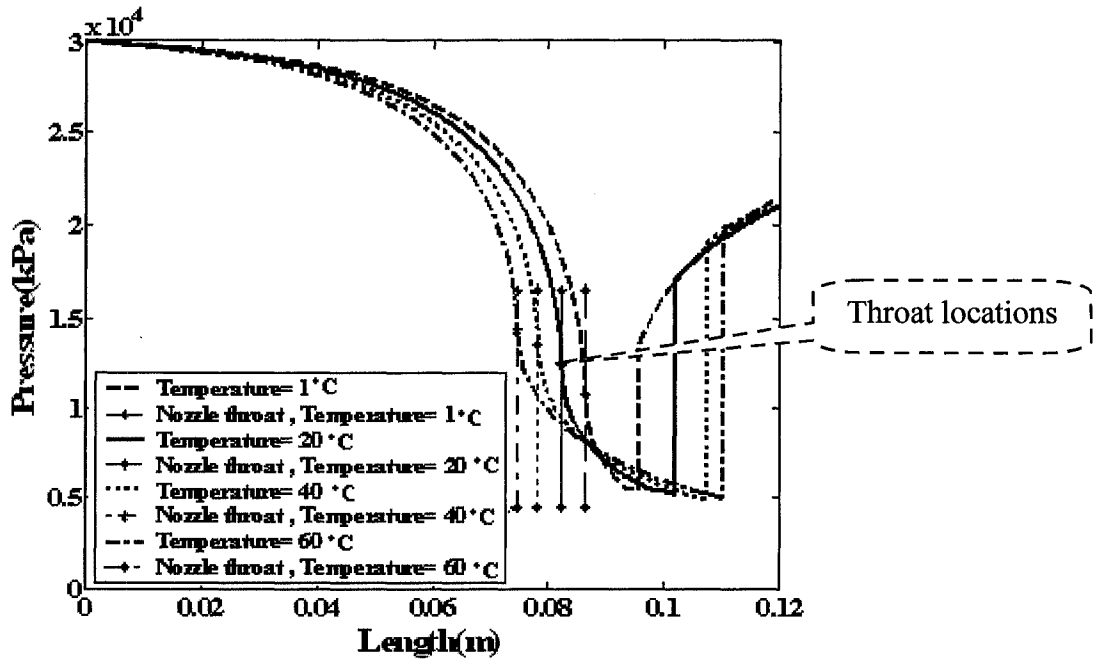

Figure 4.30: Pressure distributions and shockwave location along the designed nozzle for temperature –effect studies with 70% recovery of inlet pressure

Figure 4.30 shows the pressure distributions in the nozzle if the 70% recovery of the inlet pressure (21 MPa) is chosen as the design criteria. The throat in each nozzle is marked in this figure. While the inlet pressure and the flow rate are constant, with an increase in inlet temperature, the length of the converging part of the nozzle decreases and the flow is choked earlier in the nozzle. At the same time, the shockwave location shifts towards the nozzle exit. Therefore, the distance between the nozzle throat and the shockwave increases. As the inlet temperature decreases from 60 to 1° C, the throat cross section area decreases 24.14% and the nozzle exit cross section decreases 29.00?%.

In the nozzle with Stream 1 as the working fluid, the distance between the nozzle

throat and the shockwave location is 9.47% of the nozzle length and this distance becomes longer, up to 32.19% of the nozzle length as the temperature increases to 60 °C.

With the increase in inlet temperature from 1 to 60 ° C, the throat location shifts form 72.00% of the total length to 62.16% of the total length so the flow can become choked, up to 10% of the total length earlier. At the same situation, shockwave location varies from 79.58% of the total length to 91.66% of the total length.

Figures 4.31 and 4.32 present the temperature and velocity distributions along the nozzle with 70% recovery of the inlet pressure.

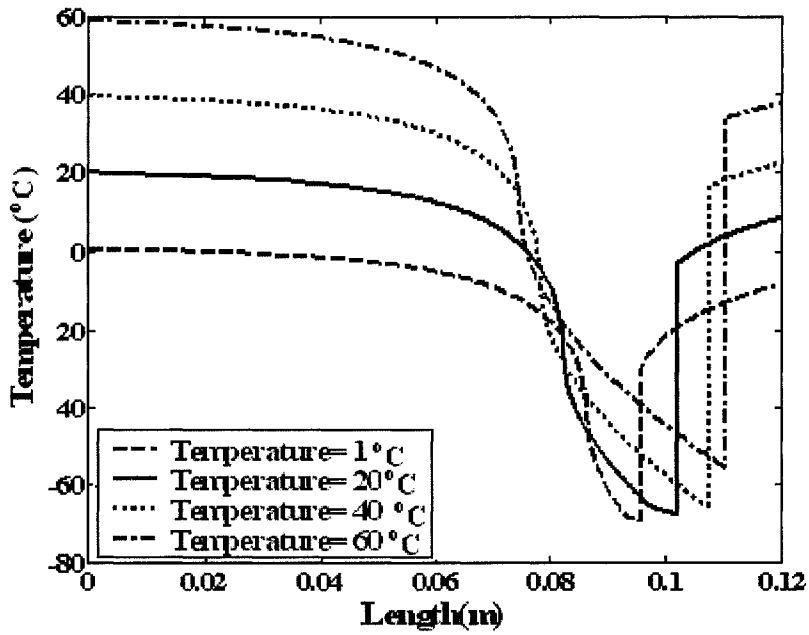

Figure 4.31: Temperature distributions and shockwave location along the designed nozzle for temperature–effect studies with 70% recovery of the inlet pressure

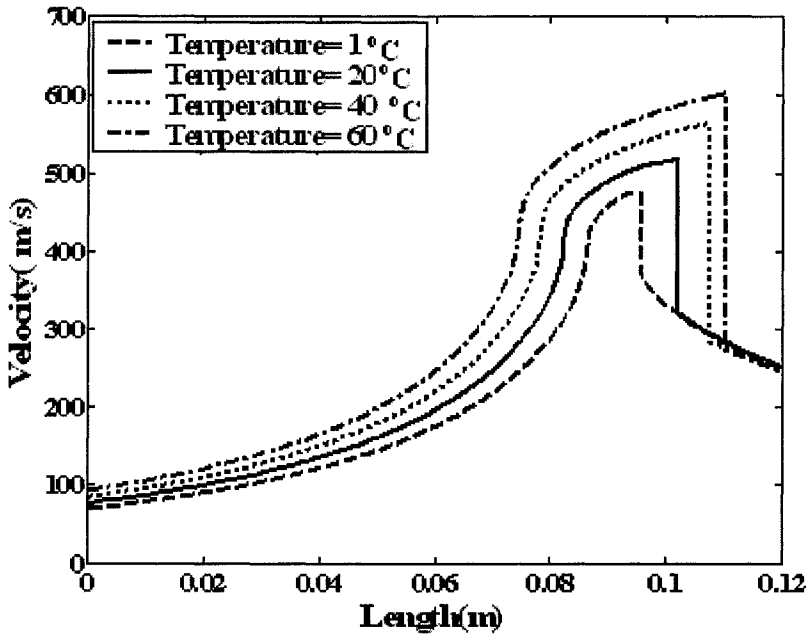

Figure 4.32: Velocity distributions and shockwave location along the designed nozzle for temperature–effect studies with 70% recovery of inlet pressure

As can be seen in Figure 4.33, smaller pressure expansions happen with temperature when the design criterion is set for 70% recovery of inlet pressure. At the temperature of 60 °C, the flow condition will be in the single phase region of the phase envelope and therefore, water phase is the only liquid phase and water can be removed selectively, without affecting the hydrocarbon content of the gas stream.

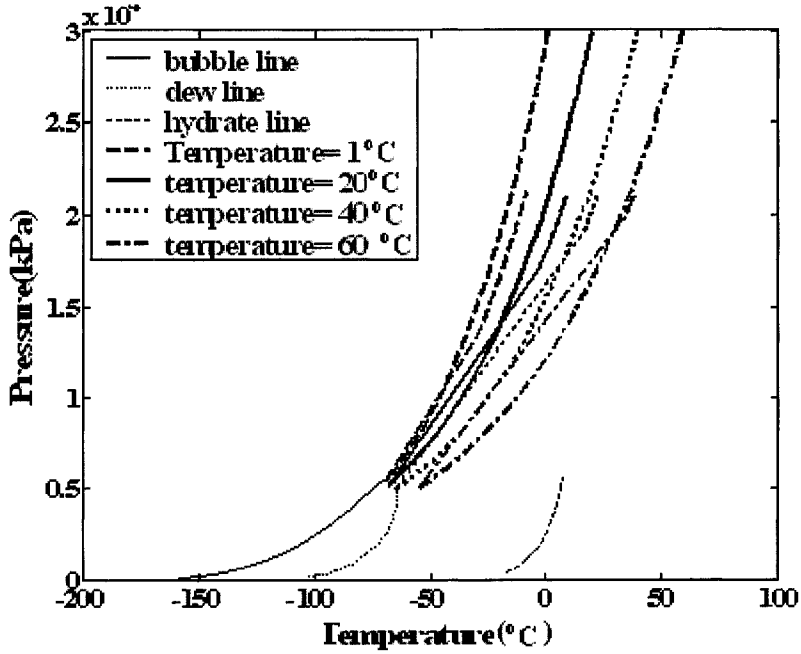

Figure 4.33: Phase envelope and Pressure- Temperature distributions along the designed nozzle and temperature-effect studies with 70% inlet pressure recovery

Table 4.19 presents the initial water content in the stream and the remained water content in the nozzle stream after separating the condensed liquid before the shockwave in a nozzle which is designed to recover 70% of the inlet pressure. In reality condensed liquids cannot be completely separated from the main stream in the nozzle, therefore the results shown here are theoretical assuming that 100% of the condensed liquid is separated. Figure 4.34 shows the gas water content along the nozzle. The water content increases with inlet temperature (see Figure 4.34). Theoretically, a close to complete water removal can be achieved in the supersonic nozzle in all the inlet conditions.

Table 4.19: Remained water content in the nozzle stream after the shockwave for the designed nozzle in temperature-effect study with 70% inlet recovery

Inlet temperature (°C)	Initial water content (mg/m3)	Remainder water content (mg/m3)
1	59.39	0.23
20	174.07	0.18
40	464.22	0.24
60	1084.30	0.84

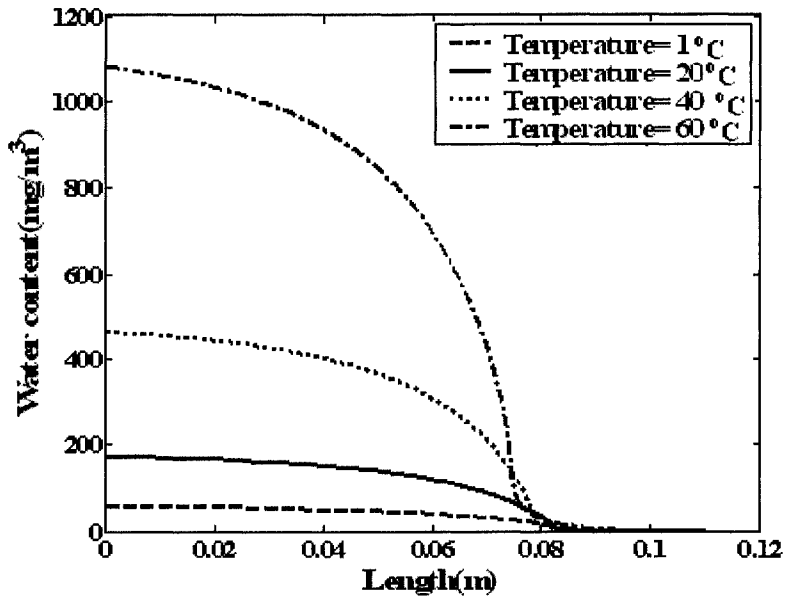

Figure 4.34: Theoretical water removal along the designed nozzle and temperature-effect studies with 70% inlet pressure recovery.

4.2.2.2 RATING NOZZLES FOR EACH GAS STREAM IN TEMPERATURE-EFFECT STUDIES

If the aim is using one nozzle for different inlet temperatures, the flow rate should be adjusted such that the sonic velocity is reached at the throat and the flow is choked. The designed nozzle using the *"Test Stream"* is used for this simulation. Table 4.20 shows the adjusted flow rates in each condition inlet temperature. The flow capacity

decreases with the increase in the inlet temperature.

Table 4.20: the adjusted flow rate to rate the nozzle in temperature –effect-studies

Stream name	**1**	***Test stream***	**2**	**3**
Molar flow Rate (kmole/h)	5,565	5,000	4,538	4,179
Exit pressure range (% of inlet pressure)	14.51,-,80.76	14.84,-,82.71	14.94,-,84.14	15.23,-,85.24

Depending on the nozzle backpressure, the exit pressure will fall in a range whose lower and upper bounds are given as a percentage of the inlet pressure in Table 4.20. In nozzles with constant lengths, as the inlet temperature increases, the maximum possible recovery of inlet pressure will increase while the lowest exit pressure will stay almost unchanged. These results are shown in Figure 4.35.

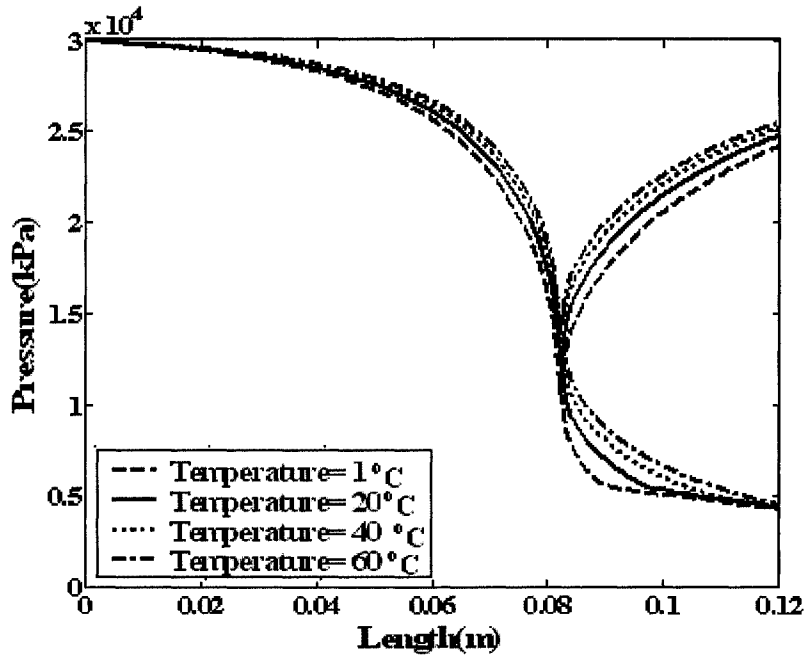

Figure 4.35: Pressure distribution along the rated nozzle in the temperature-effect-studies

If the 70% recovery of the inlet pressure is used as the design criteria, the shockwave location varies depending on the inlet conditions (see Figure 4.36). Increasing the inlet temperature from 1 to 60 ° C, shifts the shockwave location 12.82% towards the nozzle exit. The inlet pressure decreases between 82 to 83% before the shockwave happens.

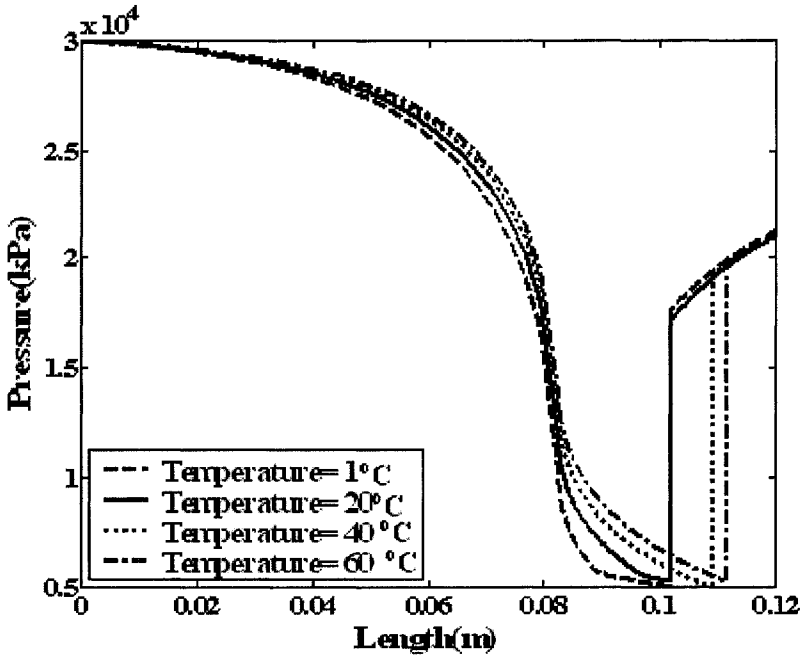

Figure 4.36: Pressure distribution and the shockwave location along a rated nozzle in temperature-effect-studies with 70% recovery of inlet pressure

Figure 4.38 illustrates that with 70% recovery of inlet pressure, as the inlet temperature increases the amount of the liquid phase decreases and finally it can be seen that with the inlet conditions for Stream 3, the flow remains in a single phase. Figures 4.39 and 4.40 show the temperature and velocity distributions along the rated nozzle in the temperature effect studies and when 70% of the inlet pressure recovery is obtained.

Figure 4.36 illustrates that close to complete water removal occurs in the nozzle before the shockwave happens (see Table 4.21).

Table 4.21: Remained water content in the nozzle stream after the shockwave for the designed nozzle in temperature-effect study with 70% inlet recovery

Inlet temperature (°C)	Initial water content (mg/m3)	Remainder water content (mg/m3)
1	59.39	0.15
20	174.07	0.18
40	464.22	0.24
60	1,084.30	0.77

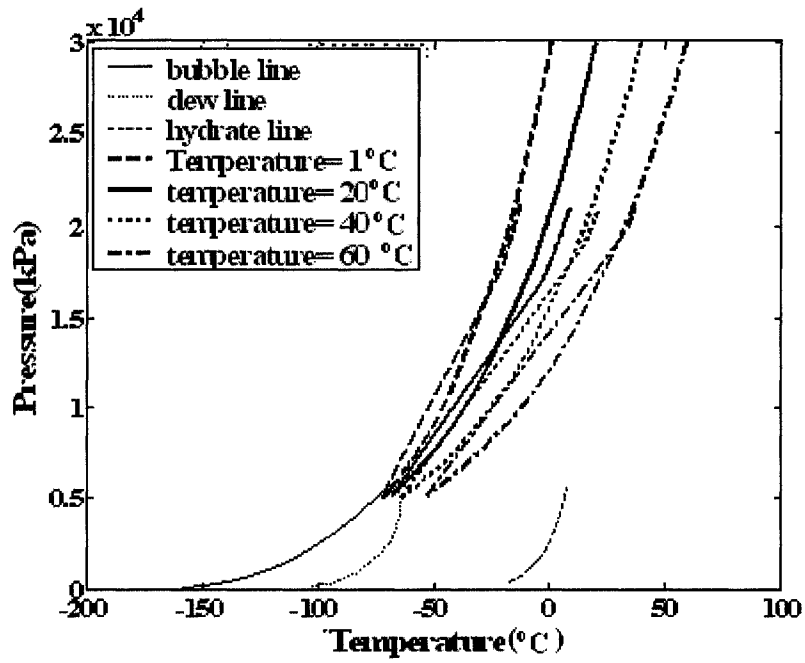

Figure 4.38: Phase envelope and Pressure- Temperature distributions along a rated nozzle in the temperature-effect studies with 70% inlet pressure recovery

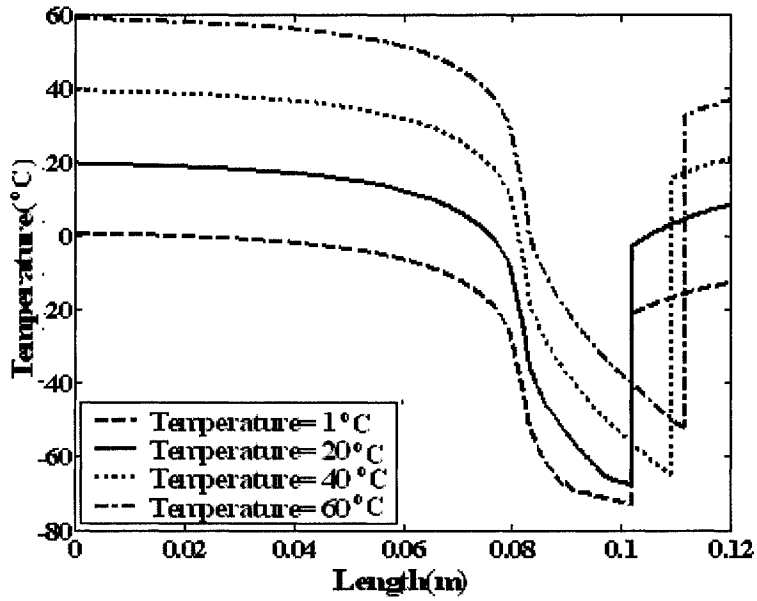

Figure 4.39: Temperature distribution and the shockwave location along a rated nozzle in the temperature-effect-studies with 70% inlet pressure recovery

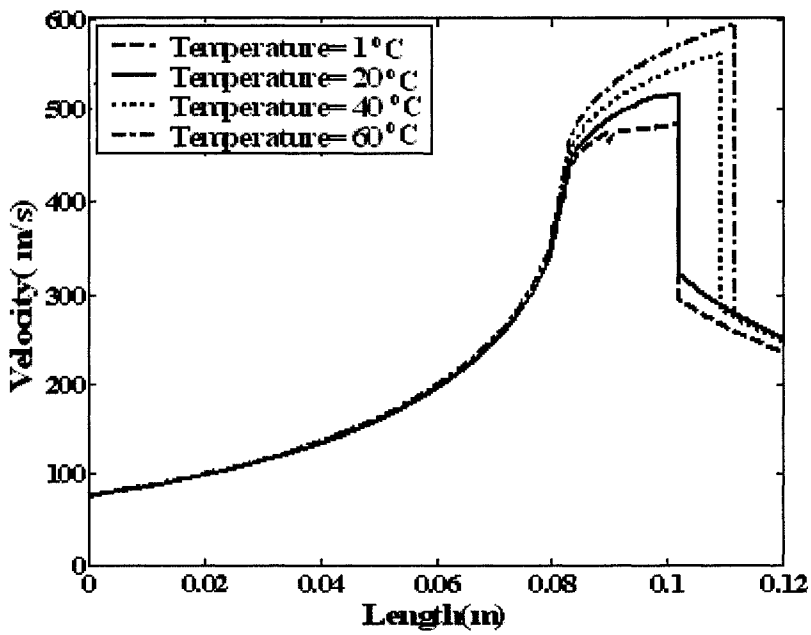

Figure 4.40: Velocity distributions and the shockwave locations along a rated nozzle in the temperature-effect-studies with 70% of inlet pressure recovery

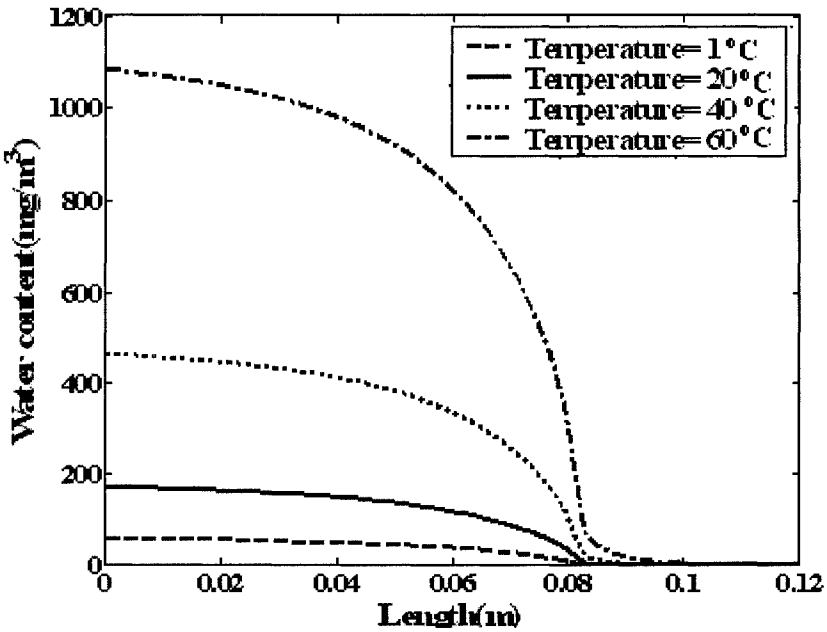

Figure 4.41: Theoretical water removal along the rated nozzle in the temperature-effect-studies with 70% inlet pressure recovery

4.2.4 Effect Of Flow Rate

4.2.4.1 Designing a nozzle for different flow rates in flow rate-effect studies

A few streams with the pressure, temperature, and composition the same as that of "*Test Stream*" but with different flow rates are considered as the working fluid and a nozzle was designed for each case. Table 4.22 shows the inlet flow rate and the range of the exit pressures as a percentage of the inlet pressure. A wider range of pressure recovery can be achieved in the nozzle with the increase in inlet flow rate. Therefore, the "*recovery pressure*" increases with inlet flow rate. In the nozzle with a length of 0.12 *m*, the highest possible pressure recovery is 64.80 and 93.03% % of the inlet pressure for

Stream 1 and 4, respectively. Figure 4.42 presents the result shown in Table 4.22.

Table 4.22: The pressure recovery range in the flow rate–effect-studies

Stream name	**1**	**2**	***Test stream***	**3**	**4**
Molar flow Rate (kmole/h)	2,000	4,000	5,000	6,000	10,000
Exit pressure range (% of inlet pressure)	20.4 - 64.8	15.6 - 79.8	14.8 - 82.7	14.4 - 85.0	13.5 - 93.0

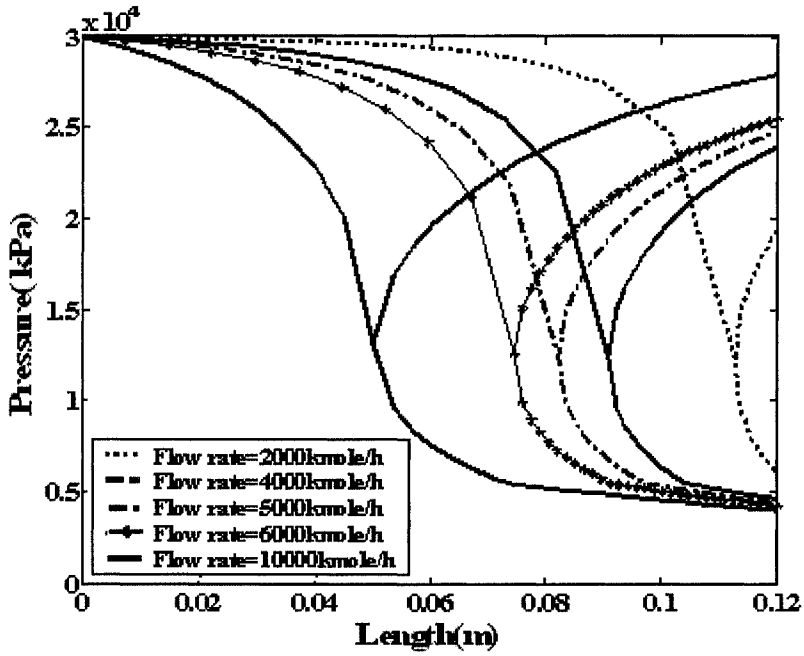

Figure 4.42: Pressure distribution along the rated nozzle in the flow rate-effect-studies

Figure 4.43 shows the different nozzle geometries. As it can be seen the flow becomes choked earlier along the nozzle as the flow rate increases. Therefore, the converging length of the nozzle is shorter and the throat diameter is bigger. These results are shown in Table 4.23.

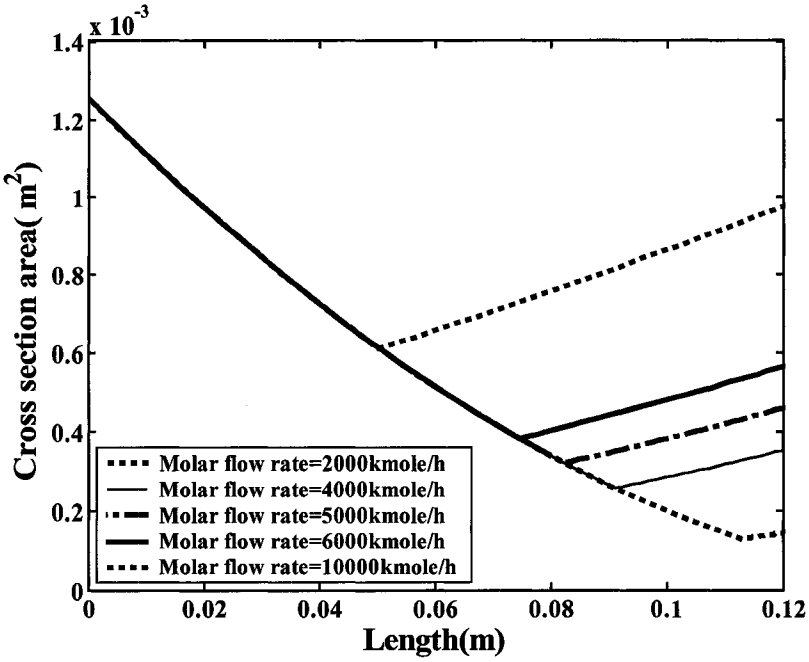

Figure 4.43: Designed nozzles geometry in flow rate-effect-studies

Table 4.23: Designed nozzle geometry in flow rate-effect studies

Stream name	1	2	*Test stream*	3	4
Throat diameter(m)	0.0129	0.0182	0.0203	0.0221	0.0279
Nozzle converging length (m)	0.1128	0.0908	0.0821	0.0744	0.0502

With the design criteria of 70% recovery of the inlet pressure, no nozzle with the length of 0.12 m can be designed for Stream 1 as 64.80% of the inlet pressure recovery is the highest possible recovery in such a nozzle. The pressure, temperature and velocity distributions and the shockwave locations along a designed nozzle with 70% inlet

pressure recovery are shown in Figure 4.44, 4.45 and 4.46. Shockwave happens at 77.07% of the total nozzle length when the molar flow rate is 10,000 *kmole/h*. The shockwave location shifts toward the nozzle exit as the molar flow rate of the nozzle decreases. When the molar flow rate is 4,000 *kmole/h,* shockwave happens at 88.33% of the total length.

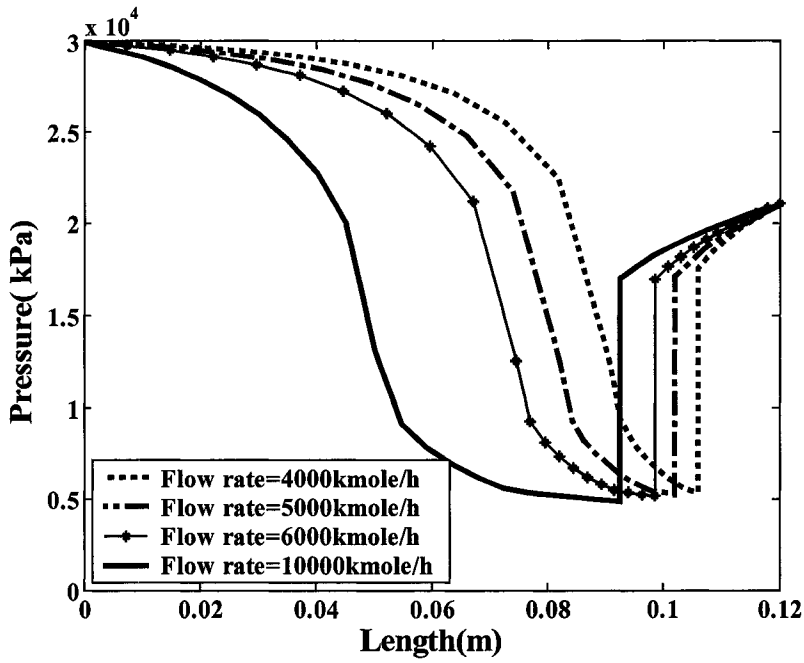

Figure4.44: Pressure distributions and the shockwave locations along the designed nozzle in flow rate-effect studies with 70%inlet pressure recovery

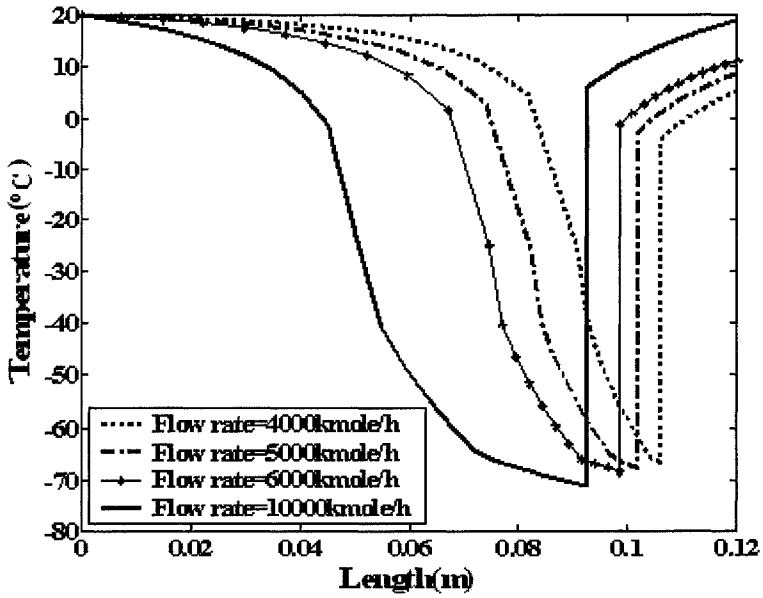

Figure4.45: Temperature distributions and the shockwave locations along the designed nozzle in flow rate-effect studies with 70%inlet pressure recovery

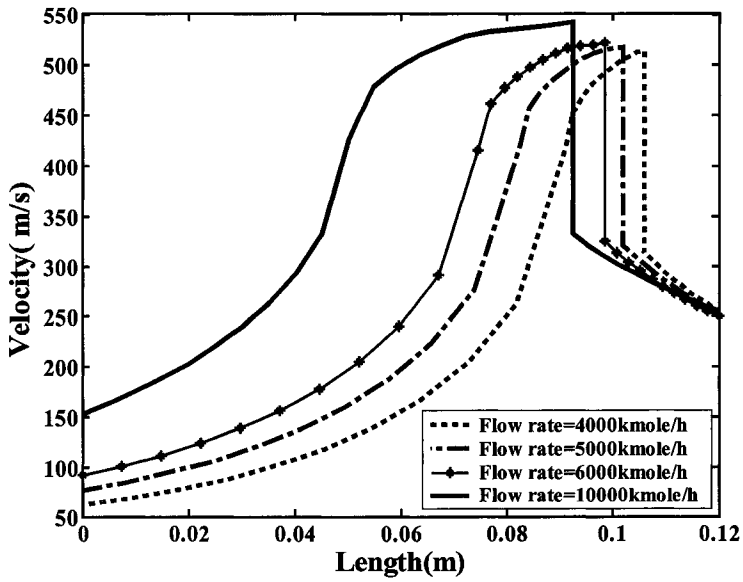

Figure4.46: Velocity distributions and the shockwave locations along the designed nozzle in flow rate-effect studies with 70%inlet pressure recovery

4.2.4.2 RATING NOZZLES FOR EACH FLOW RATE IN FLOW RATE-EFFECT STUDIES

For any each stream conditions and the specified nozzle geometry, there is a flow rate (*design flow rate*) in which the critical conditions are presents at the throat and the flow is choked. If the flow rate is lower than the specified flow rate, the Mach number will be less than unity in the throat of the nozzle and the flow will never be choked. Figures 4.47 and 4.48 show the Mach number and the pressure distributions of the streams with pressures and temperatures equal to that of the *"Test Stream"* at different flow rates. For the flow rate equal to 5,000 *kmole/h* for which the nozzle was designed, the Mach number at the throat reaches unity but for the lower flow rates the stream is always remain subsonic (see Figure 4.47).

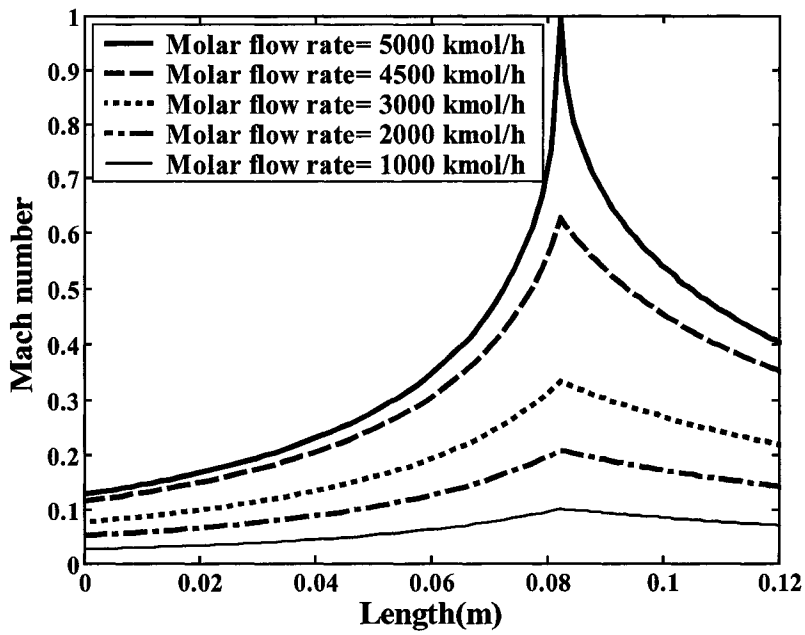

Figure 4.47: Mach number distribution along the nozzle with different flow rates

As shown in Figure 4.48, the pressure drop on both sides of the nozzle increases

as the flow rate increases to the *design flow rate.* This pressure drop is the lowest possible pressure drop along the specified nozzle, while the flow is choked.

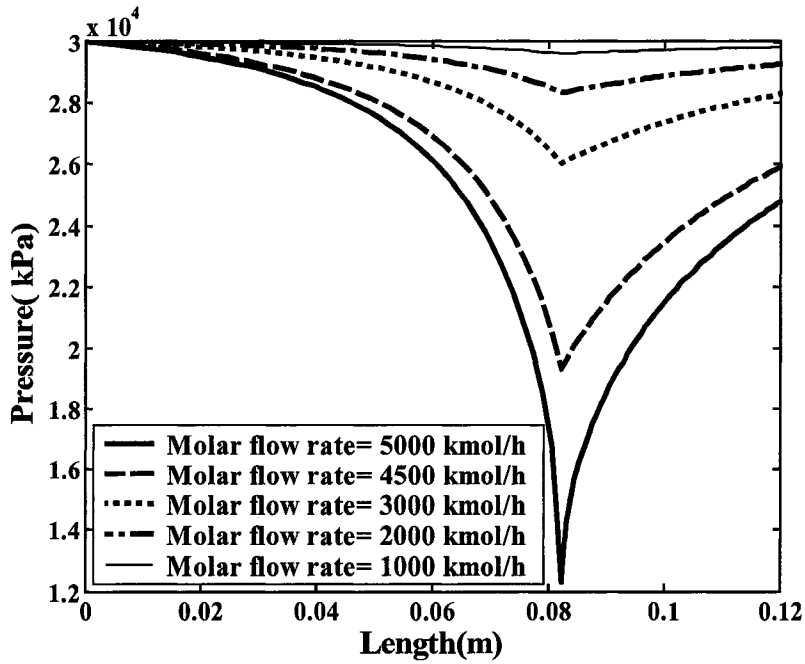

Figure 4.48: Pressure distribution along the nozzle with different flow rates

4.2.5 Effect of backpressure

The behaviour of the working fluid in the nozzle depends on the back pressure (pressure at the nozzle exit) of the nozzle. For a nozzle of 0.12 *m* long and the *"Test Stream"* as a working fluid, the backpressure should not exceed 82.71% of the inlet pressure in order to choke the flow at the throat. This exit pressure is equal to the nozzle *"recovery pressure"*. The" *design pressure"* in this condition is 14.84% of the inlet pressure. If the backpressure is between the nozzle *"recovery pressure"* and *"design pressure"*, a shockwave happens either inside or outside of the diverging part of the

nozzle. With the decrease in the backpressure, the shockwave location shifts towards the nozzle exit until when the backpressure is equal to 48.5% of the inlet pressure where the shockwave happens at the nozzle exit. The shockwave happens outside the nozzle if the backpressure decreases further down and falls between 48.50 to 14.84% of the inlet pressure.

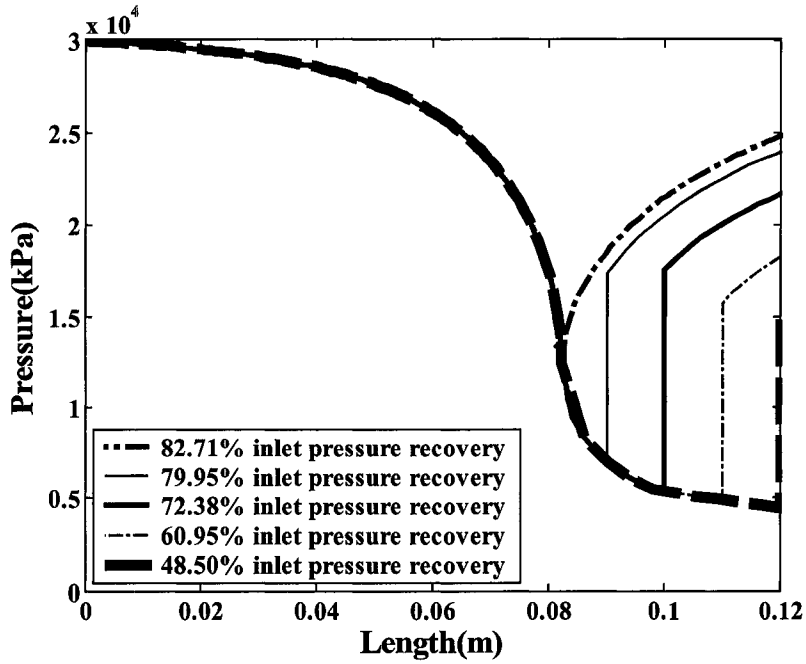

Figure 4.49: Pressure distribution along the nozzle for different back pressures

Figures 4.50 to 4.53 show the temperature-pressure variations and the location of the lowest temperature with respect to the two-phase region. It is clear that by lowering the pressure recovery (higher pressure drops along the nozzle), the gas will expand more and pressure and temperature will be lower before the shockwave happens. The pressure drop can be reduced by increasing the backpressure which results in higher pressure and

temperature before the shockwave. If the selective water removal is desired, pressure and temperature before the shock should be prevented from falling into the two-phase region. As indicated in Figures 4.50 to 4.53, higher backpressures cause the shockwave to happen earlier and less liquid hydrocarbons will form. Increasing the backpressure might reduce the water removal efficiency. Table 4.24 lists the amount of water remained in the gas at different shockwave locations along the nozzle. As it can be seen 94% of the water is removed in the converging part of the nozzle. In this condition, although about only 80% of the inlet pressure is recovered, close to complete water removal is achieved. A selective water removal is obtained in this case (see Figure 4.53) and 94% of the total amount of water in the stream will be condensed in the converging part of the nozzle. The rest of the water will start condensing in the diverging part.

Table 4.24: Water content along the nozzle

Shockwave location (m)	0.082	0.090	0.100	0.110	0.120
Pressure recovery (% of inlet pressure)	82.71	79.95	72.38	60.95	48.5
Water remainder in vapour phase (% of initial water content) (mg/m^3)	6.00	0.50	0.11	0.06	0.04

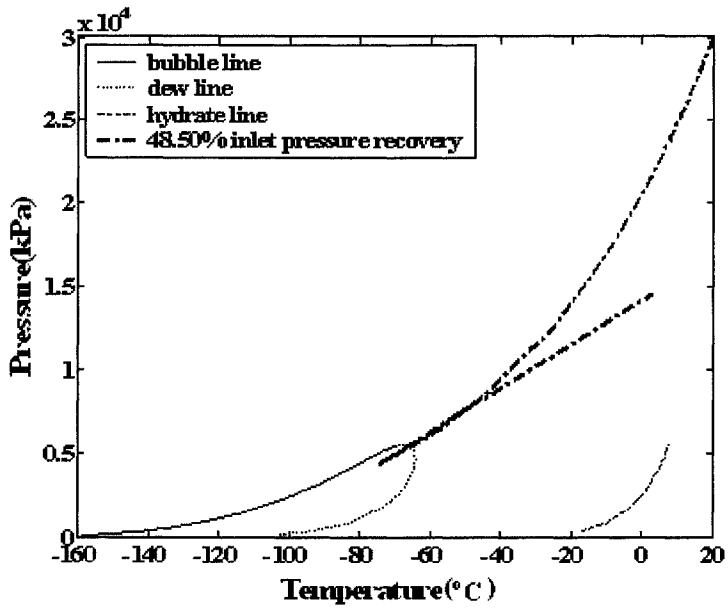

Figure 4.50: Phase envelope and Pressure-Temperature distributions with 48.5% inlet pressure recovery

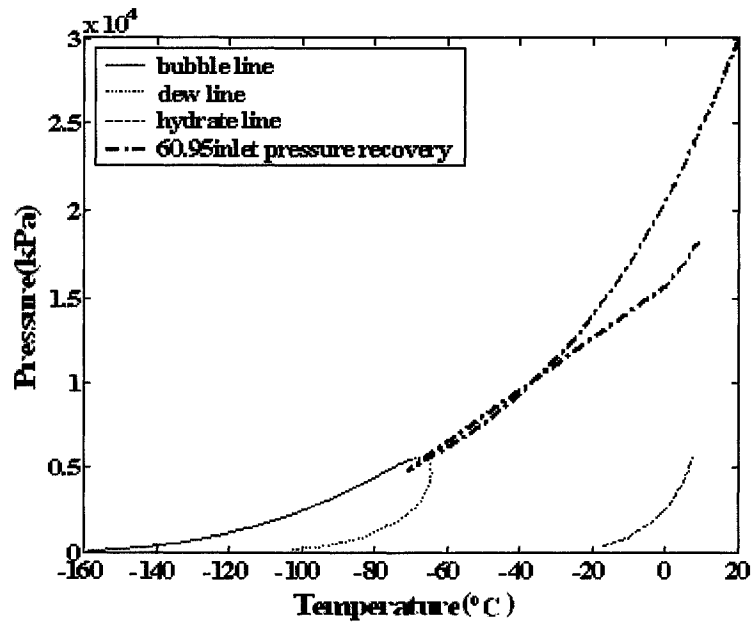

Figure 4.51: Phase envelope and Pressure-Temperature distributions with 60.95% inlet pressure recovery

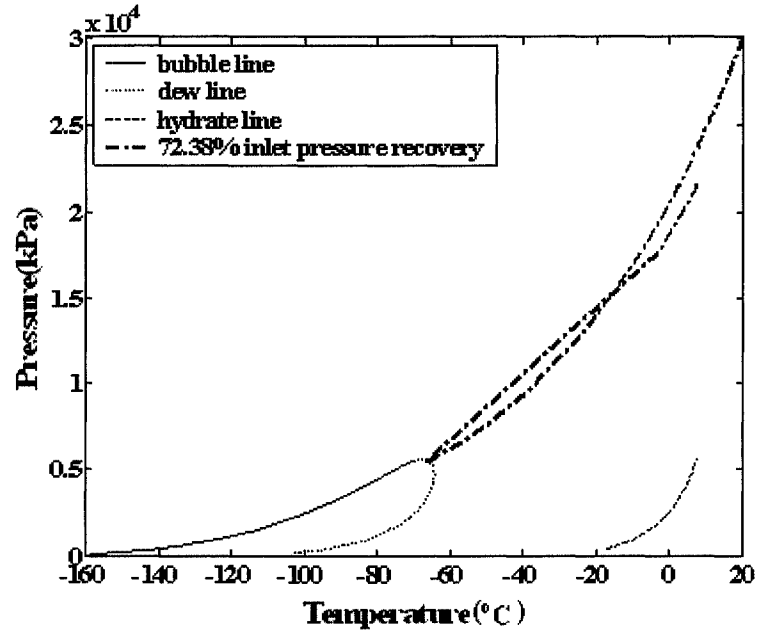

Figure 4.52: Phase envelope and Pressure-Temperature distributions with 73.38% inlet pressure recovery

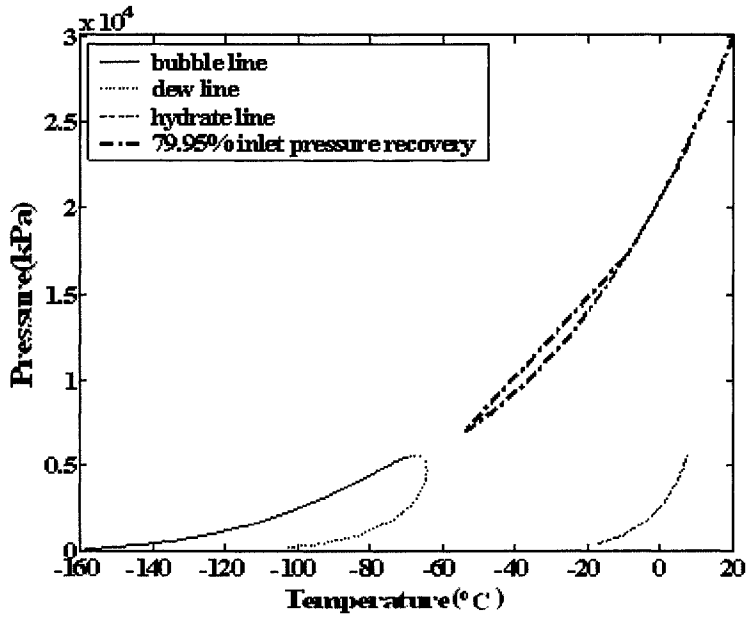

Figure 4.53: Phase envelope and Pressure-Temperature distributions with 79.95% inlet pressure recovery

4.2.6 Effect of friction

All the analyses up to this point were performed considering no friction in the nozzle; the effect of friction in the nozzle will be considered in this part of the thesis. As a result of friction, the flow will not remain isentropic and the entropy of the flow will therefore be increasing along the nozzle. The nozzle is assumed to be made of mild steel with an absolute roughness of 4.572×10^{-5} *m*. The analyses are performed by designing a nozzle in which a non-isentropic flow exists or alternatively by rating the nozzle which is designed in isentropic condition, considering the non-isentropic flow as a working fluid.

4.2.6.1 Designing a new nozzle using non-isentropic flow in frcition- effet studies

A nozzle is designed assuming that friction is present in the nozzle and the *"Test Stream"* is flowing through the nozzle. The throat diameter used in this simulation is 0.11% larger than that of the frictionless case and the converging length is 0.05% shorter than that of the case with frictionless flow. These two geometrical values affect the pressure at the throat, the *"recovery pressure"*, and the "*design pressure"* in less than 0.5%. Most probably the discrepancies are because of the errors in the developed program such as the errors such as a result of the tolerance defined in calculating the results, round off error and truncating errors, present in the computations. Therefore, the "*recovery pressure*" and the "*design pressure*" of the nozzle are the same for both frictionless and frictional flow (see Figure 4.54) but the shockwave location in the diverging part of the nozzle will be different. The differences between the shockwave

locations with the design criteria of 70 % inlet pressure recovery, is shown in Figure 4.54. In the frictionless flow, shockwave occurs at 85% of the total nozzle length and for the frictional flow it shifts 8.83% towards the nozzle exit and occurs at 93.83% of the total length. Figures 4.55 and 4.56 show the temperature and velocity distributions along the designed nozzle for the friction-effect studies.

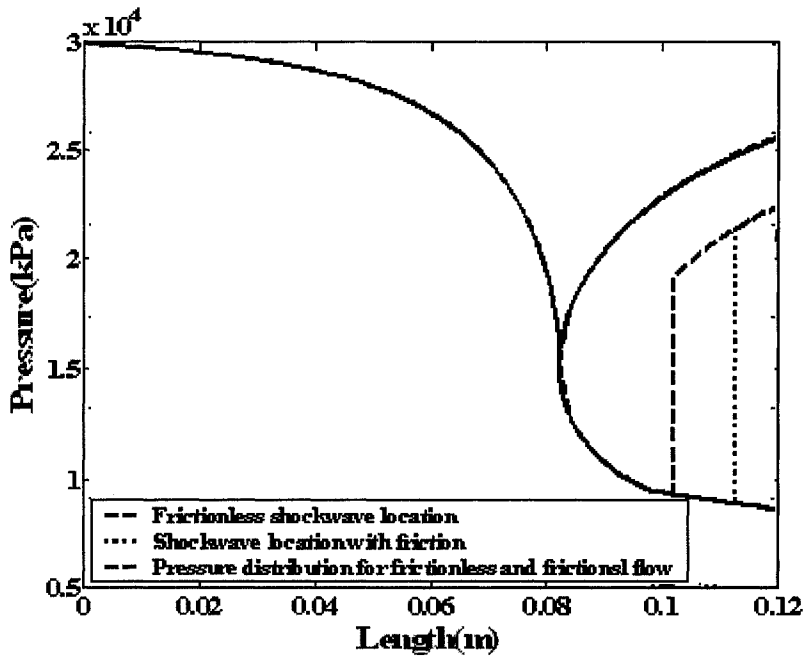

Figure 4.54: Pressure distribution and the shockwave location along the designed nozzle for the friction-effect study with 70% inlet pressure recovery

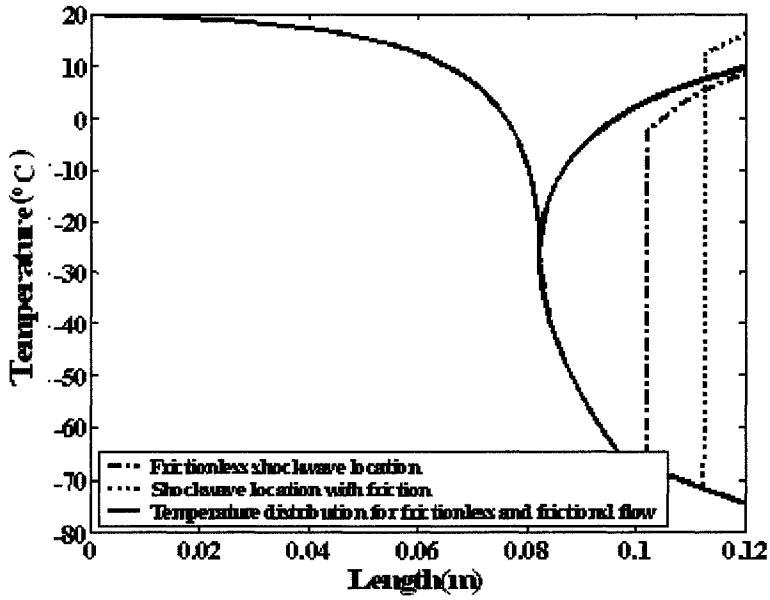

Figure 4.55: Temperature distribution and the shockwave location along the designed nozzle for the friction-effect study with 70% inlet pressure recovery

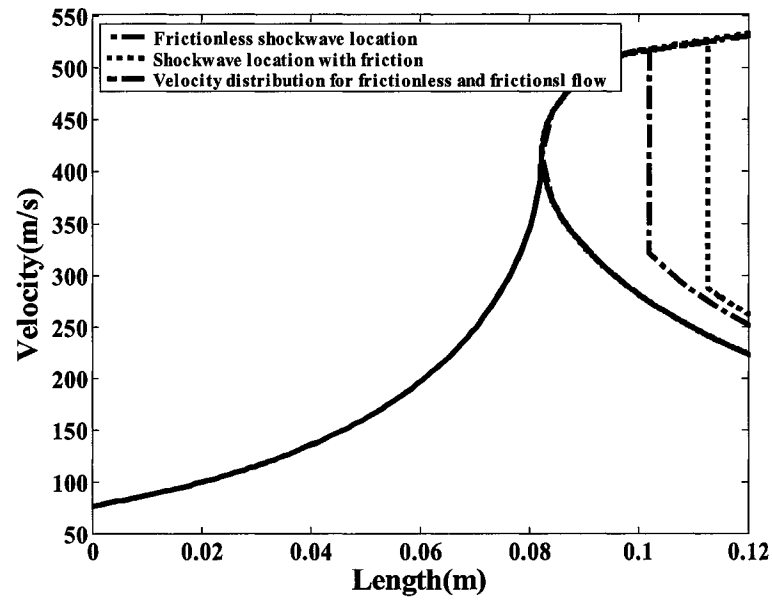

Figure 4.56: Velocity distribution and the shockwave location along the designed nozzle for the friction-effect study with 70% inlet pressure recovery

4.2.6.2 *RATING THE DESIGHNED NOZZLE WITH THE NON-ISENTROPIC FLOW IN FROCTION EFFECT STUDIES*

In order to rate the nozzle for the non-isentropic flow, we considered a nozzle previously designed for *test stream* assuming isentropic flow. For the same flow rate as in the friction less flow, the nozzle will not choke at the throat and the throat Mach number will be 0.879. Therefore, the flow rate needs to be increased. The desired flow rate in this case is 5,003 *kmole/h* instead of 5,000 *kmole/h.* the new flow rate is just 0.06% larger than the isentropic flow and also the differences between the pressure at the throat, nozzle*" recovery pressure"* and *"design pressure"* for the two cases are less than 0.5%, respectively. It can be assumed that the nozzle geometry and the flow rate are the same in an isentropic flow as well as the case when friction is present in the nozzle. The friction however affects the shockwave location in the diverging part of the nozzle. As the friction is introduced to the nozzle the shockwave location shifts towards the nozzle exit. When rating the nozzle, the shockwave is 9.48% of the total length ahead of the shockwave location in the isentropic flow and occurs at 94.5% of the total length.

Figures 4.57, 4.58, and 4.59 show the comparisons between the isentropic and non-isentropic flows.

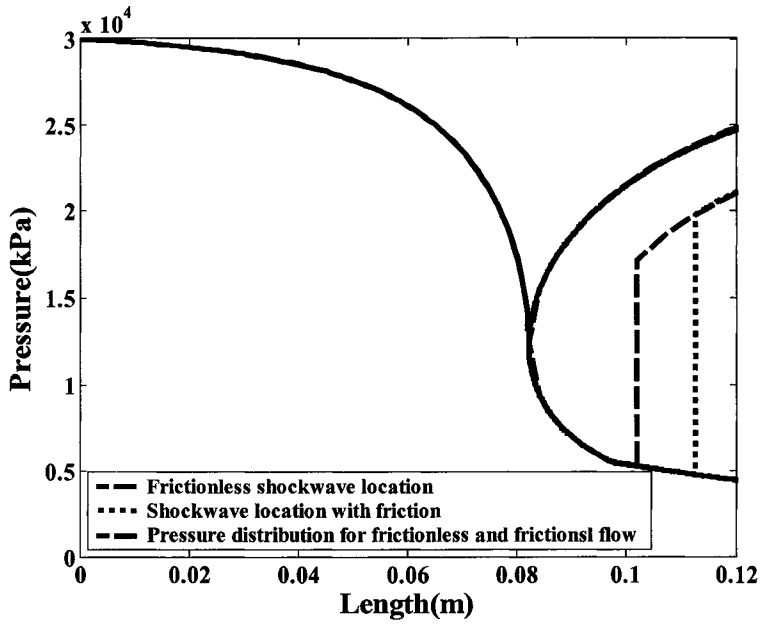

Figure 4.57: Pressure distributions and the shockwave locations along a rated nozzle with 70% inlet pressure recovery for the friction-effect study.

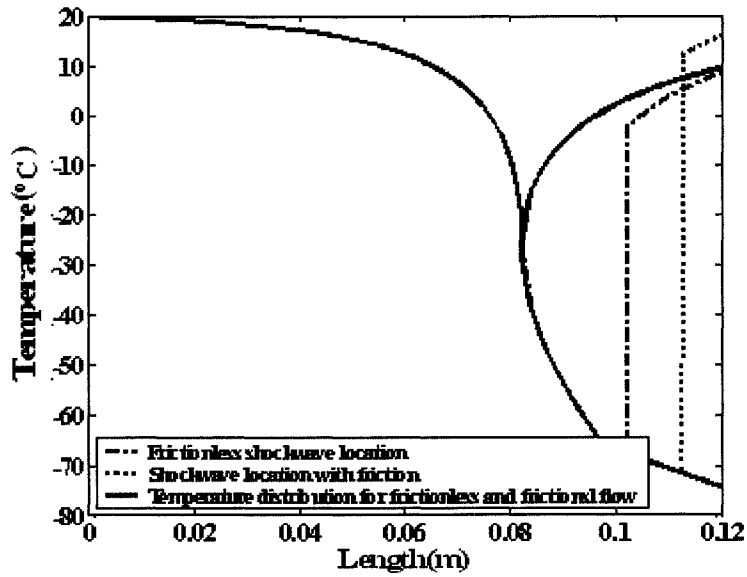

Figure 4.58: Temperature distribution and the shockwave locations along a rated nozzle with 70% inlet pressure recovery for the friction-effect study

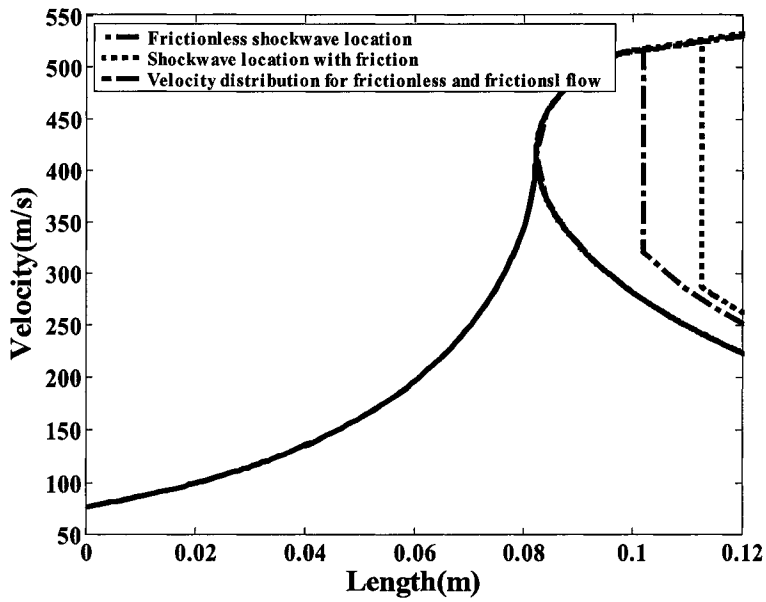

Figure 4.59: Velocity distribution and the shockwave locations along a rated nozzle with 70% inlet pressure recovery for the friction-effect study

CHAPTER 5: CASE STUDY: NATURAL GAS LIQUIDS (NGLS) RECOVERY

The recovery of natural gas constituents heavier than methane is a common process in natural gas treatment for dew point control and enhanced hydrocarbon recovery purposes. Large quantities of the produced gas used to be flared during the production of crude oil. The flaring of associated gas is gradually being abandoned and there are very strict regulations to minimize this wasteful practice, however there are still offshore facilities where a significant amount of gas has to be flared due to the lack of infrastructure to transport the gas to the market. Recovering NGL from the produced gas can significantly decrease the toxicity as well as reduce the wastage of valuable hydrocarbons of the flared gases. Supersonic separators are also used for the efficient recovery of NGLs, as natural gas condensate can be formed as a result of the expansion occurring in the nozzle. Therefore, by placing a supersonic separator within a typical crude surface production system on an offshore platform, the efficiency of the production unit can be improved. The position of the separator within the separator train will impact the recovery of the NGLs. The purpose of this chapter is to study the performance of supersonic nozzles for the recovery of NGLs. For this study a supersonic separators is placed in different positions and the crude oil production performance in each case is compared with the original production system without the NGL recovery. Membranes were studied for the NGL recovery in offshore facilities (Beronich, 2006). The

information used in Beronich's work is chosen here to study the efficiency of supersonic separators in the recovery of NGLs.

5.1 Process description

The location chosen to perform this study is the Hibernia platform located offshore of the province of Newfoundland and Labrador. A typical separation train on an offshore platform consists of series of separators at different pressures. Figure 5.1 outlines a typical diagram of this process. The pressure and temperature of the wellhead stream before entering the process are based on industry data (Beronich et al., 2006).

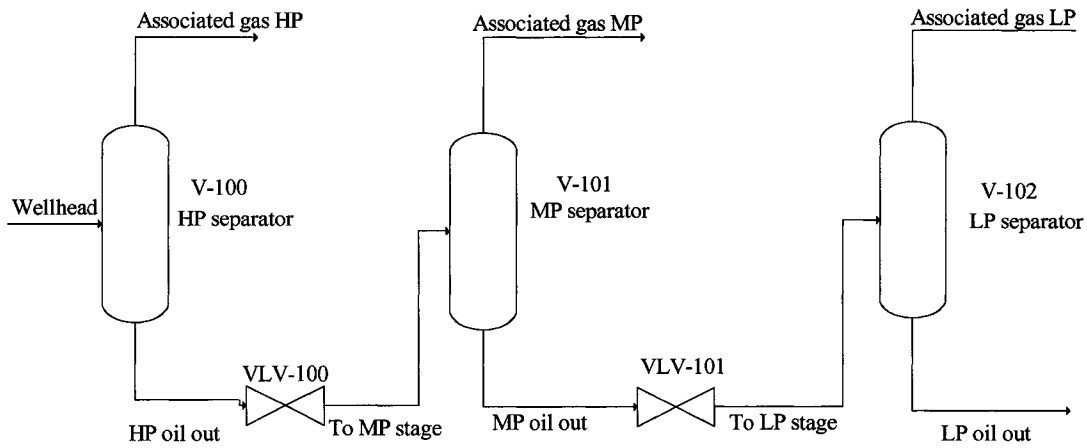

Figure 5.1: Three-stage crude oil separation

The reservoir fluid passes through a three stage separation process, where each stage works at different pressure, to optimize the crude oil production. The three separators operate at 6,998, 1,724 and 413.7 kPa, respectively. Each separator flashes the

lighter gases through the top of the column and concentrates the heavier hydrocarbons in the bottom. In the first stage, the wellhead stream enters a high-pressure separator (V-100). At each stage the pressure of the liquids leaving the separator is reduced to meet the operation criteria and sent to the next separator. The compression ratio at each stage should not be more than four as the compression ratio affect the temperature of the stream. If the compression ratio excesses four, the temperature could be high and special material should be used. Table 5.1 summarizes the inlet and outlet conditions for each separator. In this Table the total molar flow rate of each stream and its percentage of the "*wellhead*" stream are also shown. This process is called the "*Base Process*".

The composition and the molar flow of the "*Wellhead*" stream in this location and the outlet stream from the train ("*LP Out oil*") which reflects the amount of the produced crude oil, are shown in Table 5.2(more information can be found in Beronich, 2006). Also the amount of the recovered hydrocarbons in the process is indicated. The described process before locating any nozzles in the train is called "*Base Process*". The hydrocarbons heavier than ethane can be defined as C_3^+. Therefore, the compositions can be categorized as methane, ethane, C_3^+, CO_2 and N_2.

The value called the Reid Vapour Pressure (RVP) is presented for this stream .where crude oil is concentrated ("*LP oil out* ").The ideal value for RVP is 12 psia, it is safe to store crude oil at atmospheric conditions, for values close to this ideal value. When a high pressure stream is mixed with a low pressure stream, a lot of lower components are added to the stream that might increase the RVP. If the value of RVP

exceeds the ideal value, the crude may flash vapours in storage or transportation, increasing explosion and over-pressure risks. The RVP value obtained in the crude oil product is not necessary high considering that this oil goes to other facilities for further processing. The gas is going to be flashed to break emulsions at near ambient pressure which reduces the RVP value. Table 5.3 shows the crude oil production and RVP in the "*Base Process*".

Table 5.1: Inlet and Outlet conditions for each separator in "*Base Process*"

	Streams	Temperature (°C)	Pressure (kPa)	Molar Flow kgmole/h	Molar Flow (% of wellhead stream)
HP Separator	**"*Wellhead*" Stream**	42.3	6,998.0	19,975.30	100.00%
	"*Associated Gas HP*"	42.3	6,998.0	11,218.87	56.16%
	"*HP Out Oil*"	42.3	6,998.0	8,756.43	43.84%
MP Separator	**"*To MP stage*"**	40.7	1,724.0	8,756.43	43.84%
	"Associated Gas MP	40.7	1,724.0	1,670.81	8.36%
	"MP Out Oil"	40.7	1,724.0	7,085.63	35.47%
LP Separator	**"*To LP stage*"**	38.9	413.7	7,085.63	35.47%
	"*Associated Gas LP*"	38.9	413.7	584.31	2.93%
	"*LP Out Oil*"	38.9	413.7	6,501.32	32.55%

Table 5.2: Mole fractions and molar flow rates of wellhead stream and "*LP out oil*" stream in "*Base Process*"

	Wellhead		LP oil out		
	Mole Fraction	**Molar Flow (kgmole/h)**	**Mole Fraction**	**Molar Flow ((kgmole/h)**	**Recovery (% of wellhead)**
Total	1.000	1,9975.260	1.000	6,501.373	32.547
Methane	0.568	1,1347.100	0.007	45.366	0.400
Ethane	0.064	1,273.280	0.020	126.800	9.959
Propane	0.052	1,039.680	0.059	384.900	37.021
i-Butane	0.006	122.570	0.011	73.360	59.852
n-Butane	0.015	294.160	0.031	200.400	68.126
i-Pentane	0.003	53.350	0.007	44.001	82.477
n-Pentane	0.003	57.680	0.008	49.625	86.035
Hexane	0.001	21.630	0.003	20.358	94.121
C7+	0.278	5,555.290	0.854	5,554.940	99.994
C2 Plus	0.422	8,417.660	0.993	6,454.385	76.677
C3 Plus	0.358	7,144.380	0.973	6,327.585	88.567
N_2	0.009	171.590	0.000	0.041	0.024
CO_2	0.002	38.930	0.000	1.581	4.061

Table 5.3: Crude oil production of "*Base Process*"

	Molar Flow (kgmole/h)	**Recovery (%)**	**RVP (psia)**	**Volume Flow**	
				(m^3/h)	**(bbl/day)**
Total	6,501.37	32.547	19.773	1,382.64	208,716.2
Methane	45.366	0.4	-	2.431	366.963
Ethane Plus	6,454.39	76.677	-	1,380.12	208,336.3
Propane Plus	6,327.59	88.567	-	1,369.4	206,718.1

5.2 NGL RECOVERY USING A SUPERSONIC SEPARATOR

A supersonic separator was placed at different locations within the crude production train to predict the NGL recovery. Depending on the nozzle's location, the inlet conditions such as pressure, temperature, and the flow rate can be different; and therefore a different nozzle should be designed to meet the requirement for each inlet conditions (see Section 3.3). The flow is assumed to be isentropic, steady state, one dimensional and compressible. To design this nozzle the convergence half angle and the divergence half angle of the nozzle are fixed at 6.85° and 3°, respectively. The nozzle inlet diameter is fixed arbitrarily such that the inlet Mach number stays around 0.3-0.4. The maximum and minimum nozzle length can be found by applying the method discussed in Section 4.2 and the total nozzle length is chosen arbitrarily in between the minimum and maximum length.. If shockwave happens in the nozzle, the formed condensates are separated from the main stream before the shockwave. As discussed before in Section 2.1.8, they are a number of ways to separate the condensates from the main stream in the nozzle. The process was simulated in HYSYS simulator as demonstrated in the process flow diagram shown in Figure 5.2. The main stream in the nozzle, which can be in two- or three-phase flow, enters a separator. Vapour and liquid phases are separated and the liquid phase enters a splitter. A complete removal of the liquid is not possible in the nozzle, therefore it is assumed that 75% of the liquid phase will exit from bottom of the splitter and the rest remains in the main stream leaving the

nozzle with the rest of the gas. The top stream from the separator and splitter are mixed and used as the nozzle main stream after the shockwave. The liquid condensates are separated from the main stream in the nozzle. The pressure of the separated liquids should be equal to the operating pressure of the next stage; therefore, the nozzle pressure before the shockwave should stay higher than the operating pressure of the next stage. The following cases very studied to evaluate the increase in crude production using the supersonic nozzle to recover NGLs from associated gases.

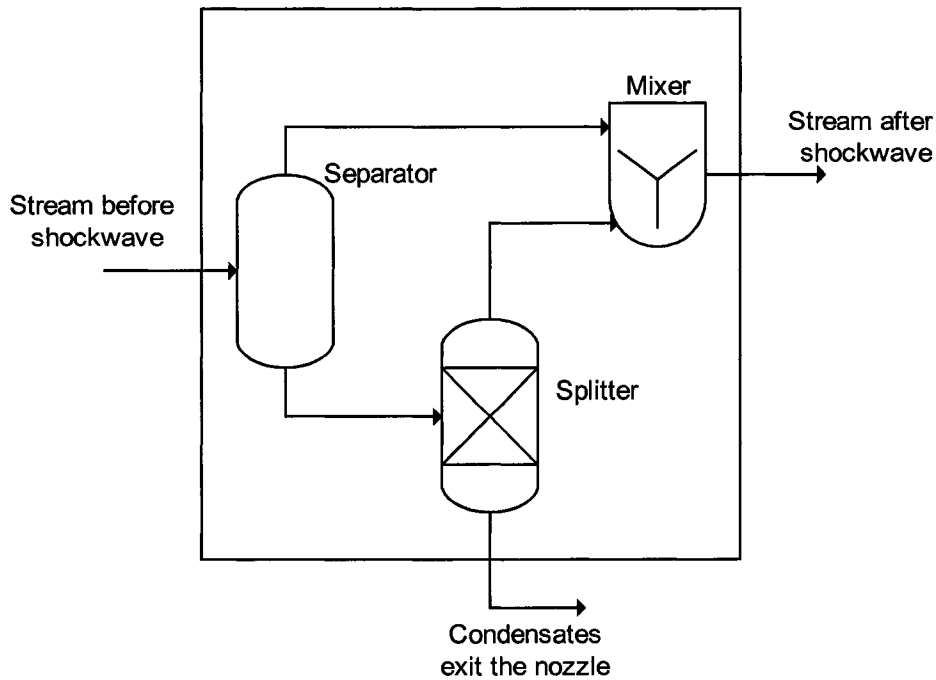

Figure 5.2: HYSYS simulation of condensate separation in the nozzle before the shockwave

5.2.1 Case 1: Supersonic nozzle at HP separator overhead

In Case 1, the supersonic nozzle is located at the overhead of the HP separator. The inlet stream of the nozzle has the same pressure, temperature, and flow rate as "*Associated Gas HP* "Stream (see Table 5.1). In Case 1.A the stream of separated liquids is mixed with the liquids from the HP separator and enters the MP separator and in Case 1.B it is mixed with the liquids from the MP separator and enters the LP separator and in Case 1.C it is mixed with the stream coming out of the train ("*LP oil out*"). Figure 5.3, 5.4, and 5.5 show the schematics of these processes.

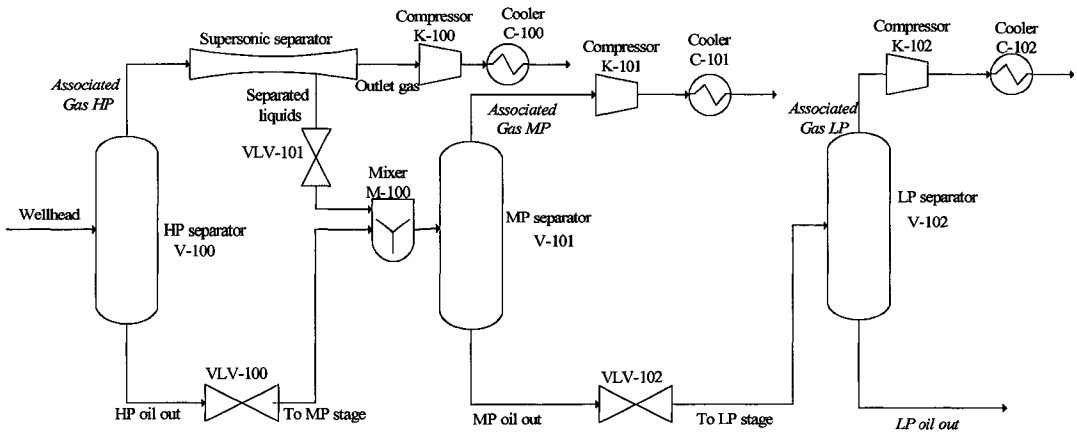

Figure 5.3: Case 1.A: Supersonic nozzle at HP Separator overhead; separated condensates routed to MP Separator

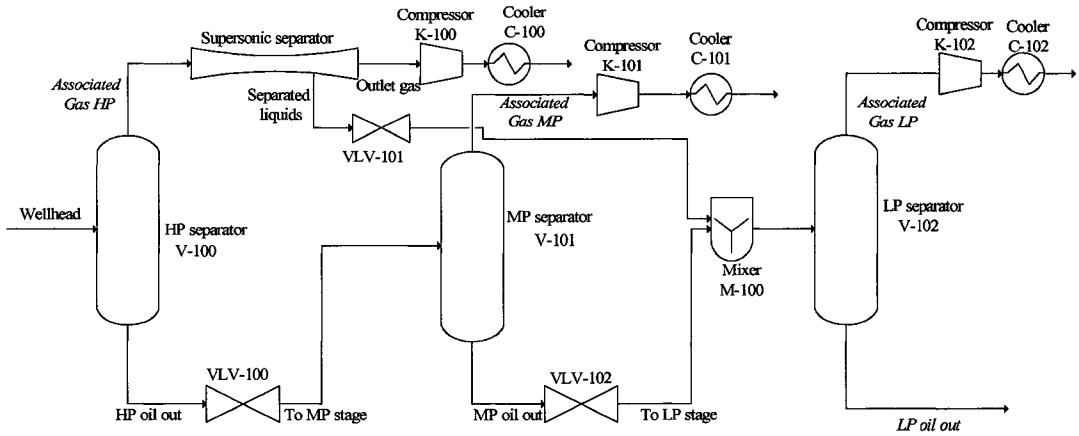

Figure 5.4: Case 1.B: Supersonic nozzle at HP Separator overhead; separated condensates routed to LP Separator

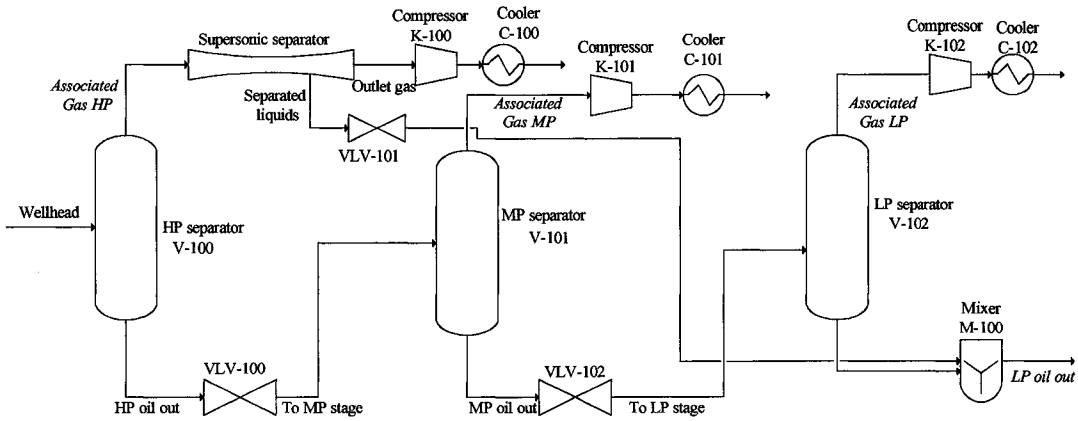

Figure 5.5: Case 1.C- Supersonic nozzle at HP Separator overhead; separated condensates routed to LP Oil Out

The feed stream is the same for these three cases so the same nozzle can be used in all the cases. Table 5.4 shows the designed nozzle geometry for this case.

Table 5.4: Nozzle geometry for case One

Inlet diameter(m)	0.1000
Throat diameter(m)	0.0718
Outlet diameter(m)	0.0910
Converging length(m)	0.1172
Diverging length (m)	0.1828
Total length (m)	0.3000
Length upper bound (m)	0.3000

Figure 5.6 shows the pressure distribution in this nozzle with 70 and 80% of the inlet pressure recovery.

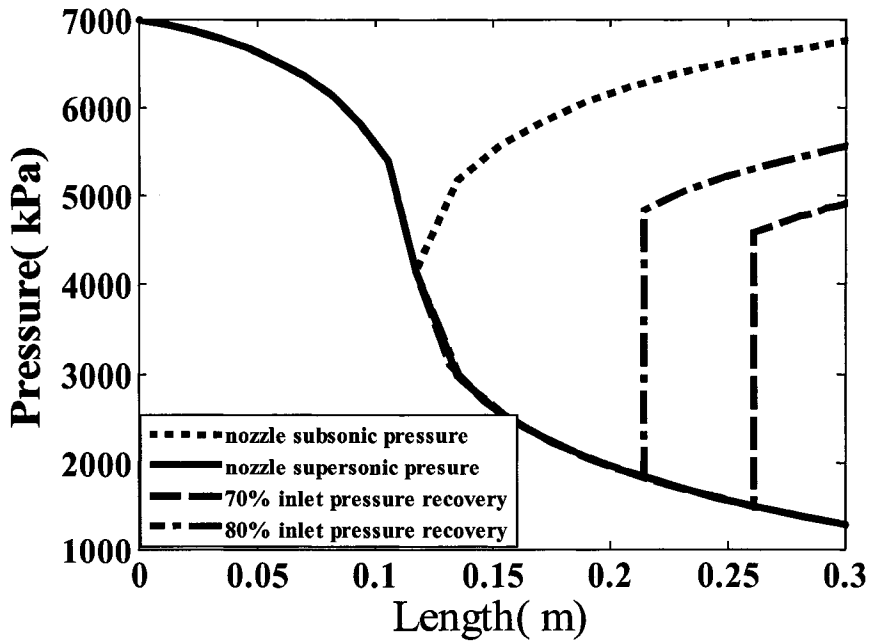

Figure 5.6: Pressure distribution along the nozzle located at HP separator overhead

In Case 1.A, the separated liquids stream enters the MP Separator. Therefore, the nozzle pressure before the shockwave should be higher than the operating pressure of the MP Separator (1,724 kPa). However, the flow has to expand to 1,409 kPa before the shockwave to recover 70% of the inlet pressure (6,998 kPa) at the nozzle exit. This problem does not exist for Cases 1.B and 1.C as the operating pressure is 413.7 kPa. So a nozzle with the backpressure such that 70% of the inlet pressure is recovered can not be used in Case 1.A. But the results of NGL recovery for Cases 1.B and 1.C are compared for the 70% inlet pressure recovery in the nozzle. Table 5.5 indicates the composition, molar flow rate and recovery for "*LP Oil Out*" and Table 5.6 indicates the crude oil production stream and RVP in both processes.

Table 5.5: Mole fractions and molar flow rates for"LP Oil Out" stream for Cases 1.B and 1.C

	Case 1.B			Case 1.C		
	Mole Fraction	**Molar Flow (kgmole/h)**	**Recovery (% of wellhead)**	**Mole Fraction**	**Molar Flow (kgmole/h)**	**Recovery (% of wellhead)**
Total	1.000	6,585.810	32.970	1.000	6,673.420	33.410
Methane	0.007	44.521	0.390	0.011	73.210	0.640
Ethane	0.020	131.370	10.320	0.023	153.680	12.071
Propane	0.065	425.490	40.920	0.068	454.170	43.680
i-Butane	0.013	82.560	67.350	0.013	85.010	69.350
n-Butane	0.034	223.640	76.020	0.034	228.080	77.530
i-Pentane	0.007	47.540	89.100	0.007	47.870	89.720
n-Pentane	0.008	52.920	91.750	0.008	53.170	92.190
Hexane	0.003	20.980	96.990	0.003	21.010	97.120
C7+	0.844	5,555.180	99.990	0.832	5,555.180	99.990
C2 Plus	0.993	6,539.690	77.690	0.989	6,598.190	78.380
C3 Plus	0.973	6,408.317	89.690	0.966	6,444.510	90.200
N2	0.000	0.041	0.024	0.000	0.132	0.076
CO2	0.000	1.558	4.002	0.000	1.885	4.840

Table 5.7: Crude oil production of the Cases 1.B, 1.C for 70% inlet pressure recovery

		Molar Flow (kgmole/h)	**Recovery (%)**	**RVP (psia)**	**Volume Flow**	
					(m^3/h)	**(bbl/day)**
Case 1.B	**Total**	6,585.810	32.970	20.960	1,390.621	20,9921.534
	Methane	44.521	0.390	-	2.387	360.306
	C2 Plus	6,539.690	77.690	-	1,388.150	209,548.468
	C3 Plus	6,408.317	89.690	-	1,377.049	207,872.756
Case 1.C	**Total**	6,673.420	33.410	24.260	1,397.244	210,921.228
	Methane	73.210	0.640	-	3.909	590.070
	C2 Plus	6,598.190	78.380	-	1,393.230	210,315.328
	C3 Plus	6,444.510	90.200	-	1,380.268	208,358.677

The "*LP Oil Out*"in the"*Base Process*" before and after the nozzle is placed, are

compared. This comparison shows that in Case 1.B, methane concentration is lower than "*Base Process*" but the concentrations of all other components are higher.

Figure 5.7 reflects the comparison between the phase envelope of the "*Base Process*" and Cases 1.B and 1.C for the "*LP Oil Out*" stream. As the stream becomes richer in lighter hydrocarbons, the bubble point curve expands toward the lower bubble point temperatures.

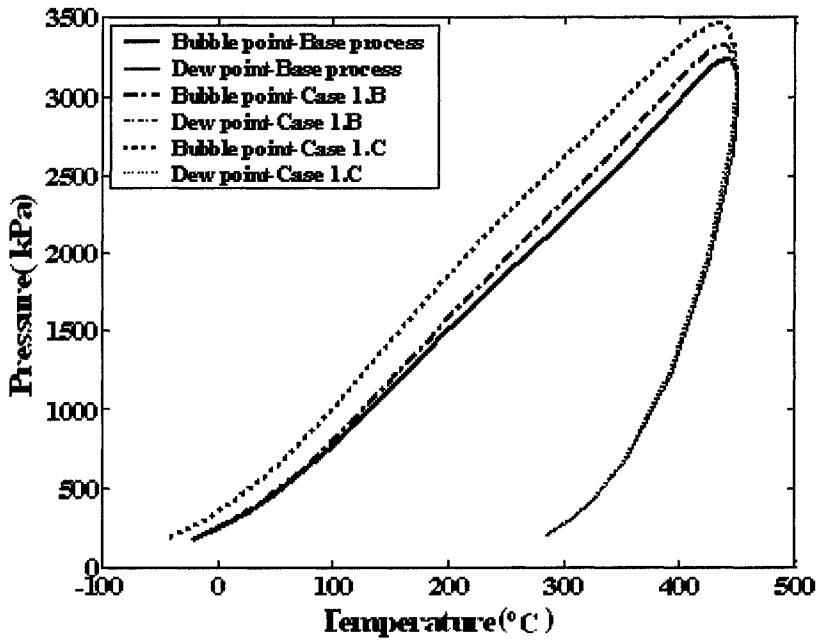

Figure 5.7: Phase envelopes for the stream "*LP Oil Out*" for "*Base Process*", Cases 1.B and 1.C with 70% inlet pressure recovery in the nozzle

As mentioned earlier, the nozzle pressure before shockwave should be kept higher than the previous case(70%) if it is desirable to locate any nozzles in case 1.A. Therefore, the a nozzle with same geometry is used in this case. The operation conditions are adjusted such that the back pressure of the nozzle is equal to 80% of the inlet pressure.

The mole fractions and the molar flow rates for "*LP Oil Out* "for three processes of case one are shown in Table 5.7. Comparison of the cases with the "*Base Process*" indicates that the lighter hydrocarbons concentration as well as the heavier components concentration is higher when a nozzle is placed in the process. Table 5.6 indicates the crude oil production stream and RVP in three processes in case one.

Table 5.7: Mole fractions and molar flow rates for"LP Oil Out" stream for three processes in case one for 80% pressure recovery

	Case 1.A			Case 1.B			Case 1.C		
	Mole Fraction	**Molar Flow (kgmole/h)**	**Recovery (% of wellhead)**	**Mole Fraction**	**Molar Flow (kgmole/h)**	**Recovery (% of wellhead)**	**Mole Fraction**	**Molar Flow (kgmole/h)**	**Recovery (% of wellhead)**
Total	1.000	6,553.150	32.810	1.000	6,553.250	32.810	1.000	6,605.190	33.070
Methane	0.007	44.910	0.400	0.007	45.020	0.400	0.010	63.360	0.560
Ethane	0.020	129.480	10.170	0.020	129.030	10.130	0.021	141.670	11.130
Propane	0.062	406.310	39.080	0.062	406.570	39.110	0.064	422.540	40.640
i-Butane	0.012	79.000	64.450	0.012	79.100	64.540	0.012	80.580	65.740
n-Butane	0.033	216.080	73.460	0.033	216.270	73.520	0.033	219.100	74.480
i-Pentane	0.007	46.960	88.030	0.007	46.960	88.030	0.007	47.200	88.460
nPentane	0.008	52.550	91.110	0.008	52.540	91.090	0.008	52.720	91.400
Hexane	0.003	20.970	96.960	0.003	20.970	96.930	0.003	20.980	97.010
C7+	0.848	5,555.190	100.000	0.848	5,555.190	100.000	0.841	5,555.190	100.000
C2 Plus	0.993	6,506.540	77.300	0.990	6,506.620	77.300	0.990	6,539.970	77.690
C3 Plus	0.973	6,377.060	89.260	0.970	6,377.600	89.270	0.970	6,398.300	89.560
N2	0.000	0.040	0.020	0.000	0.040	0.020	0.000	0.110	0.060
CO2	0.000	1.580	4.070	0.000	1.570	4.020	0.000	1.760	4.520

Table 5.8: Crude oil production of the three processes in case one for 80% inlet pressure recovery

		Molar Flow (kgmole/h)	Recovery (%)	RVP (psia)	Volume Flow	
					(m^3/h)	(bbl/day)
Case 1.A	**Total**	6,553.150	32.810	20.453	1,387.671	209,476.151
	Methane	44.910	0.400	-	2.407	363.336
	C2 Plus	6,506.540	77.300	-	1,385.178	209,099.822
	C3 Plus	6,377.060	89.260	-	1,374.230	207,447.164
Case 1.B	**Total**	6,553.250	32.810	20.446	1,387.681	209,477.663
	Methane	45.020	0.400	-	2.412	364.104
	C2 Plus	6,506.620	77.300	-	1,385.189	209,101.483
	C3 Plus	6,377.600	89.270	-	1,374.276	207,454.108
Case 1.C	**Total**	6,605.190	33.070	22.471	1,391.626	210,073.181
	Methane	63.360	0.560	-	3.396	512.644
	C2 Plus	6,539.970	77.690	-	1,388.133	209,545.895
	C3 Plus	6,398.300	89.560	-	1,376.155	207,737.753

The composition differences in Stream "*LP Oil Out*" are also reflected in the phase envelopes. The envelopes for both processes are shown in Figure 5.8. The dew point curves of these processes are similar; however, the bubble point curve for Case one is above the bubble point of the "*Base Process*". The reason is that the stream is richer in lighter hydrocarbons, which expands the two-phase region of the envelope towards lower bubble point temperatures.

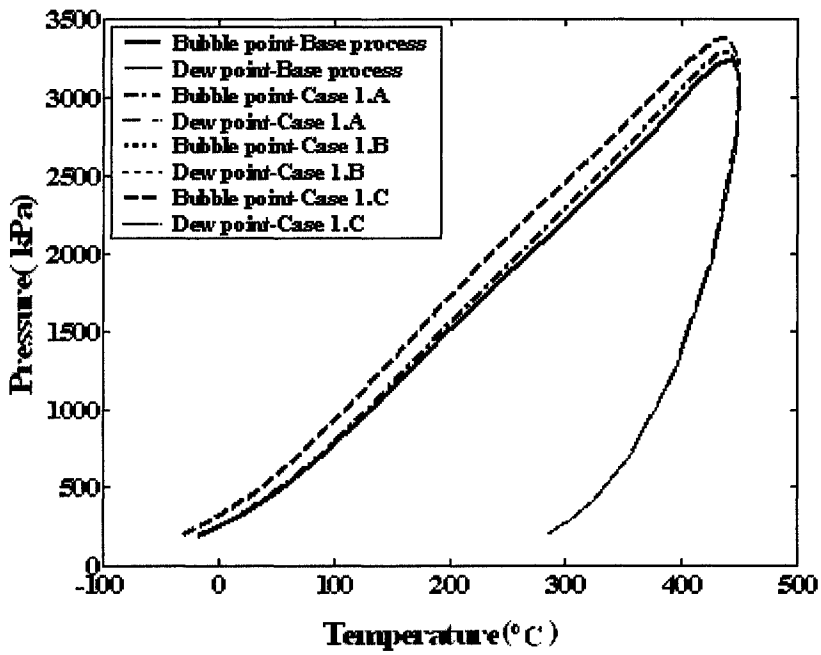

Figure 5.8: Phase envelopes for Stream "*LP Oil Out*" for "*Base Process*", Cases 1.A, 1.B and 1.C with 80% inlet pressure recovery in the nozzle

For the latter case (80% of inlet pressure recovery), the same results for the NGL recovery can be obtained by designing a shorter nozzle where 70% of the inlet pressure (exit pressure = 4,898 kPa) will be recovered. This length will be 0.2203 *m*.

5.2. 2 Case 2: Supersonic nozzle at MP Separator overhead

In this case the supersonic nozzle is located at overhead of the MP Separator; therefore the nozzle inlet stream is "*Associated Gas MP*". The pressure of separated liquid stream from the supersonic nozzle is adjusted to meet the operating pressure of the LP Separator and it is mixed with the Stream "*To LP Stage* " in Case 2.A and the stream

from bottom of the LP Separator in Case 2.B. The schematic of these two processes are shown in Figures 5.9 and 5.10.

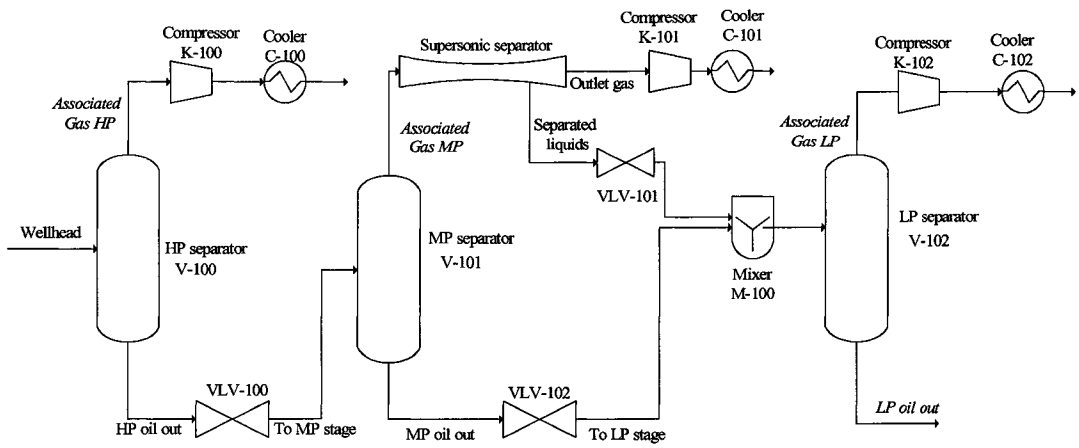

Figure 5.9: Case 2.A: Supersonic nozzle at MP Separator overhead; separated condensates routed to LP Separator

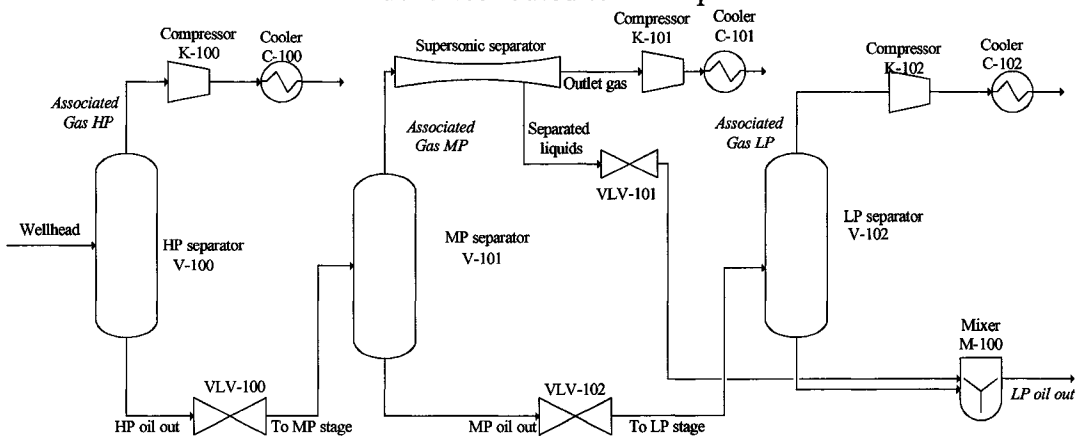

Figure 5.10: Case 2.B: Supersonic nozzle at MP Separator overhead; separated condensates routed to LP Oil Out

A nozzle with the geometry shown in Table 5.9 is designed for this purpose.

Table 5.9: Nozzle geometry for case two

Inlet diameter(m)	0.1000
Throat diameter(m)	0.0605
Outlet diameter(m)	0.0747
Converging length(m)	0.1644
Diverging length (m)	0.1356
Total length (m)	0.3000
Length upper bound (m)	0.4000

As shown in Figure 5.11, if the recovery of 70% of the inlet pressure is obtained, the nozzle pressure before the shockwave is (359.64 kPa) which is lower than the operating pressure of LP Separator. Therefore, the pressure before shockwave should stay higher. If the backpressure is adjusted at 80% of the inlet pressure, the pressure in side the nozzle and before the shockwave will be 466.47 kPa, which is higher than LP separator operating pressure (413.7 kPa). The supersonic nozzle used in this processes is considered to have a pressure recovery of 80%.

Table 5.10 and Figure 5.12 outline the composition of Stream "*LP Oil Out*" in Cases 2.A and 2.B. Comparison of these processes with the "*Base Process*" show that the composition will remain almost the same when a supersonic nozzle is introduced after the MP separator. Plotting the results for the three cases results in almost overlapped lines . Table 5.11 presents the crude oil production and the RVP of the "*LP oil out*"stream in case 2.

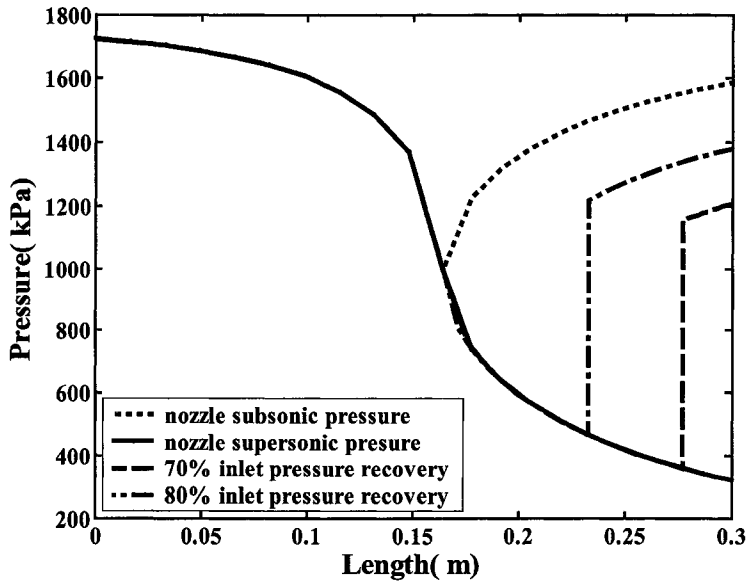

Figure 5.11: Pressure distribution along the nozzle located at MP Separator overhead with 80% inlet pressure recovery

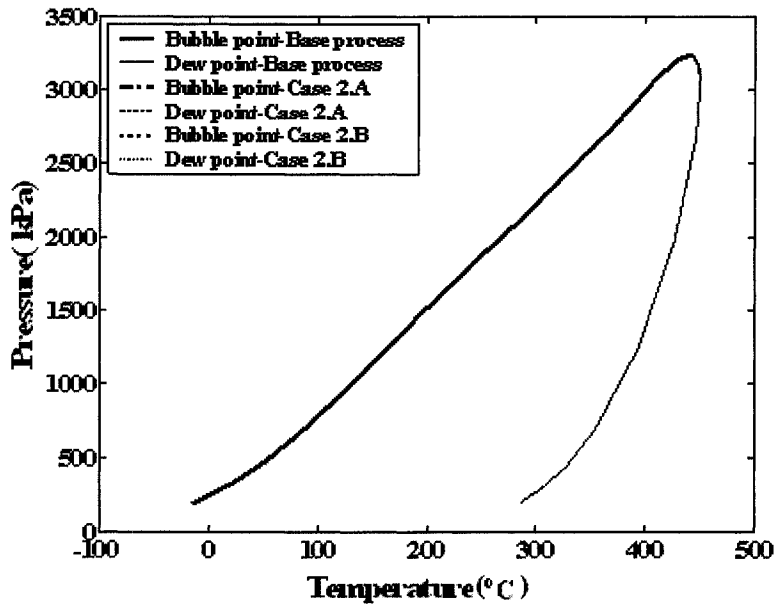

Figure 5.12: Phase envelopes for Stream "*LP Oil Out*" for "*Base Process*" and Case 2 with 80% inlet pressure recovery

Table 5.10: Mole fractions and molar flow rates of"*LP Oil Out*" Stream in Case 2 with 80% inlet pressure recovery

	Case 2.A			Case 2.B		
	Mole Fraction	**Molar Flow (kgmole/h)**	**Recovery (% of wellhead)**	**Mole Fraction**	**Molar Flow (kgmole/h)**	**Recovery (% of wellhead)**
Total	1.000	6,501.550	32.550	1.000	6,501.430	32.550
Methane	0.007	45.370	0.400	0.007	45.370	0.400
Ethane	0.020	126.800	9.960	0.020	126.810	9.960
Propane	0.059	384.910	37.020	0.059	384.920	37.020
i-Butane	0.011	73.360	59.850	0.011	73.360	59.850
n-Butane	0.031	200.410	68.130	0.031	200.410	68.130
i-Pentane	0.007	44.000	82.480	0.007	44.000	82.480
n-Pentane	0.008	49.630	86.040	0.008	49.630	86.040
Hexane	0.003	20.360	94.130	0.003	20.360	94.140
C7+	0.854	5,554.950	99.990	0.854	5,554.950	99.990
C2 Plus	0.993	6,454.440	76.680	0.993	6,454.440	76.680
C3 Plus	0.973	6,327.640	88.570	0.973	6,327.640	88.570
N2	0.000	0.040	0.020	0.000	0.040	0.020
CO2	0.000	1.580	4.060	0.000	1.580	4.060

Table 5.11: Crude oil production of the three processes in case 2 for 80% inlet pressure recovery

		Molar Flow (kgmole/h)	**Recovery (%)**	**RVP (psia)**	**Volume Flow**	
					(m^3/h)	**(bbl/day)**
Case 2.A	**Total**	6,501.550	32.550	19.774	1382.643	208717.151
	Methane	45.370	0.400	-	2.431	366.972
	C2 Plus	6,454.440	76.680	-	1380.126	208337.211
	C3 Plus	0.993	88.570	-	1369.406	206718.957
Case 2.B	**Total**	6,501.430	32.550	19.774	1382.643	208717.151
	Methane	45.370	0.400	-	2.431	366.972
	C2 Plus	6,454.440	76.680	-	1380.126	208337.196
	C3 Plus	6,327.640	88.570	-	1369.406	206718.957

A shorter nozzle with the length of 0.2523 *m* can be designed to recover 70% of the inlet pressure with the same result in the stream composition.

5.2.3 Case 3: Supersonic nozzle at LP Separator overhead

Figure 5.13 shows the process that the supersonic nozzle is places at the overhead of LP Separator and the separated liquid stream from the nozzle is mixed with the stream from the bottom of the LP Separator after the pressure reduction. The feed stream of the nozzle is "*Associated Gas LP*" .This stream has a very low pressure and any small reduction in pressure of the stream can cause it to fall below the LP separator operating pressure , so the supersonic nozzle can not be placed after the LP separator

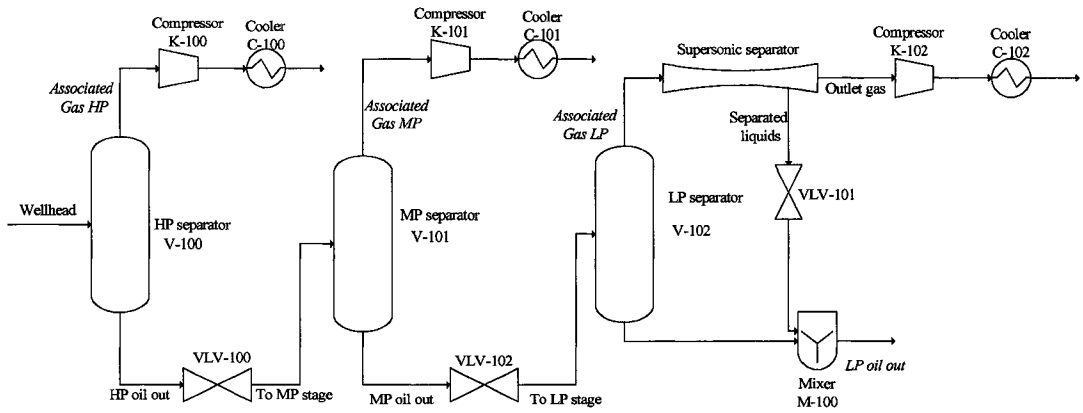

Figure 5.13: Case 3: Supersonic nozzle at LP Separator overhead; separated condensates routed to LP Oil Out

In the following cases, the pressure of the stream separated from the top of the separators is increased; the stream is cooled and entered the supersonic nozzle.

5.2.4 Case 4: Supersonic nozzle at HP compressor discharge

The pressure of the "*Associated Gas HP*"stream from the HP separator is 6,998 kPa, this pressure is increased to 10,000 kPa in a compressor and cooled to the stream initial temperature. So the inlet properties are the same as the "*Associated Gas HP*" except the pressure which is 10,000 kPa. This stream is entered the supersonic nozzle. A nozzle with the geometry shown in Table 5.11 is designed for this condition. The nozzle backpressure is adjusted to recover 70% of the inlet nozzle pressure (7,000 kPa).

Table 5.11: Nozzle geometry for Case 4

Inlet diameter(m)	0.0800
Throat diameter(m)	0.0586
Outlet diameter(m)	0.0778
Converging length(m)	0.0891
Diverging length (m)	0.1829
Total length (m)	0.2720
Length upper bound (m)	0.2720

Three processes were considered in this case. In case 4.A the "*separated liquids*" stream is mixed with "*HP Oil Out*" and entered MP Separator, in Case 4.B, it is mixed with "*MP Oil Out*" and enters LP Separator and in the last case (Case 4.C) it is mixed with the stream from the bottom of the LP separator (See Figure 5.14 to 5.16).

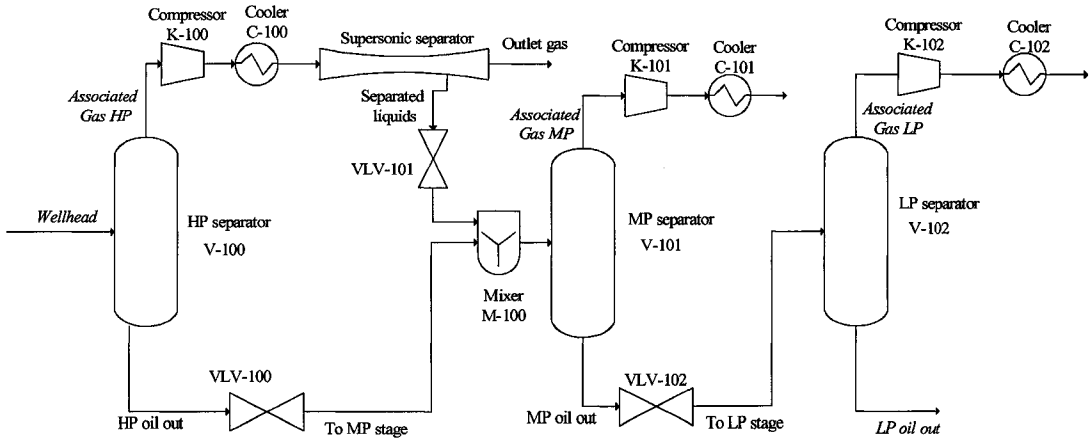

Figure 5.14: Case 4.A: Supersonic separator at HP compressor discharge; separated condensates routed to MP Separator

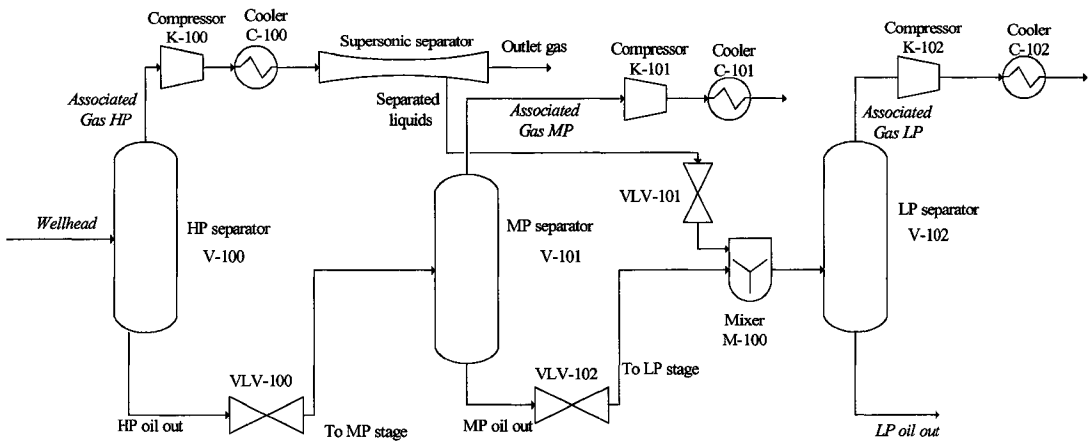

Figure 5.15: Case 4.B: Supersonic separator at HP compressor discharge; separated condensates routed to LP Separator

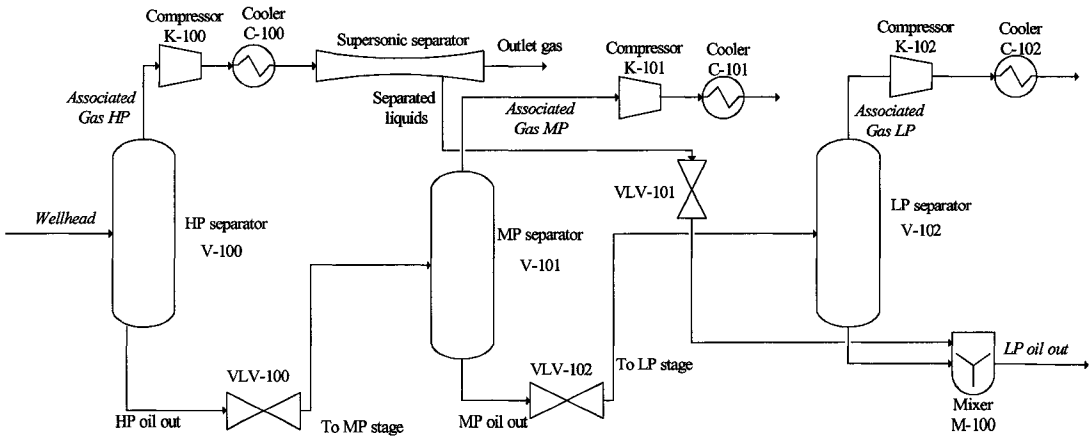

Figure 5.16: Case 4.C: Supersonic separator at HP compressor discharge; separated condensates routed to LP Oil Out

Figure 5.17 indicates the pressure distribution along the nozzle with 70 % recovery of the inlet pressure. As it can be seen the pressure before the shockwave is above the operating pressures of the MP and LP separators. In Table5.12 the mole fractions and mole flows of each component of the "*LP Oil Out*" stream are shown. This stream is richer in lighter hydrocarbons in this case than the same stream in the "*Base Process*" which results in the bubble point curve expansion toward the lower bubble point temperatures (see Figure 5.18).Table 5.13 shows the crude oil production and RVP for the "*LP oil out* " stream in case 4.

Table 5.12: Mole fractions and molar flow rates for Stream"*LP Oil Out*" in Case 4 with 70% inlet pressure recovery

	Case 4.A			Case 4.B			Case 4.C		
	Mole Fraction	**Molar Flow (kgmole/h)**	**Recovery (% of wellhead)**	**Mole Fraction**	**Molar Flow (kgmole/h)**	**Recovery (% of wellhead)**	**Mole Fraction**	**Molar Flow (kgmole/h)**	**Recovery (% of wellhead)**
Total	1.000	6,622.790	33.150	1.000	6,613.900	33.110	1.000	6,808.270	34.080
Methane	0.010	43.660	0.380	0.010	44.330	0.390	0.020	116.270	1.020
Ethane	0.020	137.030	10.760	0.020	135.150	10.610	0.030	185.810	14.590
Propane	0.070	450.050	43.290	0.070	445.510	42.850	0.070	503.050	48.380
i-Butane	0.010	85.180	69.500	0.010	84.450	68.900	0.010	88.820	72.460
n-Butane	0.030	228.150	77.560	0.030	226.310	76.930	0.030	234.060	79.570
i-Pentane	0.010	47.800	89.590	0.010	47.550	89.130	0.010	48.140	90.230
n-Pentane	0.010	53.100	92.060	0.010	52.870	91.660	0.010	53.330	92.460
Hexane	0.000	21.000	97.080	0.000	20.960	96.910	0.000	21.010	97.140
C7+	0.840	5,555.190	100.000	0.840	5,555.190	100.000	0.820	5,555.190	100.000
C2 Plus	0.990	6,577.490	78.140	0.990	6,567.990	78.030	0.980	6,689.410	79.470
C3 Plus	0.970	6,440.460	90.150	0.970	6,432.840	90.040	0.960	6,503.600	91.030
N_2	0.000	0.040	0.020	0.000	0.040	0.020	0.000	0.290	0.170
CO_2	0.000	1.600	4.100	0.000	1.540	3.950	0.000	2.300	5.920

Table 5.13: Crude oil production of the three processes in case 4 for 70% inlet pressure recovery

		Molar Flow (kgmole/h)	Recovery (%)	RVP (psia)	Volume Flow	
					(m^3/h)	(bbl/day)
Case 4.A	Total	6,622.790	33.150	21.717	1394.047	210438.644
	Methane	43.660	0.380	-	210438.6924	31766814.895
	C2 Plus	6,577.490	78.140	-	353.1708843	53312.981
	C3 Plus	6,440.460	90.150	-	1380.036	208323.610
Case 4.B	Total	6,613.900	33.110	21.567	1393.207	210311.841
	Methane	44.330	0.390	-	210311.8663	31747669.835
	C2 Plus	6,567.990	78.030	-	358.5699143	54127.993
	C3 Plus	6,432.840	90.040	-	1379.322	208215.828
Case 4.C	Total	6,808.270	34.080	29.328	1407.755	212507.938
	Methane	116.270	1.020	-	212508.5081	32079264.348
	C2 Plus	6,689.410	79.470	-	940.538945	141979.245
	C3 Plus	6,503.600	91.030	-	1385.685	209176.356

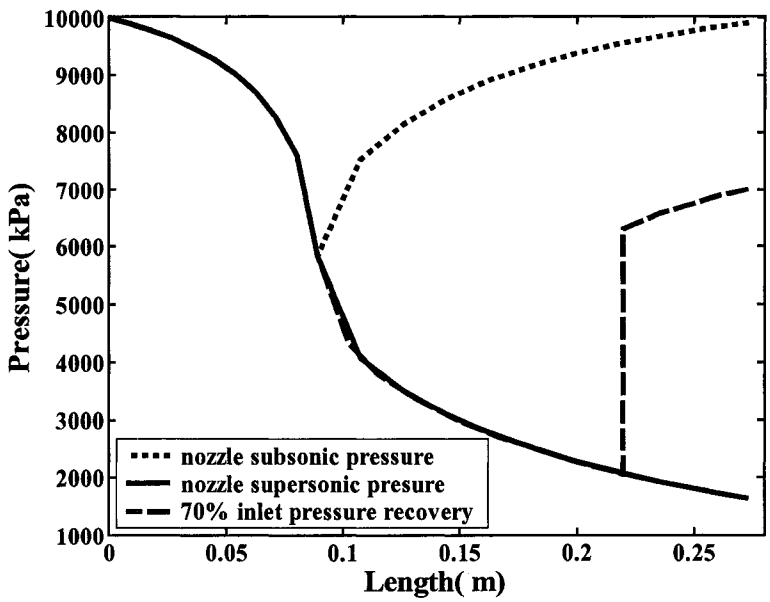

Figure 5.17: Pressure distribution along the nozzle with 70% pressure recovery in Case 4

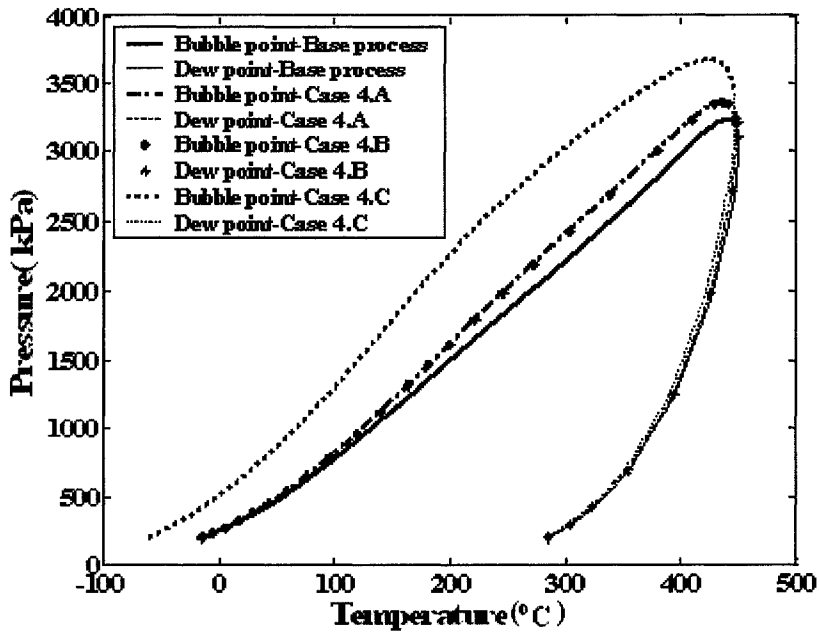

Figure 5.18: Phase envelopes for Stream "*LP Oil Out*" for "*Base Process*" and Case 4 with 70% pressure recovery

5.2.5 CASE 5: SUPERSONIC SEPARATOR AT MP COMPRESSOR DISCHARGE

The pressure of "*Associated Gas MP*"is 1,724 kPa, this pressure with the pressure compression ratio of 4 (6,896 kPa) cooled to the initial stream temperature (40.72 °C). The inlet properties are the same as the "*Associated Gas MP*" except the pressure which is 6,896 kPa. This stream enters the supersonic nozzle. A nozzle with the geometry shown in Table 5.14 is designed for this condition. The nozzle backpressure is adjusted to recover 70% of the inlet nozzle pressure (4,827 kPa).

Table 5.14: Nozzle geometry for case 5

Inlet diameter(m)	0.0400
Throat diameter(m)	0.0284
Outlet diameter(m)	0.0391
Converging length(m)	0.0481
Diverging length (m)	0.1019
Total length (m)	0.1500
Length upper bound (m)	0.1500

Two different processes are considered in this case, the "*separated liquids*" stream from the supersonic nozzle is mixed with "*MP Oil Out*" stream from the bottom of MP Separator and it is entered LP Separator in Case 5.A and mixed with the stream from the bottom of LP Separator in Case 5.B. These two processes are shown in Figures 5.19 and 5.20. As shown in Figure 5.21, the pressure upstream of the shockwave is above the MP and LP separators operating pressures and as a result, this nozzle with 70% of the inlet pressure recovery can be used in the system.

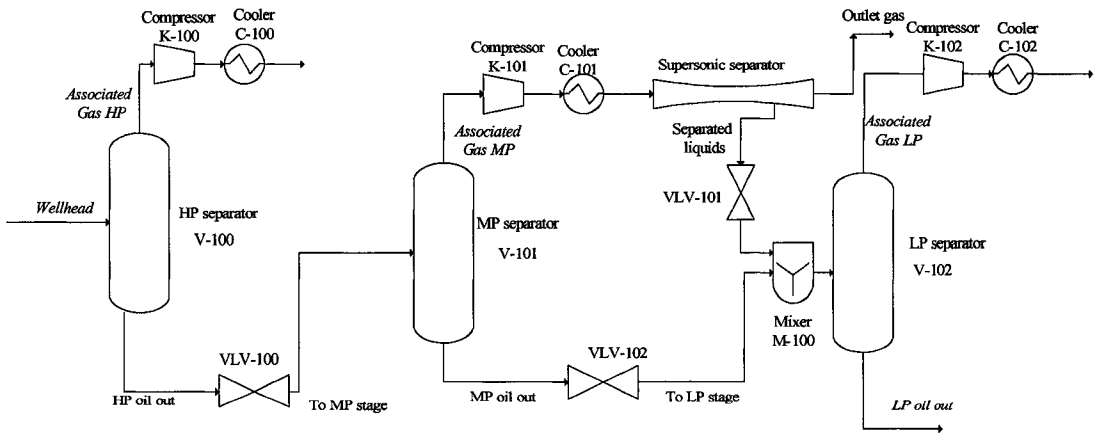

Figure 5.19: Case 5.A: Supersonic separator at MP compressor discharge; separated condensates routed to LP Separator

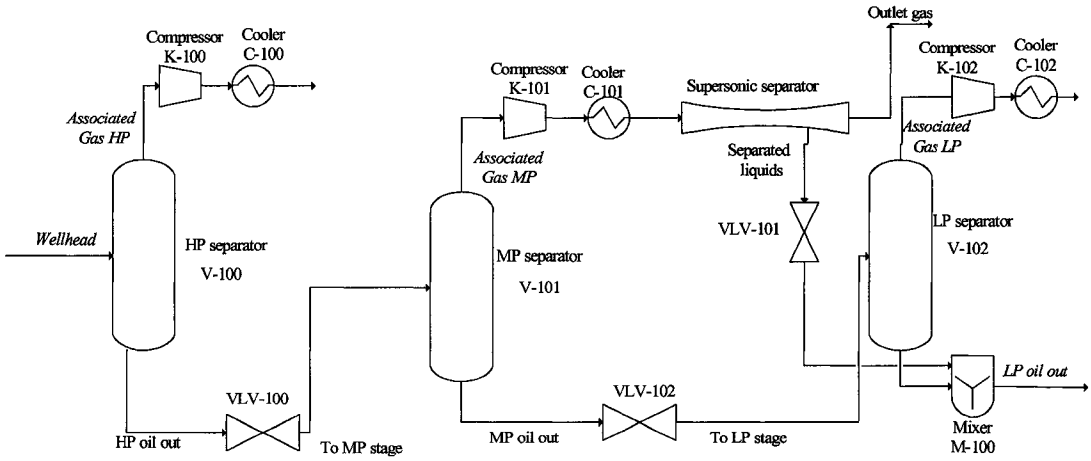

Figure 5.20: Case 5.B: Supersonic separator at MP compressor discharge; separated condensates routed to LP Oil Out

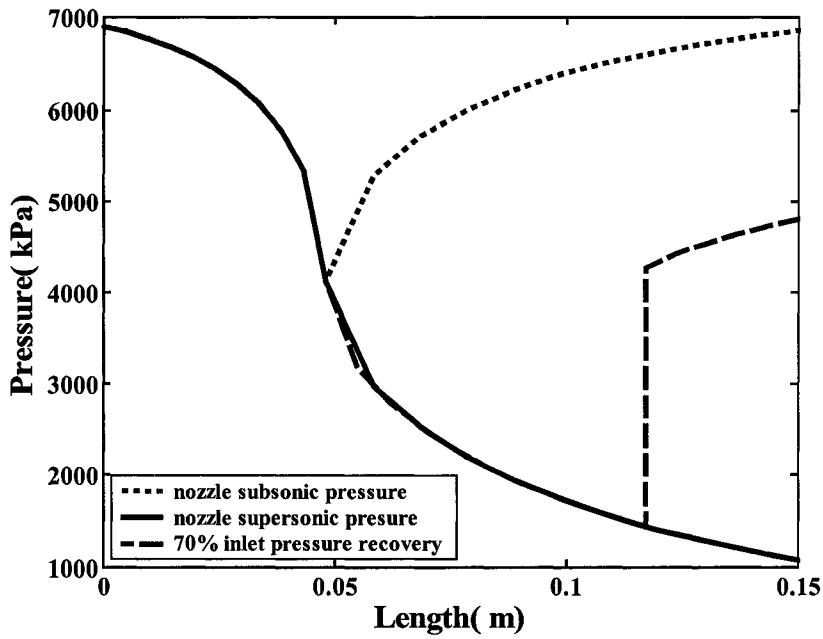

Figure 5.21: Pressure distribution along the nozzle with 70% pressure recovery in Case 5

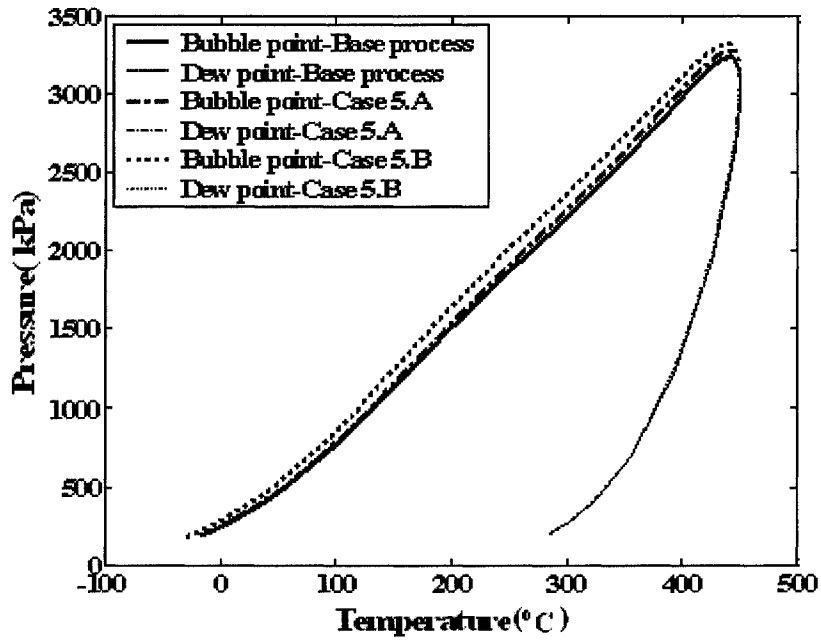

Figure 5.22: Phase envelopes for the stream "*LP Oil Out*" for "*Base Process*" and Case 5 with 70% pressure recovery

In Table5.15, the mole fractions and mole flows of each component of the "*LP oil out*" stream in case Five are shown. This stream is richer in lighter hydrocarbons in this case, especially in case 5.B, than the same stream in the "*Base process*" which results in the bubble point curve expansion toward the lower bubble point temperatures (see Figure 5.22).Table 5.16 shows the crude oil production and RVP for the *"LP oil out"* stream for the case 5 .

Table 5.15: Mole fractions and molar flow rates for Stream "*LP Oil Out*" for two processes in Case 5

	Case 5.A			Case5.B		
	Mole Fraction	**Molar Flow (kgmole/h)**	**Recovery (% of wellhead)**	**Mole Fraction**	**Molar Flow (kgmole/h)**	**Recovery (% of wellhead)**
Total	1.000	6,537.920	32.730	1.000	6,575.860	32.920
Methane	0.007	44.580	0.390	0.008	54.650	0.480
Ethane	0.020	130.190	10.220	0.022	141.600	11.120
Propane	0.062	405.540	39.010	0.064	418.920	40.290
i-Butane	0.012	76.800	62.660	0.012	77.770	63.450
n-Butane	0.032	208.320	70.820	0.032	210.020	71.400
i-Pentane	0.007	44.960	84.270	0.007	45.080	84.500
n-Pentane	0.008	50.470	87.510	0.008	50.570	87.670
Hexane	0.003	20.490	94.720	0.003	20.500	94.770
C_7^+	0.850	5,554.950	99.990	0.845	5,554.950	99.990
C_2 Plus	0.993	6,491.730	77.120	0.991	6,519.420	77.450
C_3 Plus	0.973	6,361.540	89.040	0.970	6,377.810	89.270
N_2	0.000	0.040	0.020	0.000	0.060	0.030
CO_2	0.000	1.580	4.050	0.000	1.740	4.470

Table 5.16: Crude oil production of the three processes in case 5 for 70% inlet pressure recovery

		Molar Flow (kgmole/h)	**Recovery (%)**	**RVP (psia)**	**Volume Flow**	
					(m^3/h)	**(bbl/day)**
Case 5.A	**Total**	6,537.92	32.73	20.38	1,386.05	209,231.52
	Methane	44.58	0.39	-	2.39	360.57
	C2 Plus	6,491.73	77.12	-	1,383.58	208,858.04
	C3 Plus	0.991	89.04	-	1,372.57	207,196.56
Case 5.B	**Total**	6,575.86	32.92	21.78	1,389.02	209,680.50
	Methane	54.65	0.48	-	2.93	442.09
	C2 Plus	6,519.42	77.45	-	1,386.00	209,224.12
	C3 Plus	6,377.81	89.27	-	1,374.03	207,417.01

5.2.6 CASE 6: SUPERSONIC SEPARATOR AT LP COMPRESOR DISCHARGE

In Case 6, the possibility of locating the supersonic nozzle with 70% of pressure recovery at the discharge of LP compressor is investigated (see Figure 5.23).

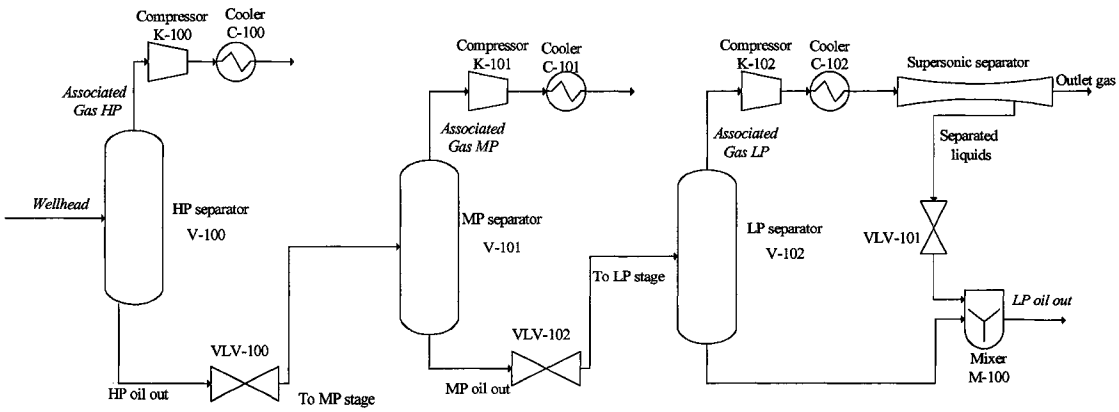

Figure 5.23: Case 6: Supersonic separator at LP compressor discharge; separated condensates routed to LP Oil Out

The pressure of Stream "*Associated Gas LP*"is increased to 1,655 kPa with the compression ratio of 4, cooled to the same temperature as the temperature before the compressor and entered the supersonic nozzle. This stream has the same inlet properties as the "*Associated Gas LP*"with a higher pressure. Table 5.17 shows the geometry of the nozzle designed with this stream as the working fluid. The pressure upstream of the shockwave should be kept above the operating pressure of LP Separator as it is the pressure of the stream exiting the bottom of LP Separator. As shown in Figure 5.24, if backpressure of the nozzle is adjusted to recover 70% of the inlet pressure, the pressure upstream of the shockwave will fall below the operating pressure of LP Separator (413.7

kPa) and as a result, such a nozzle can not be located in this position.

Table 5.17: Nozzle geometry for Case 6

Inlet diameter(m)	0.0520
Throat diameter(m)	0.0385
Outlet diameter(m)	0.0484
Converging length(m)	0.0559
Diverging length (m)	0.0941
Total length (m)	0.1500
Length upper bound (m)	0.1500

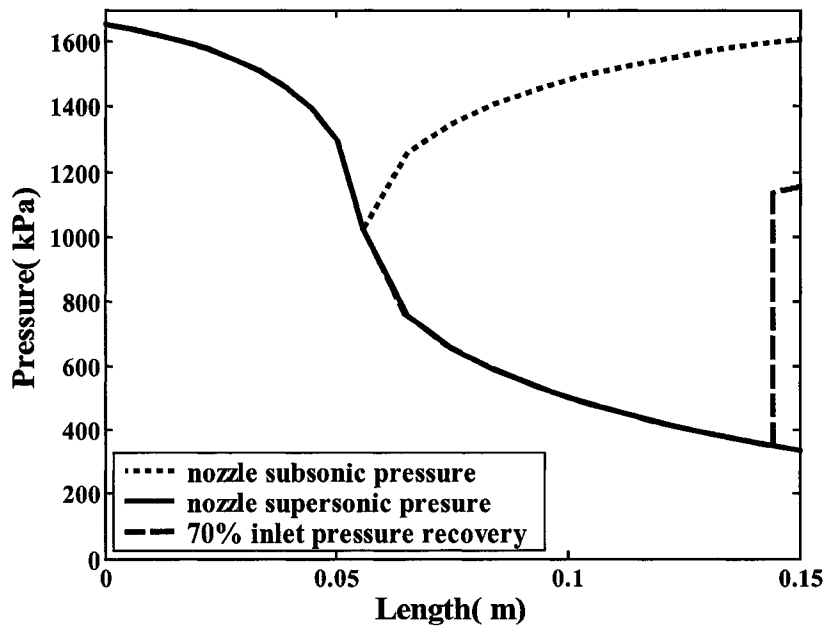

Figure 5.24: Pressure distribution along the nozzle with 70% pressure recovery in Case 6

5.2.7 CASE 7: NOZZLES AT OVERHEADS OF HP AND MP COMPRESSORS

As shown in the previous cases, it is more efficient to locate the nozzle after the compressor of each separator. Two processes are considered in this case. In the Case 7.A the stream "*separated liquids*" from the HP nozzle is mixed with the stream "*HP Oil Out* " and entered MP Separator after pressure adjustment. The same stream from MP nozzle is mixed with "*MP Oil Out*" and entered the LP separator. In Case 7.B the stream "*separated liquids*" from both nozzles are mixed with the "*MP Oil Out*" and entered LP Separator. These processes are outlined in Figures 5.25 and 5.26.

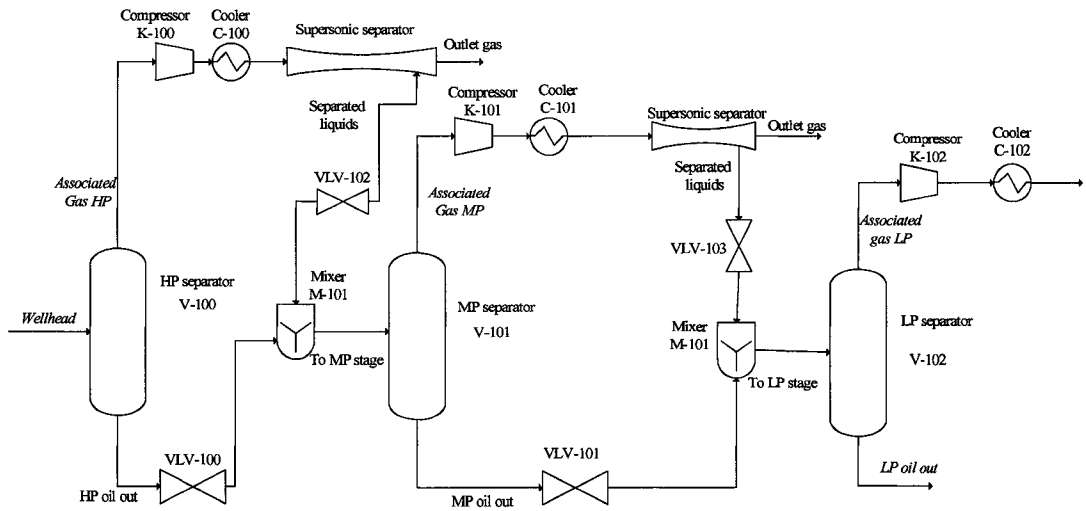

Figure 5.25: Case 7.A: Two supersonic nozzles at discharges of HP and MP compressors; separated liquids to MP and LP separators

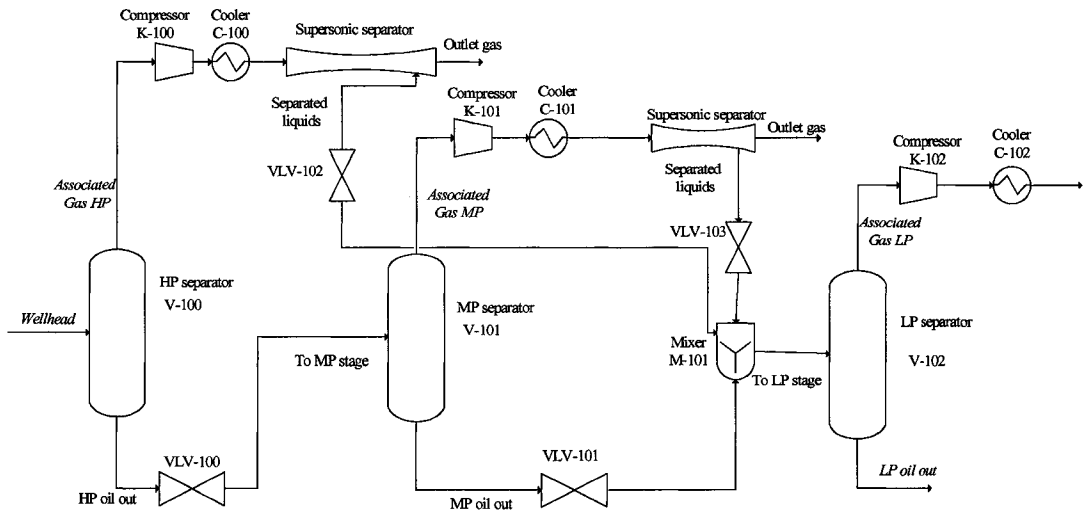

Figure 5.26: Case 7.B: Two supersonic nozzles at discharges of HP and MP compressors; separated liquids to LP Separator

The first nozzle, "*HP nozzle*", is located after the HP compressor. The inlet properties and therefore the nozzle geometry are the same as Case 4. The other nozzle,"*MP nozzle*", is located after the MP compressor. The inlet pressure and temperature is the same as Case 5 but the molar flow rate (1,797 kmole/h) is higher than that of Case 5. The nozzlespecifications designed for this purpose are listed in Table 5.18. The pressure distributions in the "*HP and MP nozzles*" in Case 7.A, show that the nozzles can be used in the system because the pressure upstream of the shockwave in the nozzle is higher than the operating pressure of the next stage (see Figure 5.17 and Figure 5.27). In Case 7.B, the inlet stream for both nozzles is the "*Associated Gas HP*" and "*Associated Gas MP*", respectively as the "*separated liquids*" from both nozzles are entered the LP Separator. The nozzles designed in Cases4 and 5 are used as "*HP and MP*

nozzles" (see Figures 5.17 and 5.21 for the pressure distributions along the nozzles). In Table 5.14, the mole fractions and molar flows of each component of "*LP Oil Out*" stream in Case 7 are shown.

Table 5.18: "*MP Nozzle*" geometry for case 7.A

Inlet diameter(m)	0.0400
Throat diameter(m)	0.0294
Outlet diameter(m)	0.0395
Converging length(m)	0.0439
Diverging length (m)	0.0961
Total length (m)	0.1400
Length upper bound (m)	0.1400

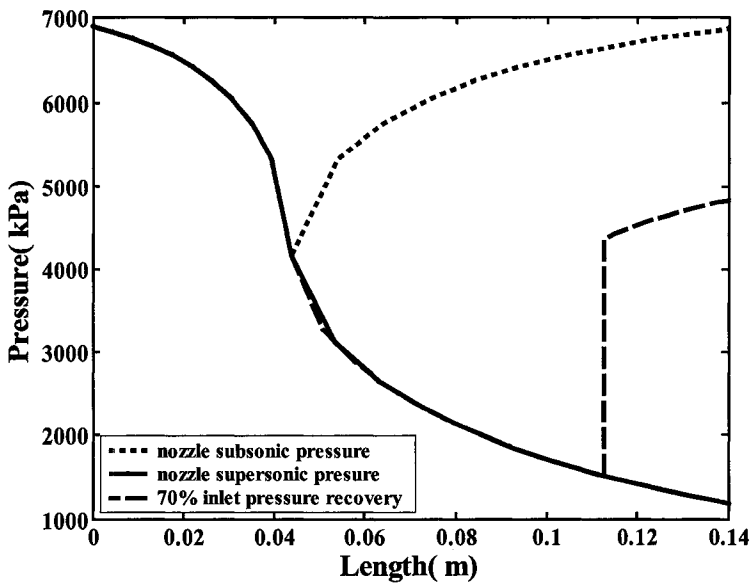

Figure 5.27: Pressure distribution along MP nozzle with 70% pressure recovery in Case 7 with 70% inlet pressure recovery

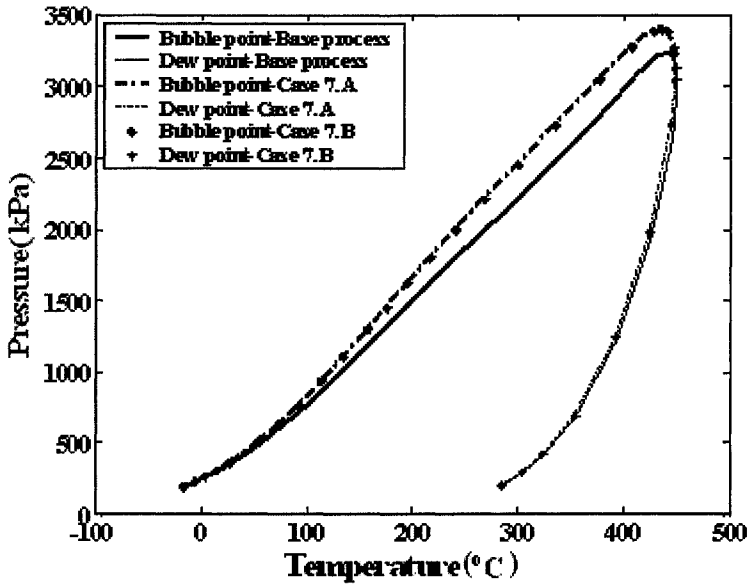

Figure 5.28: Phase envelopes for the stream "*LP Oil Out*" for "*Base Process*" and Case 7 with 70% pressure recovery

Table 5.19: Mole fractions and molar flow rates of" LP Oil Out" for Case 7

	Case 7.A			Case 7.B		
	Mole Fraction	**Molar Flow (kgmole/h)**	**Recovery (% of wellhead)**	**Mole Fraction**	**Molar Flow (kgmole/h)**	**Recovery (% of wellhead)**
Total	1.000	6,663.980	33.360	1.000	6,648.630	33.280
Methane	0.006	42.910	0.380	0.007	43.760	0.390
Ethane	0.021	140.660	11.050	0.021	138.140	10.850
Propane	0.071	473.560	45.550	0.070	464.760	44.700
i-Butane	0.013	89.090	72.680	0.013	87.790	71.630
n-Butane	0.036	236.980	80.560	0.035	234.080	79.580
i-Pentane	0.007	48.830	91.520	0.007	48.500	90.920
n-Pentane	0.008	54.000	93.620	0.008	53.720	93.140
Hexane	0.003	21.130	97.690	0.003	21.090	97.510
C7+	0.834	5,555.200	100.000	0.836	5,555.200	100.000
C2 Plus	0.993	6,619.440	78.640	0.993	6,603.290	78.450
C3 Plus	0.972	6,478.780	90.680	0.972	6,465.150	90.490

N2	0.000	0.040	0.020	0.000	0.040	0.020
CO2	0.000	1.590	4.090	0.000	1.540	3.950

Table 5.20: Crude oil production of the three processes in case 7 for 70% inlet pressure recovery

		Molar Flow (kgmole/h)	Recovery (%)	RVP (psia)	Volume Flow (m^3/h)	Volume Flow (bbl/day)
Case 7.A	Total	6,663.980	33.360	22.335	1,397.633	210,980.017
	Methane	42.910	0.380	-	2.303	347.635
	C2 Plus	6,619.440	78.640	-	1,395.244	210,619.371
	C3 Plus	6,478.780	90.680	-	1,383.379	208,828.227
Case7.B	Total	6,648.630	33.280	22.163	1,396.690	210,837.618
	Methane	43.760	0.390	-	2.343	353.643
	C2 Plus	6,603.290	78.450	-	1,394.262	210,471.165
	C3 Plus	6,465.150	90.490	-	1,382.574	208,706.775

In Figure 5.28, the phase envelopes are shown for *"Base Process"*, Cases 7.A, and 7.B. The bubble point curve of the process for Case 7 is shifted slightly to the left indicating a larger amount of heavy hydrocarbons. The small difference between the bubble curve line of Cases 7.A and 7.B, illustrates the higher concentration of heavy hydrocarbons in Case 7.A.

5.2.8 Case 8: One nozzle after the separated stream from the HP and MP separator are mixed

In this case the stream *"Associated Gas MP* "is compressed with the compression ratio of 4 to 6,896 kPa and cooled to the stream temperature, before entering the

compressor. This stream is mixed with the "*Associated Gas HP* "and entered a supersonic nozzle. This process is outlined in Figure 5.29.

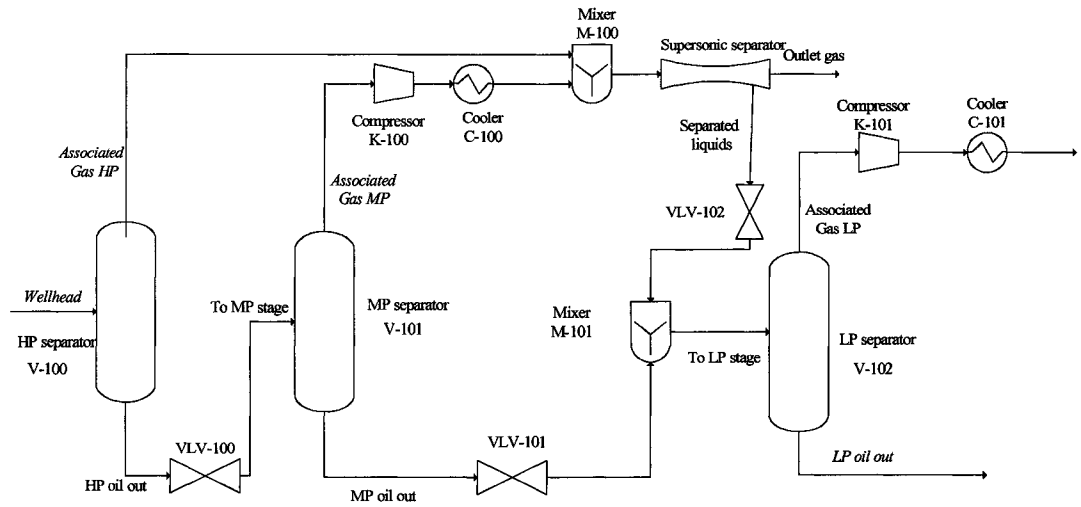

Figure 5.29: Case 8; Supersonic nozzle after the mixed stream from HP and MP separators

In this process, the streams from the high and medium pressure separators are mixed and therefore, the inlet properties of the nozzle are changed. Table 5.21 lists the inlet properties of the fluid entering the nozzle. In Table 5.22 the geometry of the designed nozzle for this case is outlined.

Table 5.21: Properties of nozzle inlet stream in Case 8

Pressure (kPa)	6,896
Temperature (C)	41.6
Molar flow (kmole /h)	1,2889.67

Table 5.22: Nozzle geometry for Case 8

Inlet diameter(m)	0.1060

Throat diameter(m)	0.0774
Outlet diameter(m)	0.1017
Converging length(m)	0.1186
Diverging length (m)	0.2313
Total length (m)	0.3500
Length upper bound (m)	0.3500

As the stream from the nozzle is entering the LP separator, the pressure upstream of the shockwave is needed to be kept above the operating pressure of LP Separator (413.7 kPa). The "*design pressure*" of this nozzle is above the LP separator operating pressure ,so there will not be any limitation in how much the gas is expanded.theerefore the londest possible nozzle in this case 0..35 m is designed. In Table 5.23, the mole fractions and mole flows for all components in Stream "*LP Oil Out*" in Case 8 are shown. Higher concentration of heavy hydrocarbons in Stream "*LP Oil Out*" in Case 8 is also reflected in Figure 5.31. It is clear that the bubble point curve is shifted to the left of the curve for the "*Base Process*".

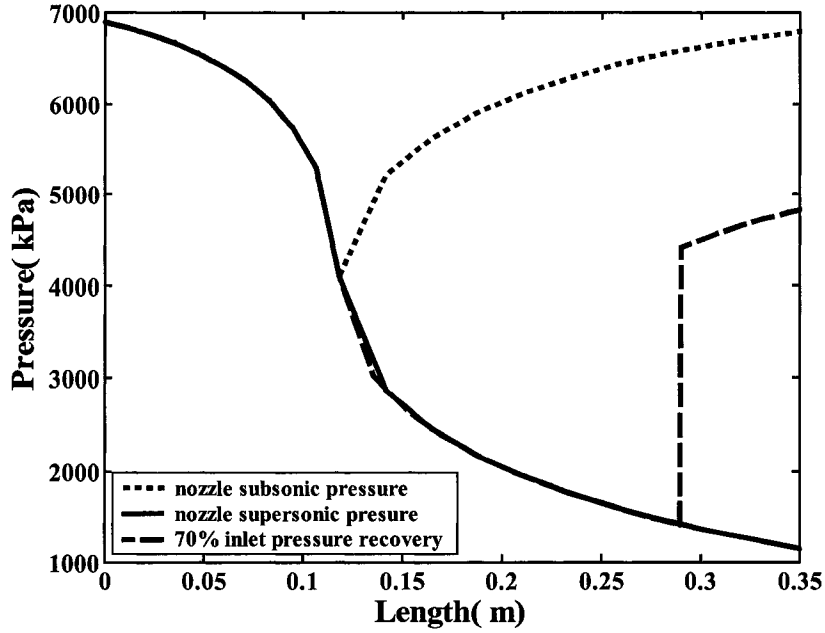

Figure 5.30: Pressure distribution along the nozzle with 70% pressure recovery in Case 8

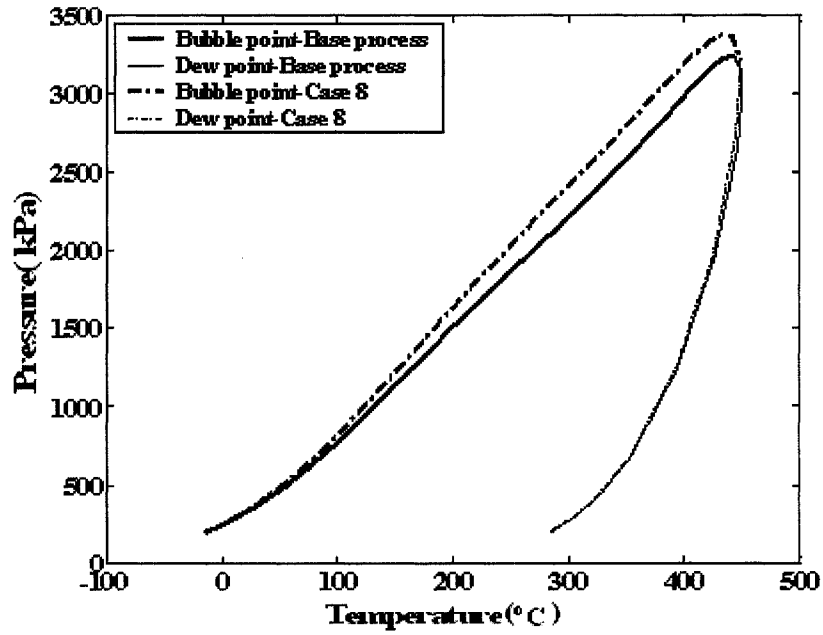

Figure 5.31: Phase envelopes for the stream "*LP Oil Out*" for "*Base process*" and Case 8 with 70% pressure recovery

Table 5.23: Mole fractions and molar flow rates of the" *LP oil out"* stream in case eight

	Case 8		
	Mole Fraction	**Molar Flow (kgmole/h)**	**Recovery (% of wellhead)**
Total	1.000	6,663.980	33.360
Methane	0.007	43.810	0.390
Ethane	0.020	134.960	10.600
Propane	0.068	451.450	43.420
i-Butane	0.013	86.940	70.930
n-Butane	0.035	233.350	79.330
i-Pentane	0.007	48.600	91.100
n-Pentane	0.008	53.840	93.340
Hexane	0.003	21.110	97.610
C7+	0.838	5,555.200	100.000
C2 Plus	0.993	6,585.450	78.230
C3 Plus	0.973	6,450.490	90.290
N2	0.000	0.040	0.020
CO2	0.000	1.550	3.990

Table 5.24 Crude oil production of the three processes in case 8 for 70% inlet pressure recovery

		Molar Flow (kgmole/h)	**Recovery (%)**	**RVP (psia)**	**Volume Flow**	
					(m^3/h)	**(bbl/day)**
Case 8	**Total**	6,663.980	33.360	21.713	1394.896	210566.747
	Methane	43.810	0.390	-	2.348	354.413
	C2 Plus	6,585.450	78.230	-	1392.464	210199.633
	C3 Plus	6,450.490	90.290	-	1381.054	208477.225

5.3 Review of eigth cases

Table 5.25 summarizes the results obtained for the "*Base Process*" and Cases 1 to

8. In this table the final compositions of each exit stream (*LP Oil Out*) as well as their exit RVP are shown. The objective is to reach a higher recovery of the heavy hydrocarbons in Stream *"LP Oil Out"*. It is also important that the quality of the final product in terms of vapour pressure be maintained. The preferred processes have a higher recovery of heavy hydrocarbons compared to the "*Base Process*" while the amount of methane is similar or lower than the "*Base process*". It is disadvantageous to mix the "*separated liquids*" with the stream exiting the bottom of LP Separator. The separated liquids are at higher pressure and contined larger amount of higher boiling hydrocarbons (methane and ethane) which increase the vapour pressure of the final crude product. Cases 4.A, 4.B, 7.A, 7.B, and 8 show good performance for increasing the crude oil production efficiency. However, Case 7.A seems to be the most attractive process, although two nozzles have to be used. Case 8 also is a promising option. Althugh the size of the nozzle is bit larger however the recovery is very close to that of Case 7A.

Table 5.25: Final compositions in the exit streams (*LP Oil Out)* for Cases 1 to 8

Case	Methane Flow rate (kmole/h)	C_2^+ Flow rate (kmole/h)	C_3^+ Flow rate (kmole/h)	RVP (Psia)
Base process	0.40	76.68	88.57	19.773
1.A	0.40	77.3	89.26	20.453
1.B	0.40	77.3	89.27	20.446
1.C	0.56	77.69	89.56	22.471
2.A	0.40	76.68	88.57	19.774
2.B	0.40	76.68	88.57	19.774
3	----	----	----	----
4.A	0.38	78.14	90.15	21.717
4.B	0.39	78.03	90.04	21.567
4.C	1.02	79.47	91.03	29.328
5.A	0.39	77.12	89.04	20.377
5.B	0.48	77.45	89.27	21.778
6	----	----	----	---
7.A	0.38	78.64	90.68	22.335
7.B	0.39	78.45	90.49	22.163
8	0.39	78.23	90.29	21.713

CHAPTER 6: CONCLUSIONS

6.1 SUMMARY

The propose of this thesis was to develop a compact high pressure system which is capable of removing water vapour from natural gas without affecting the heavy hydrocarbons. The proposed system in this work was compared with the traditional dehydration and hydrate inhibition processes such as absorption, adsorption, refrigeration, and membranes. In order to model and simulate the supersonic separators, the continuity and momentum equations, the first and the second laws of thermodynamics, along with a suitable equation of state had to be used to set a set of non-linear equations. The non-linear equations had to be solved numerically to analyze the performance of the nozzle under various conditions. In order to study the performance of the supersonic separators, two software packages, namely MATLAB and HYSYS were linked. MATLAB was used to numerically solve the governing non-linear equations. The necessary informations were transferred between the two software packages. In this study a specific nozzle could be designed for the desired conditions. The model could also be used to rate a previously designed nozzle. The effect of the feed pressure, temperature, flow rate, backpressure (pressure at the nozzle exit), and friction on the design of the nozzle and the flow behaviour inside the nozzle were evaluated. In order to demonstrate the capability of the developed model, the model was used to simulate the

production system within a three-stage separation train to examine its ability in recovering the NGLs from the associated gases. The model and simulation runs indicated that the use of a supersonic nozzle can improve the economy of crude production in offshore facilities.

6.2 Conclusions and Future Work

The following conclusions could be drawn from this work:

1. Dehydration and water removal is an important process in natural gas treatment. Therefore, there is a need to develop a method which:
    - works at different pressures
    - is suitable for different applications; compactness is one of the attractive features for offshore applications,
    - does not need a large initial investment and operates at low cost,
    - is environmental friendly, and
    - is selective towards water removal
2. Line heating is not an efficient method, as it does not remove the water although it is a simple process and does not need much investment. Hydrate inhibitor injection is costly and is not an environmental friendly process. Absorption using liquid desiccants is a simple process which can be automated for unmanned operations but needs a large footprint and therefore not suitable for offshore production facilities where compactness is of critical

importance. Adsorption using solid desiccants also requires large facility requiring large amount of energy to regenerate the desiccants. Refrigeration needs a large facility, can be costly to operate. Membranes require lower energy to operate, pose minimal environmental impact over the others, however are not selective for water removal.

3. Supersonic separators have several advantages over the previously mentioned methods and can present attractive features especially for offshore and subsea applications. Such as the compactness, self-induced refrigeration and the high gas velocity in the nozzle.
4. The Newton-Raphson was used as a numerical method to solve the non-linear equation involved in modelling the supersonic nozzle. This technique is an efficient method to simulate the supersonic nozzles. The only pitfall of this method is its sensitivity to the initial guesses. An unsuitable initial guess can result in divergence of the solution from the correct values.
5. The results of modelling also indicated the importance of choosing a suitable equation of state. Ideal gas assumption resulted in inaccurate predictions.
6. When a nozzle is designed, the increase in nozzle inlet pressure, results in an increase in the nozzle length and the converging nozzle length and a decrease in the throat diameter. When the nozzle is rated, the flow capacity increases with inlet pressure. Fixing the backpressure, at a constant percentage of the inlet pressure recovery, the shockwave happens earlier in the nozzle for the

higher inlet pressures. At both cases the "*design pressure*" of the nozzle will remain constant with the increase in the inlet pressure but the "*recovery pressure*" decrease with the increase in inlet pressure.

7. Designing a nozzle for higher inlet temperatures, results in a larger throat diameter in a shorter converging nozzle. The results of nozzle rating show that the flow capacity varies inversely with inlet temperature. For both, designing and rating a nozzle, the *"design pressure*" of the nozzle remains constant as the inlet pressure varies but the "*recovery pressure*" increases with the inlet temperature. For the same pressure recovery, the shockwave location shifts towards the nozzle exit as the inlet temperature increases.
8. There is a maximum possible flow rate for each nozzle. For the flow rates lower than this maximum value, the nozzle will not be choked at the throat (Mach number is lower than unity) and therefore flow will be subsonic along the nozzle. If it is desirable to have choked flow at the throat for lower flow rates, the nozzle will have a longer converging length with a smaller throat diameter. For the higher flow rates, a nozzle with shorter converging part and a larger throat should be designed.
9. The nozzle exit pressure (backpressure) affects the shockwave location in the diverging part of the nozzle. The higher the backpressure, the earlier the shockwave happens. The back pressure can be chosen between the "*recovery pressure*" and the "*design pressure*". Designers have to compromise between

higher separation and a better pressure recovery.

10. Presence of friction inside the nozzle does not significantly affect the flow behaviour in the nozzle. It would however affect the location of the shockwave in the diverging aprt of the nozzle. For the chosen flow in this study, the shockwave in frictional flow was predicted later in the nozzle when compared with frictionless flow.
11. The water content of the gas increases with inlet temperature but decreases with increase in inlet pressure. Close to complete water removal may be achieved using the supersonic nozzles. At constant inlet temperature, with increase in pressure, the pressure-temperature of the system is more likely to remain in the dense phase. Therefore selective water removal can be achieved by controlling the design parameters: e.g.,increasing the inlet pressure with constant temperature, increasing the inlet temperature with constant outlet pressure and controlling the backpressure. As mentioned, shockwave happens earlier in the nozzle when the backpressure is higher and in this case the pressure is recovered without any further pressure reduction. This causes the pressure to remain above the cricondenbar.
12. The efficiency of supersonic nozzles in improving the capacity of crude production trains comprising three separation stages was examined. The results with variable nozzle locations were studied. Eight cases were presented. The performance criterion was the highest recovery of heavy

hydrocarbons with similar or lower amount of methane and lighter hydrocarbons in the crude oil. A case (Case 7.A) where two nozzles were placed in the crude separation system, showed the most attractive performance among all the other studied cases. This study is assumed that two supersonic nozzles can be used in one platform due to their compactness. However, the feasibility study should be done to prove if this case is practical and economical.

Proposed Future Work

The following research activities are recommended as future work:

1. Since the analyses and conclusions in this work are based on the computational simulations, several assumptions were made to perform this study. Therefore, it is recommended to design and construct a pilot plant to confirm the results achieved with the computational simulation. This study is specially recommended for the cases where more than one nozzle is used on the platform.
2. Some of the common equations of state fail to work in all pressure and temperature conditions. Therefore, the tuning the equations of state is recommended. In order to tune equations, PVT tests need to be conducted.
3. The developed program needs a relatively long time to design a nozzle. The program needs to be modified in order to reduce the time of

computation and it can be improved to become more user-friendly.

4. The design of supersonic nozzles can be combined with the study of separated liquids or solid (ice or hydrate) particles from the nozzle stream.
5. Study of the possibility of using the supersonic nozzles for the other applications such as cryogenic separation, deep cut, ethane recovery and air separation is also recommended.
6. The effect of having multiple nozzles in the crude production or high pressure dehydration processes was not studied in this work. It would add to the work if in the future work the effect of having several nozzles could be studied.

REFERENCES

Alfyorov, V., Bagirov, L., Imayev, S., Lacey, J., Dmitriey, L. and Feygin, V.:"supersonic gas conditioning: First Commercial Offshore Experience", *Oil and Gas Journal* (May 2005).

Arnold, K. and Stewart, M.:, "Surface Production Operations; Volume 2; Design of Gas Handling Facilities", 2nd Edition, Gulf Professional Publishing, Huston, TX, (1999)46 .

Ballard, D.: "Fundamentals of Gas Dehydration", Proceeding of the Gas Conditioning Conference, Okla, Norman, Mar 5-7, 1979.

Berger, B. D. and Anderson, K. E., "Gas Handling and Field Processing", Pennwell Corp, Tulsa, Ok. (1980)59.

Beronich, E. L., Hawboldt, K., Abdi, M., "Recovering Natural Gas Liquids in Atlantic Canada's Offshore Petroleum Production Projects", paper presented at the 85th Annual Convention of the Gas Processors Association, Grapevine,TX, March 5-8 , 2006.

Beronich, E. L.: "Recovery of Natural Gas Liquids with Membranes from Associated Gas on Newfoundland and Labrador Offshore Production Facilities", Masters Thesis, Faculty of Engineering and Applied Science, Memorial University of Newfoundland, 2006.

Beronich, E. L., Hawboldt, K., Abedinzadegan Abdi, M., "Linking a Process Simulator (HYSYS) with MATLAB, a Powerful Modeling Tool for Continuous Process Industry: a Tutorial", paper presented at the annual NECEC conference, Newfoundland,

Nov.9th, 2005.

Campbell, J.M., "Gas Conditioning and Processing", Volume 1, Campbell Petroleum Series, Norman, Ok (1992)61.

Covington, K., Collie, T., Behrens, S., "Selection of Hydrate Suppression Methods for Gas Streams", paper presented at the 78th GPA Annual Convention, Nashville, TN, March , 1999

Fox, R. W., McDonald, A. T., "Introduction to Fluid Mechanics", 3rd Edition, John Wiley & Sons Inc. Hoboken, NJ, (1985)561

Gas Processors Suppliers Association, "GPSA Engineering Data Book", 12th Edition, Tulsa, OK, (2004).

Greitzer, E. M., Tan, C. S., Graf, M. B., "Internal Flow Concepts and Applications" Cambridge, UK, (2004) 40.

Hengwei, L., Zhonggliang, L., Yongxun, F., Keyu, G. and Tingmin, Y., "Characteristic of a Supersonic Swirling Dehydration System of Natural Gas", *Chinese Journal of Chemical Eng.*, (2005)**13**

Hollis, R. B., "Real-Gas Flow Properties for NASA Langley Research Center Aerothermodynamics Facilities Complex Wind Tunnels", Langley Research Center, Hampton, Virginia, Sep. 1996

Iluhi, M., "Cold Flow Concepts Compared", Masters thesis, Norwegian University of Science and Technology, Dec. 2005

Jacobsen, R. T., Penoncello, S. G., Lemmon, E. W., "Thermodynamic Properties

of Cryogenic Fluids", Springer, verlag (1997)8

Karimi, A., Abedinzadegan Abdi, M., "Selective Water Removal From Supercritical Natural Gas", paper presented in SPE Gas Technology Symposium, Calgary, Alberta, Canada, 15-18 May, 2006

Khezzar, L, Benayoune, M., "Application of a Design Method of a Supersonic Nozzle", *Journal of Engineering and Applied science*, (1997) **44**

Kidnay, A. J., Paqrrish,W. R., "Fundamentals of Natural Gas Processing", Taylor and Francis Group,LLC., (2006)9

Man, H. C., Duan, J., Yue, T. M., "Design and characteristic of supersonic nozzle of high pressure laser cutting ", *Journal of Materials Processing Technology*, (1997)**63**

Manning, F.S., Thompson, R., "Oilfield Processing of Petroleum, Volume 1: Natural Gas", Pennwell Corp,Tulsa,Ok, (1991) 19

Mohitpour, M., Golshan, H., and Murray, A., "Pipeline Design and Construction, a Practical Approach", 2nd Edition, ASME press, NY, (2003)57

Molleson, G. V., Stasenko, A. L., "An Axsimmetric Flow of a Mixture of Real Gases With a Condensing Component", *High Temperature*, (2005)**43**

Moraitis, C.S, Akritidis, C. B., "Optimization of the Operation of a Drying Heat Pump Using Superheated Steam", *Drying Technology*,(1997)**15**

Prast, B., Schinkelshoek, P., Lammers, B., Betting, M., "CFD for Supersonic Gas Processing", paper presented in Multiphase Separation and Multiphase Pumping Technologies Conference, 1-2 September 2005

Schinkelshoek, P., Epsom, H., "Supersonic Gas Conditioning Introduction of the Lower Pressure Drop Twister" , paper presented in at the GPA 85th Annual Convention, Grapevine, TX, 5-8 March 2006

APPENDIX: MATLAB CODE

The process showed in Figure A.1 is used to design a nozzle. A gas stream called "strGas" is mixed with the water stream called " strWater" in the mixer to get the water saturated gas stream. The composition properties in the length stream called" strLength" is transferred to inlet stream, "strInlet". To predict the "*recovery properties*" and "*design properties*", the properties distribution is extracted from "strInlet" by applying Newton-Raphon method at each cross section. If shockwave happens in the diverging part of the nozzle, the condensed liquids are separated from the main stream of the nozzle and the remained stream will be the dry gas stream, "strDrygas". The composition properties of this stream are transferred to the nat gas stream, "strNatgas" and by applying Newton-Raphson method, the properties in the nozzle after the shockwave will be found.

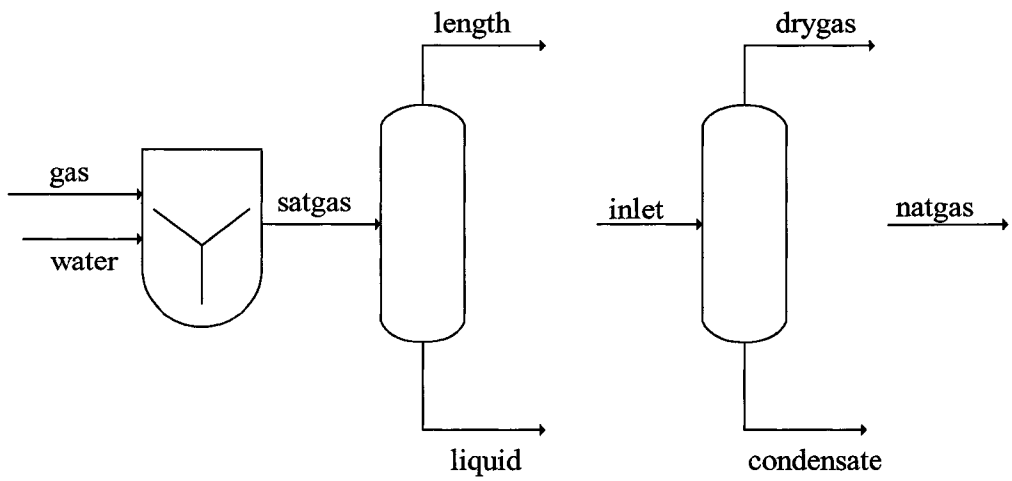

Figure A.1: The process used in HYSYS

The developed MATLAB program to do this simulation, in both isentropic and non-isentropic cases, is given in the following pages.

A.1 Isentropic flow

A.1.1 Finding nozzle throat

```
clear all;
clc;

% % % % % % % % % % %

% Variable name legend
%
% T: temperature (C)
% P: pressure (kPa)
% A: x-section area (m^2)
% L: length (m)
% mDot: flow rate (kmole/hr)
% entr: entropy ()
% enrg: enthalpy ()
% momt: momentum ()
% v: velocity (m/s)
% machNum: mach number
% ro: density (kg/m ^3)
% seg: segement count
% shock: shock location measured from inlet (m)
% alpha: half angle (degrees)
% vFrac: saturated gas vapour fraction

% % % % % % % % % % %
% Postfix legend
%
% (entr, engr, momt, ro, v)_W: water stream
% (T, P, mach, v)1: inlet
% (L, seg, alpha)_c: converging part
% (L, seg, alpha)_d: diverging part
```

```
% (L, mDot)_as: after shock
% (L)_bs: before shock

%Parameters
T1   = 20;
P1   = 30000;
A1   = 0.001257;
L    = 0.12;
mDot = 5000;


% Linking with hysys
hyApp    = feval('actxserver', 'Hysys.Application');
hysolver = hyApp.ActiveDocument.Solver;
solver.CanSolve = 1; %Start solver
hysolver.CanSolve = 0;

strInlet     = hyApp.ActiveDocument.Flowsheet.MaterialStreams.Item('inlet');
strLength    = hyApp.ActiveDocument.Flowsheet.MaterialStreams.Item('length');
strNatgas    = hyApp.ActiveDocument.Flowsheet.MaterialStreams.Item('natgas');
strGas       = hyApp.ActiveDocument.Flowsheet.MaterialStreams.Item('gas');
strWater     = hyApp.ActiveDocument.Flowsheet.MaterialStreams.Item('water');
strSatgas    = hyApp.ActiveDocument.Flowsheet.MaterialStreams.Item('satgas');
strDrygas    =hyApp.ActiveDocument.Flowsheet.MaterialStreams.Item('drygas');
hySS         = hyApp.ActiveDocument.Flowsheet.Operations.Item('SPRDSHT-1');

% Gas saturation
vFrac = 1;
mDot_W = 0;
[entr1, enrg1, momt1, ro1, v1] = funcs(solver, strGas, T1, P1, A1, mDot);
while vFrac==1
   mDot_W=mDot_W+0.001;
    [entr_W, enrg_W, momt_W, ro_W, v_W] = funcs(hysolver,strWater, T1, P1,
A1, mDot_W);
   vFrac = hySS.Cell('B6').CellValue;
end

% Saturated gas properties
T1 = hySS.Cell('B7').CellValue;
P1 = hySS.Cell('B8').CellValue;
mDot = hySS.Cell('C1').CellValue;
```

```
% Nozzle design
seg_c = 30;
alpha_c = 6.85;
alphaRad_c = (alpha_c*pi) / 180;

seg_d = 300;
alpha_d = 3;
alphaRad_d = (alpha_d*pi) / 180;


A(1) = A1
T(1) = T1;
P(1) = P1;
[entr(1), enrg(1), momt(1), ro(1), v(1)] = funcs(solver, strInlet, T(1), P(1), A(1),
mDot);
[machNum1, v1] = mach(T1, P1, A1, mDot);
machNum(1) = machNum1;
v(1) = v1;
water(1) = hySS.Cell('D1').CellValue;
r1 = sqrt(A1/pi);
ID(1) = 2*r1;
p(1) = 0;


i = 1;
L_segment = 0.0009;
x = tan(alphaRad_c)*L_segment;
hySS.Cell('B1').CellValue = L_segment;

% Finding the throat
converged(i) = true;
exception(i) = false;

while converged(i) == true && exception(i) == false && abs(1-machNum(i))>0.2
   i = i + 1;
   ID(i) = ID(i-1)-(2*x);
   A(i) = (pi*(ID(i))^2)/4;
   p(i) = p(i-1)+L_segment;
     [T(i), P(i), machNum(i), v(i),converged(i), exception(i)] = tpDistr(T1, P1,
A1,T1,P1, A(i), mDot);
if converged(i) == true && exception(i) == false
   [entr(i), enrg(i), momt(i), ro(i), v(i)] = funcs(hysolver, strInlet, T(i), P(i), A(i),
```

```
mDot);
        end
        end

        L_segment = 0.0000009;
        x = tan(alphaRad_c)*L_segment;
        hySS.Cell('B1').CellValue = L_segment;
        hysolver.CanSolve = 1 % start solver
        hysolver.CanSolve = 0;
        converged(i)=1;
        converged(i) == true
        exception(i)=0;

        while converged(i) == true && exception(i) == false
          i = i + 1;
          ID(i)=ID(i-1)-(2*x);
          A(i)=(pi*(ID(i))^2)/4;
          p(i)=p(i-1)+L_segment;
           [T(i), P(i), machNum(i), v(i),converged(i), exception(i)] = tpDistr(T(1), P(1),
A(1),T(1),P(1), A(i), mDot);
        if converged(i) == true && exception(i) == false
           [entr(i), enrg(i), momt(i), ro(i), v(i)] = funcs(hysolver, strInlet, T(i), P(i), A(i),
mDot);
        end
        end

        ithroat=i-1; % throat index


        % saving the throat properties
        save nozzlethroat A T P machNum v p ID ithroat  entr ro momt enrg mDot
```

A.1.2 FINDING THE NOZZLE "RECOVERY PROPERTIES"

```
        clear all
        clc

        load nozzlethroat   % Calling the properties at the converging part
         i=ithroat;
```

```
L    = 0.12;
mDot = 5000;

% Linking with hysys
hyApp = feval('actxserver', 'Hysys.Application');
hysolver = hyApp.ActiveDocument.Solver;
solver.CanSolve = 1;
hysolver.CanSolve = 0;

strInlet     = hyApp.ActiveDocument.Flowsheet.MaterialStreams.Item('inlet');
strLength    = hyApp.ActiveDocument.Flowsheet.MaterialStreams.Item('length');
strOutlet    = hyApp.ActiveDocument.Flowsheet.MaterialStreams.Item('outlet');
strNatgas    = hyApp.ActiveDocument.Flowsheet.MaterialStreams.Item('natgas');
strGas       = hyApp.ActiveDocument.Flowsheet.MaterialStreams.Item('gas');
strWater     = hyApp.ActiveDocument.Flowsheet.MaterialStreams.Item('water');
strSatgas    = hyApp.ActiveDocument.Flowsheet.MaterialStreams.Item('satgas');
strDrygas    =hyApp.ActiveDocument.Flowsheet.MaterialStreams.Item('drygas');
hySS         = hyApp.ActiveDocument.Flowsheet.Operations.Item('SPRDSHT-1');

% Nozzle design
seg_c = 30;
alpha_c = 6.85;
alphaRad_c = (alpha_c*pi) / 180;

seg_d = 30;
alpha_d = 3;
alphaRad_d = (alpha_d*pi) / 180;


L_c = ( (sqrt( A(1)/pi)) - (sqrt(A(ithroat)/pi)) )/ (tan (alphaRad_c)) ;
L_d = L-L_c;
rt = sqrt(A(ithroat)/pi);

dL_c=L_c/seg_c;
dL_d=L_d/seg_d;


 for h = L_c+dL_d:dL_d:L
    i = i+1;
    p(i) = h
    R = (p(i)-L_c)*tan(alphaRad_d);
    A(i) = ((R+rt)^2) *pi;
```

```
        [T(i), P(i), machNum(i), v(i), converged, exception] = tpDistr(T(1), P(1),
A(1),T(1 ),P(1),A(i),mDot1);
        [entr(i), enrg(i), momt(i), ro(i), v(i)] = funcs(hysolver, strInlet, T(i), P(i), A(i),
mDot1);
    end
```

A.1.3 FINDING THE DESIGN PROPERTIES

```
clear all
clc

load nozzlethroat   % Calling the properties at the converging part
 i=ithroat;

 L   = 0.12;
 mDot = 5000;

% Linking with hysys
hyApp = feval('actxserver', 'Hysys.Application');
hysolver = hyApp.ActiveDocument.Solver;
solver.CanSolve = 1;
hysolver.CanSolve = 0;

strInlet     = hyApp.ActiveDocument.Flowsheet.MaterialStreams.Item('inlet');
strLength    = hyApp.ActiveDocument.Flowsheet.MaterialStreams.Item('length');
strOutlet    = hyApp.ActiveDocument.Flowsheet.MaterialStreams.Item('outlet');
strNatgas    = hyApp.ActiveDocument.Flowsheet.MaterialStreams.Item('natgas');
strGas       = hyApp.ActiveDocument.Flowsheet.MaterialStreams.Item('gas');
strWater     = hyApp.ActiveDocument.Flowsheet.MaterialStreams.Item('water');
strSatgas    = hyApp.ActiveDocument.Flowsheet.MaterialStreams.Item('satgas');
strDrygas    =hyApp.ActiveDocument.Flowsheet.MaterialStreams.Item('drygas');
hySS         = hyApp.ActiveDocument.Flowsheet.Operations.Item('SPRDSHT-1');

% Nozzle design
seg_c = 30;
alpha_c = 6.85;
alphaRad_c = (alpha_c*pi) / 180;

seg_d = 30;
alpha_d = 3;
alphaRad_d = (alpha_d*pi) / 180;
```

```
L_c = ( (sqrt( A(1)/pi)) - (sqrt(A(ithroat)/pi)) )/ (tan (alphaRad_c)) ;
L_d = L-L_c;
rt = sqrt(A(ithroat)/pi);

dL_c=L_c/seg_c;
dL_d=L_d/seg_d;


for h=L_c+dL_d:dL_d:L
        i=i+1;
        p(i)=h
        R=(p(i)-L_c)*tan(alphaRad_d);
        A(i)= ((R+rt)^2) *pi;
        [T(i), P(i), machNum(i), v(i), converged, exception] = tpDistr(T(1),
P(1),   A(1),-120 ,1000,A(i),mDot1);
        [entr(i), enrg(i), momt(i), ro(i), v(i)] = funcs(hysolver, strInlet, T(i),
P(i), A(i), mDot1);

 end
```

A.1.4 SHOCKWAVE PREDICTION

```
clear all
clc

load nozzlethroat   % Calling the properties at the converging part
 i=ithroat;

 L   = 0.12;
 mDot = 5000;
 Pexit=70/100*P1;  % Desired pressure recovery
 Shock=0.1;  % first guess for shocklocation, L_c <shock<L

% Linking with hysys
hyApp = feval('actxserver', 'Hysys.Application');
hysolver = hyApp.ActiveDocument.Solver;
solver.CanSolve = 1;
hysolver.CanSolve = 0;
```

```
strInlet     = hyApp.ActiveDocument.Flowsheet.MaterialStreams.Item('inlet');
strLength    = hyApp.ActiveDocument.Flowsheet.MaterialStreams.Item('length');
strOutlet    = hyApp.ActiveDocument.Flowsheet.MaterialStreams.Item('outlet');
strNatgas    = hyApp.ActiveDocument.Flowsheet.MaterialStreams.Item('natgas');
strGas       = hyApp.ActiveDocument.Flowsheet.MaterialStreams.Item('gas');
strWater     = hyApp.ActiveDocument.Flowsheet.MaterialStreams.Item('water');
strSatgas    = hyApp.ActiveDocument.Flowsheet.MaterialStreams.Item('satgas');
strDrygas    =hyApp.ActiveDocument.Flowsheet.MaterialStreams.Item('drygas');
hySS         = hyApp.ActiveDocument.Flowsheet.Operations.Item('SPRDSHT-1');

% Nozzle design
seg_c = 30;
alpha_c = 6.85;
alphaRad_c = (alpha_c*pi) / 180;

seg_d = 30;
alpha_d = 3;
alphaRad_d = (alpha_d*pi) / 180;


L_c = ( (sqrt( A(1)/pi)) - (sqrt(A(ithroat)/pi)) )/ (tan (alphaRad_c)) ;
L_d = L-L_c;
rt = sqrt(A(ithroat)/pi);

dL_c=L_c/seg_c;
dL_d=L_d/seg_d;

L_bs=Shock-L_c;;
dL_bs=L_bs/seg_d;
L_as=L-L_c-L_bs;
dL_as=L_as/seg_d;
Abs=(( (L_bs*(tan (alphaRad_d)))+(sqrt(A(ithroat)/pi)) )^2)*pi;
Aex=(( (L_d*(tan (alphaRad_d)))+(sqrt(A(ithroat)/pi)) )^2)*pi;

[Tbs, Pbs, machNumbs, vbs, vFracbs,convergedbs, exceptionbs] =
tpDistr(T(ithroat), P(ithroat), A(ithroat),-120,1000, Abs, mDot);
[entrbs, enrgbs, momtbs, robs, vbs] = funcs(hysolver, strInlet, Tbs, Pbs, Abs,
mDot);
mDot_as= hySS.Cell('A7').CellValue;
[Tas,Pas ,machNumas, vas, converged, exception] = tpDistr_as(Tbs, Pbs,
Abs,T(1) ,P(1),Abs, mDot,mDot_as);
```

```
[Tex, Pex, machNumex, vex, vFracex,convergedex, exceptionex] =
tpDistrdrygas(Tas, Pas, Abs,T1,P1, Aex,mDot_as);

if Pex>Pexit
   display ('choose bigger shock')
else if Pex<Pexit
      display('choose lower shock')
   else display ('shocklocation is correct')

end
end
Aas=Abs;
[entras, enrgas, momtas, roas, vas] = funcs(hysolver, strNatgas, Tas, Pas, Aas,
mDot_as);

for h=L_c+dL_bs:dL_bs:Shock
   i=i+1;
   p(i)=h;
   R=(p(i)-L_c)*tan(alphaRad_d);
   A(i)= ((R+rt)^2) *pi;
     [T(i), P(i), machNum(i), v(i), vFrac, converged, exception] = tpDistr(T(1),
P(1), A(1),-120, 1000, A(i), mDot);
     [entr(i), enrg(i), momt(i), ro(i), v(i)] = funcs(hysolver, strInlet, T(i), P(i), A(i),
mDot);

end


pas=L_c+(L_bs);
i=i+1;
p(i)= pas;
A(i)=Aas;
T(i)= Tas;
P(i)= Pas;
machNum(i)= machNumas;
v(i)=vas;
entr(i) = entras;
enrg(i)=enrgas;
momt(i) = momtas;
ro(i)=roas;
```

```
for h=Shock+dL_as:dL_as:L
  i=i+1;
  p(i)=h
  R=(p(i)-L_c)*tan(alphaRad_d);
  A(i)= ((R+rt)^2) *pi;
   [T(i), P(i), machNum(i), v(i), converged, exception] = tpDistrdrygas(Tas, Pas,
Aas,T1 ,P1,A(i),mDot1);
    [entr(i), enrg(i), momt(i), ro(i), v(i)] = funcs(hysolver, strNatgas, T(i), P(i),
A(i), mDot1);

end
```

A.1.5 FUNCTIONS

A.1.5.1 ERROREVAL

```
% % % % % % % % % % %
% errorEval - computes error in one iteration of newton raphson
%
% Input:
%  solver - hysys solver
%  stream - stream name
%  entr1 - inlet enthalpy
%  enrg1 - inlet energy
%  T - temperature guess
%  P - pressure guess
%  a - xsection
%  mDot - flow rate
% Output:
%  err - error in current newton raphson iteration

function [err] = errorEval(solver, stream, entr1, enrg1, T, P, a, mDot)

dT = 0.1;
dP = 0.1;

[entr, enrg,momt,ro,v] = funcs(solver, stream, T, P, a, mDot);
f1 = entr - entr1;
```

```
f2 = enrg - enrg1;

[entr_Tinc, enrg_Tinc,momt_Tinc,ro,v] = funcs(solver, stream, T + dT/2, P, a,
mDot);
[entr_Tdec, enrg_Tdec,momt_Tdec,ro,v] = funcs(solver, stream, T - dT/2, P, a,
mDot);
[entr_Pinc, enrg_Pinc,momt_pinc,ro,v] = funcs(solver, stream, T, P + dP/2, a,
mDot);
[entr_Pdec, enrg_Pdec,momt_Pdec,ro,v] = funcs(solver, stream, T, P - dP/2, a,
mDot);

df1_dT = (entr_Tinc - entr_Tdec) / dT;
df2_dT = (enrg_Tinc - enrg_Tdec) / dT;
df1_dP = (entr_Pinc - entr_Pdec) / dP;
df2_dP = (enrg_Pinc - enrg_Pdec) / dP;

jacobean = [df1_dT df1_dP; df2_dT df2_dP];
err = -inv(jacobean)*[f1; f2]; % 2x1 matrix
```

A.1.5.2 FUNCS

```
% % % % % % % % % % %
% funcs - computes stream properties
%
% Input:
%  solver - hysys solver
%  stream - stream name
%  T - temperature
%  P - pressure
%  a - xsection
%  mDot - flow rate
% Output:
%  entr - enthalpy
%  enrg - energy
%  momt - momentum
%  ro - density
%  v - velocity

function [entr, enrg, momt, ro, v] = funcs(solver, stream, T, P, a, mDot)
```

```
% % linking with hysys

stream.Temperature.SetValue(T,'C')
stream.pressure.SetValue(P,'kPa')
stream.MolarFlow.SetValue(mDot,'kgmole/h')
solver.CanSolve = 1; %Start solver
solver.CanSolve = 0; %Stop solver

S  = stream.MassEntropyValue;        % (kJ / kg*C)
h  = stream.MassEnthalpyValue * 1000; % (J / kg)
ro =    stream.MassDensityValue ;    % (kg / m^3)


Mw = stream.MolecularWeightValue;
m = mDot*Mw; % (kg / hr)

v = (m/3600) / (ro*a); % (m / s)

entr = S;          % (kJ / kg*C)
enrg = h + (v^2)/2; % (m^2 / s^2)
momt= ((P*1000)*a)+((m/3600)*v);
```

A.1.5.3 tpDistr

The function tpDistrdrygas follow the same procedure for "strNatgas"

```
% % % % % % % % % % %
% tpDistr - computes stream properties in next xsection
%
% Input:
%  T1 - current temperature
%  P1 - current pressure
%  A1 - current xsection size
%  T2i - next temperature initial guess
%  P2i - next pressure initial guess
%  A2 - next xsection size
%  mDot - flow rate
% Output:
%  T2 - next temperature
%  P2 - next pressure
```

```
%  v - next velocity
%  vFrac - next vapour fraction
%  converged - NR convergence flag
%  exception - erroneous parameter flag

function [T2, P2, machNum, v, vFrac, converged, exception] = tpDistr(T1, P1,
A1, T2i, P2i, A2, mDot)

% linking with hysys
hyApp    = feval('actxserver', 'Hysys.Application');
hysolver = hyApp.ActiveDocument.Solver;
solver.CanSolve = 1; %Start solver
hysolver.CanSolve = 0;

strInlet  = hyApp.ActiveDocument.Flowsheet.MaterialStreams.Item('inlet');
% strLength = hyApp.ActiveDocument.Flowsheet.MaterialStreams.Item('length');
hySS      = hyApp.ActiveDocument.Flowsheet.Operations.Item('SPRDSHT-1');

% Newton-Raphson
[entr1, enrg1, momt1, ro1, v1] = funcs(hysolver, strInlet, T1, P1, A1, mDot);

tol = 0.001; % tolerance for error
kmax = 100;  % maximum number of iterations

% set initial guess
T2 = T2i;  % (C)
P2 = P2i; % (kPa)

k = 0;
pres = tol + 1.;
tres = tol + 1.;
exception = false;
while (exception == false) && (tres >= tol || pres >= tol) && k <= kmax
   err = errorEval(hysolver, strInlet, entr1, enrg1, T2, P2, A2, mDot);
   T2 = T2 + err(1, 1);
   P2 = P2 + err(2, 1);
   if P2 < 0 || T2 < -273
      exception = true;
   else
      tres = abs( err(1,1) );
      pres = abs( err(2,1) );
      k = k + 1;
```

```
    end
end

converged = false;
machNum = 0;
v = 0;
vFrac = 0;
if exception == false
    if k > kmax
        converged = false;
    else
        converged = true;
        [machNum, v] = mach(T2, P2, A2, mDot);
    end
end
```

A.1.5.4 MACH

The function machdrygas follow the same procedure for "strNatgas"

```
% % % % % % % % % % %
% machNum - computes mach number & velocity
%
% Input:
%   T - temperature
%   P - pressure
%   A - xsection
%   mDot - flow rate
% Output:
%   machNum - mach number
%   v - velocity

function [machNum,v] = mach(T, P, A, mDot)

hyApp    = feval('actxserver', 'Hysys.Application');
hysolver = hyApp.ActiveDocument.Solver;
solver.CanSolve = 1;
hysolver.CanSolve = 0;
strInlet= hyApp.ActiveDocument.Flowsheet.MaterialStreams.Item('inlet');

dT = 0.1;
```

```
[entr1, enrg1,momt1,ro1,v1] = funcs(hysolver,strInlet, T, P, A, mDot);

tol = 0.005; % tolerance for error
kmax = 200;  % maximum number of iterations

% % % % % % % % % % %
% Speed of sound computation
%
P2_inc=P;
k = 0;
pres = tol + 1.;
exception = false;
while (exception == false) &&  (pres >= tol) && k <= kmax
  err = errorEval_mach(hysolver, strInlet,T+dT/2, P2_inc, A, mDot,entr1);
    P2_inc = P2_inc + err;
   if P2_inc< 0
      exception = true;
   else
      pres = abs( err );
      k = k + 1;
   end
end

[entr, enrg,momt,ro_inc,v_inc] = funcs(hysolver,strInlet, T+dT/2, P2_inc, A,
mDot);
P2_dec=P;
k = 0;
pres = tol + 1.;
exception = false;
while (exception == false) && (pres >= tol) && k <= kmax
  err = errorEval_mach(hysolver, strInlet,  T-dT/2, P2_dec, A, mDot,entr1);
   P2_dec = P2_dec + err;
   if P2_dec < 0
      exception = true;
   else
      pres = abs( err );
      k = k + 1;
   end
end

[entr, enrg,momt,ro_dec,v_dec] = funcs(hysolver,strInlet, T-dT/2, P2_dec, A,
mDot);
```

```
c = sqrt( abs( (P2_inc-P2_dec)*1000/(ro_inc - ro_dec) ) ); % (m/s)
[entr, enrg,momt,ro,v] = funcs(hysolver,strInlet, T, P, A, mDot);
machNum = v / c;
```

A.1.6 errorEvalmach

```
% % % % % % % % % % %
% errorEval - computes error in one iteration of newton raphson to cpmpute
% Machnumber
%
% Input:
%  solver - hysys solver
%  stream - stream name
%  T - temperature
%  P - pressure
%  a - xsection
%  mDot - flow rate
% entr1- entropy inlet
% Output:
%  err - error in current newton raphson iteration to compute Mach number

function [err] = errorEval_mach(solver, stream, T, P, A, mDot,entr1)
dP = 0.1;
[entr, enrg,momt,ro,v] = funcs(solver, stream, T, P, A, mDot);
f1 = entr - entr1;
[entr_Pinc, enrg_Pinc,momt_Pinc,ro,v] = funcs(solver, stream, T, P + dP/2, A,
mDot);
[entr_Pdec, enrg_Pdec,momt_Pdec,ro,v] = funcs(solver, stream, T, P - dP/2, A,
mDot);

df1_dP = (entr_Pinc - entr_Pdec) / dP;
err = -f1/df1_dP; % 2x1 matrix
```

A.1.5.7 tpDistr_as

```
% % % % % % % % % % %
% tpDistr - computes stream properties after downstream the shockwave
% Input:
%  T1 - current temperature
%  P1 - current pressure
```

```
%  A1 - current xsection size
%  T2i - next temperature initial guess
%  P2i - next pressure initial guess
%  A2 - next xsection size
%  mDot - flow rate
% Output:
%  T2 - next temperature
%  P2 - next pressure
%  v - next velocity
%  vFrac - next vapour fraction
%  converged - NR convergence flag
%  exception - erroneous parameter flag


function [T2,P2, machNum, v, converged, exception] = tpDistr_as(Tt, Pt, At,
T2i,P2i,Aas, mDot)

% linking with hysys
hyApp    = feval('actxserver', 'Hysys.Application');
hysolver = hyApp.ActiveDocument.Solver;
solver.CanSolve = 1; %Start solver
hysolver.CanSolve = 0;

strInlet  = hyApp.ActiveDocument.Flowsheet.MaterialStreams.Item('inlet');
 strNatgas = hyApp.ActiveDocument.Flowsheet.MaterialStreams.Item('natgas');
hySS      = hyApp.ActiveDocument.Flowsheet.Operations.Item('SPRDSHT-1');

% Newton-Raphson
[entrt, enrgt,momtt,rot,vt] = funcs(solver, strInlet, Tt, Pt, At, mDot);

tol = 0.005; % tolerance for error
kmax = 100;   % maximum number of iterations

% set initial guess
Tas = T2i;% (C)
Pas =P2i;
k = 0;
tres = tol + 1.;
pres = tol + 1.;

exception = false;
while (exception == false) && (tres >= tol|| pres >= tol) && k <= kmax
```

```
    err = errorEval_as(hysolver, strNatgas,enrgt,momtt ,Tas, Pas, Aas, mDot);
    Pas = abs(Pas + err(2, 1));
    Tas = Tas + err(1, 1);
    if  Tas < -273  || Pas < 0
      exception = true;
    else
      tres = abs( err(1,1) );
     pres = abs( err(2,1) );
      k = k + 1;
    end
  end
  T2=Tas;
  P2=Pas;
  converged = false;
  machNum = 0;
  v = 0;
  vFrac = 0;
  if exception == false
    if k > kmax
      converged = false;
    else
      converged = true;
      [machNum, v] = machdrygas(Tas, Pas, Aas, mDot);

    end
  end
```

A.1.5.8 ERRORVAL_AS

```
  % % % % % % % % % % %
  % errorEval_as - computes error in one iteration of newton raphson to predict
%       upstream properties of shockwave
  % Input:
  %  solver - hysys solver
  %  stream - stream name
  % enrg1 - inlet energy
  %  momt1 - inlet momentum
  %  T - temperature guess
  %  P - pressure guess
  %  a - xsection
```

```
%  mDot - flow rate
% Output:
%  err - error in current newton raphson iteration


function [err] = errorEval_as(solver, stream,enrg1,momt1, T, P, a, mDot)

dT = 0.1;
dP = 0.1;


[entr, enrg,momt,ro,v] = funcs(solver, stream, T, P, a, mDot);
f1 = enrg - enrg1;
f2 = momt - momt1;


[entr_Tinc, enrg_Tinc,momt_Tinc,ro,v] = funcs(solver, stream, T + dT/2, P, a,
mDot);
[entr_Tdec, enrg_Tdec,momt_Tdec,ro,v] = funcs(solver, stream, T - dT/2, P, a,
mDot);
[entr_Pinc, enrg_Pinc,momt_Pinc,ro,v] = funcs(solver, stream, T, P+dP/2 , a,
mDot);
[entr_Pdec, enrg_Pdec,momt_Pdec,ro,v] = funcs(solver, stream, T, P- dP/2, a,
mDot);

df2_dT = (momt_Tinc - momt_Tdec) / dT;
df1_dT = (enrg_Tinc - enrg_Tdec) / dT;
df2_dP = (momt_Pinc - momt_Pdec) / dP;
df1_dP = (enrg_Pinc - enrg_Pdec) / dP;

jacobean = [df1_dT df1_dP; df2_dT df2_dP];
err = -inv(jacobean)*[f1; f2]; % 2x1 matrix
```

A.2 Non-isentropic

A.2.1 finding the nozzle throat

```
clear all;
clc;
```

```
% Parameters
T1   = 20;
P1   = 30000;
A1   = 0.001257;
L    = 0.12;
mDot = 5000;

% Linking with hysys
hyApp = feval('actxserver', 'Hysys.Application');
hysolver = hyApp.ActiveDocument.Solver;
solver.CanSolve = 1;
hysolver.CanSolve = 0;

strInlet     = hyApp.ActiveDocument.Flowsheet.MaterialStreams.Item('inlet');
strLength    = hyApp.ActiveDocument.Flowsheet.MaterialStreams.Item('length');
strOutlet    = hyApp.ActiveDocument.Flowsheet.MaterialStreams.Item('outlet');
strNatgas    = hyApp.ActiveDocument.Flowsheet.MaterialStreams.Item('natgas');
strGas       = hyApp.ActiveDocument.Flowsheet.MaterialStreams.Item('gas');
strWater     = hyApp.ActiveDocument.Flowsheet.MaterialStreams.Item('water');
strSatgas    = hyApp.ActiveDocument.Flowsheet.MaterialStreams.Item('satgas');
strDrygas    = hyApp.ActiveDocument.Flowsheet.MaterialStreams.Item('drygas');
strCondensate = hyApp.ActiveDocument.Flowsheet.MaterialStreams.Item('condensate');
hySS         = hyApp.ActiveDocument.Flowsheet.Operations.Item('SPRDSHT-1');

% Gas saturation
vFrac = 1;
mDot_W = 0;
[entr1, enrg1, momt1, ro1, v1] = funcs(solver, strGas, T1, P1, A1, mDot);
while vFrac==1
   mDot_W=mDot_W+0.001;
   [entr_W, enrg_W, momt_W, ro_W, v_W] = funcs(hysolver,strWater, T1, P1, A1,
mDot_W);
   vFrac = hySS.Cell('B6').CellValue;
end
%
% Saturated gas properties
T1 = hySS.Cell('B7').CellValue;
P1 = hySS.Cell('B8').CellValue;
mDot = hySS.Cell('C1').CellValue;

% Nozzle design
seg_c = 30;
```

```
alpha_c = 6.85;
alphaRad_c = (alpha_c*pi) / 180;

seg_d = 300;
alpha_d = 3;
alphaRad_d = (alpha_d*pi) / 180;

A(1) = A1
T(1) = T1;
P(1) = P1;
[entr(1), enrg(1), momt(1), ro(1), v(1)] = funcs(solver, strInlet, T(1), P(1), A(1), mDot);
[machNum1, v1] = mach(T1, P1, A1, mDot);
machNum(1) = machNum1;
v(1) = v1;
water(1) = hySS.Cell('D1').CellValue;
r1 = sqrt(A1/pi);
ID(1) = 2*r1;
p(1) = 0;

i = 1;
L_segment = 0.0009;
x = tan(alphaRad_c)*L_segment;
hySS.Cell('B1').CellValue = L_segment;

% Finding the throat
converged(i) = true;
exception(i) = false;

while converged(i) == true && exception(i) == false && abs(1-machNum(i))>0.2
   i = i + 1;
   ID(i) = ID(i-1)-(2*x);
   A(i) = (pi*(ID(i))^2)/4;
   p(i) = p(i-1)+L_segment;
   [T(i), P(i), machNum(i), v(i), vFrac(i),converged(i), exception(i)] = tpDistr_as(T(i-1),
P(i-1), A(i-1)1,T1,P1, A(i), mDot);
  if converged(i) == true && exception(i) == false
   [entr(i), enrg(i), momt(i), ro(i), v(i)] = funcs(hysolver, strInlet, T(i), P(i), A(i), mDot);
end
end

L_segment = 0.0000009;
x = tan(alphaRad_c)*L_segment;
```

```
hySS.Cell('B1').CellValue = L_segment;
hysolver.CanSolve = 1 % start solver
hysolver.CanSolve = 0;
converged(i)=1;
converged(i) == true
exception(i)=0;
while converged(i) == true && exception(i) == false
   i = i + 1;
   ID(i)=ID(i-1)-(2*x);
   A(i)=(pi*(ID(i))^2)/4;
   p(i)=p(i-1)+L_segment;
   [T(i), P(i), machNum(i), v(i), vFrac(i),converged(i), exception(i)] = tpDistr_as(T(i-1),
P(i-1), A(i-1),T1,P1, A(i), mDot);
   if converged(i) == true && exception(i) == false
   [entr(i), enrg(i), momt(i), ro(i), v(i)] = funcs(hysolver, strInlet, T(i), P(i), A(i), mDot);
end
end
ithroat=i-1; % throat index

save nozzlethroat A T P machNum v p ID ithroat entr ro momt enrg mDot
```

A.2.2 NOZZLE RECOVERY PROPERTIES

```
clear all
clc

load nozzlethroat   % Calling the properties at the converging part
 i=ithroat;

 L    = 0.12;
 mDot = 5000;

% Linking with hysys
hyApp = feval('actxserver', 'Hysys.Application');
hysolver = hyApp.ActiveDocument.Solver;
solver.CanSolve = 1;
hysolver.CanSolve = 0;

strInlet     = hyApp.ActiveDocument.Flowsheet.MaterialStreams.Item('inlet');
strLength    = hyApp.ActiveDocument.Flowsheet.MaterialStreams.Item('length');
```

```
strOutlet    = hyApp.ActiveDocument.Flowsheet.MaterialStreams.Item('outlet');
strNatgas    = hyApp.ActiveDocument.Flowsheet.MaterialStreams.Item('natgas');
strGas       = hyApp.ActiveDocument.Flowsheet.MaterialStreams.Item('gas');
strWater     = hyApp.ActiveDocument.Flowsheet.MaterialStreams.Item('water');
strSatgas    = hyApp.ActiveDocument.Flowsheet.MaterialStreams.Item('satgas');
strDrygas    = hyApp.ActiveDocument.Flowsheet.MaterialStreams.Item('drygas');
strCondensate = hyApp.ActiveDocument.Flowsheet.MaterialStreams.Item('condensate');
hySS         = hyApp.ActiveDocument.Flowsheet.Operations.Item('SPRDSHT-1');

% Nozzle design
seg_c = 30;
alpha_c = 6.85;
alphaRad_c = (alpha_c*pi) / 180;

seg_d = 30;
alpha_d = 3;
alphaRad_d = (alpha_d*pi) / 180;


L_c = ( (sqrt( A(1)/pi)) - (sqrt(A(ithroat)/pi)) )/ (tan (alphaRad_c)) ;
L_d = L-L_c;
rt = sqrt(A(ithroat)/pi);

dL_c=L_c/seg_c;
dL_d=L_d/seg_d;

hySS.Cell('B1').CellValue=dL_d;
 for h = L_c+dL_d:dL_d:L
    i = i+1;
    p(i) = h
    R = (p(i)-L_c)*tan(alphaRad_d);
    A(i) = ((R+rt)^2) *pi;
    [T(i), P(i), machNum(i), v(i), converged, exception] = tpDistr_as(T(i-1), P(i-1), A(i-
1),T(1) ,P(1),A(i),mDot);
    [entr(i), enrg(i), momt(i), ro(i), v(i)] = funcs(hysolver, strInlet, T(i), P(i), A(i), mDot);
 end
```

A.2.3 NOZZLE DESIGN PROPERTIES

```
clear all
clc
```

```
load nozzlethroat   % Calling the properties at the converging part
 i=ithroat;

 L    = 0.12;
 mDot = 5000;

% Linking with hysys
hyApp = feval('actxserver', 'Hysys.Application');
hysolver = hyApp.ActiveDocument.Solver;
solver.CanSolve = 1;
hysolver.CanSolve = 0;

strInlet     = hyApp.ActiveDocument.Flowsheet.MaterialStreams.Item('inlet');
strLength    = hyApp.ActiveDocument.Flowsheet.MaterialStreams.Item('length');
strOutlet    = hyApp.ActiveDocument.Flowsheet.MaterialStreams.Item('outlet');
strNatgas    = hyApp.ActiveDocument.Flowsheet.MaterialStreams.Item('natgas');
strGas       = hyApp.ActiveDocument.Flowsheet.MaterialStreams.Item('gas');
strWater     = hyApp.ActiveDocument.Flowsheet.MaterialStreams.Item('water');
strSatgas    = hyApp.ActiveDocument.Flowsheet.MaterialStreams.Item('satgas');
strDrygas    = hyApp.ActiveDocument.Flowsheet.MaterialStreams.Item('drygas');
strCondensate = hyApp.ActiveDocument.Flowsheet.MaterialStreams.Item('condensate');
hySS         = hyApp.ActiveDocument.Flowsheet.Operations.Item('SPRDSHT-1');

% Nozzle design
seg_c = 30;
alpha_c = 6.85;
alphaRad_c = (alpha_c*pi) / 180;

seg_d = 30;
alpha_d = 3;
alphaRad_d = (alpha_d*pi) / 180;


L_c = ( (sqrt( A(1)/pi)) - (sqrt(A(ithroat)/pi)) )/ (tan (alphaRad_c)) ;
L_d = L-L_c;
rt = sqrt(A(ithroat)/pi);

dL_c=L_c/seg_c;
dL_d=L_d/seg_d;

hySS.Cell('B1').CellValue=dL_d;
```

```
for h=L_c+dL_d:dL_d:L
        i=i+1;
        p(i)=h
        R=(p(i)-L_c)*tan(alphaRad_d);
        A(i)= ((R+rt)^2) *pi;
        [T(i), P(i), machNum(i), v(i), converged, exception] = tpDistr_as(T(i-1), P(i-
1), A(i-1),-120 ,1000,A(i),mDot);
        [entr(i), enrg(i), momt(i), ro(i), v(i)] = funcs(hysolver, strInlet, T(i), P(i),
A(i), mDot);

 end
```

4.2.4 SHOCKWAVE PREDICTION

```
clear all
clc

load nozzlethroat   % Calling the properties at the converging part
 i=ithroat;

 L    = 0.12;
 mDot = 5000;
 Pexit=70/100*P(1);  % Desired pressure recovery
 Shock=0.1;  % first guess for shocklocation, L_c <shock<L

% Linking with hysys
hyApp = feval('actxserver', 'Hysys.Application');
hysolver = hyApp.ActiveDocument.Solver;
solver.CanSolve = 1;
hysolver.CanSolve = 0;

strInlet     = hyApp.ActiveDocument.Flowsheet.MaterialStreams.Item('inlet');
strLength    = hyApp.ActiveDocument.Flowsheet.MaterialStreams.Item('length');
strOutlet    = hyApp.ActiveDocument.Flowsheet.MaterialStreams.Item('outlet');
strNatgas    = hyApp.ActiveDocument.Flowsheet.MaterialStreams.Item('natgas');
strGas       = hyApp.ActiveDocument.Flowsheet.MaterialStreams.Item('gas');
strWater     = hyApp.ActiveDocument.Flowsheet.MaterialStreams.Item('water');
strSatgas    = hyApp.ActiveDocument.Flowsheet.MaterialStreams.Item('satgas');
strDrygas    = hyApp.ActiveDocument.Flowsheet.MaterialStreams.Item('drygas');
strCondensate = hyApp.ActiveDocument.Flowsheet.MaterialStreams.Item('condensate');
hySS         = hyApp.ActiveDocument.Flowsheet.Operations.Item('SPRDSHT-1');
```

```
% Nozzle design
seg_c = 30;
alpha_c = 6.85;
alphaRad_c = (alpha_c*pi) / 180;

seg_d = 30;
alpha_d = 3;
alphaRad_d = (alpha_d*pi) / 180;


L_c = ( (sqrt( A(1)/pi)) - (sqrt(A(ithroat)/pi)) )/ (tan (alphaRad_c)) ;
L_d = L-L_c;
rt = sqrt(A(ithroat)/pi);

dL_c=L_c/seg_c;
dL_d=L_d/seg_d;

L_bs=Shock-L_c;;
dL_bs=L_bs/seg_d;
L_as=L-L_c-L_bs;
dL_as=L_as/seg_d;
Abs=(( (L_bs*(tan (alphaRad_d)))+(sqrt(A(ithroat)/pi)) )^2)*pi;
Aex=(( (L_d*(tan (alphaRad_d)))+(sqrt(A(ithroat)/pi)) )^2)*pi;

% Properties distributions from throat to shockwave location
hySS.Cell('B1').CellValue=dL_bs;
for h=L_c+dL_bs:dL_bs:Shock
   i=i+1;
   p(i)=h;
   R=(p(i)-L_c)*tan(alphaRad_d);
   A(i)= ((R+rt)^2) *pi;
   [T(i), P(i), machNum(i), v(i), vFrac, converged, exception] = tpDistr_as(T(i-1), P(i-1),
A(i-1),-70, 5000,  A(i), mDot);
   [entr(i), enrg(i), momt(i), ro(i), v(i)] = funcs(hysolver, strInlet, T(i), P(i), A(i), mDot);

end

Tbs=T(i);
Pbs=P(i);
machNumbs=machNum(i);
vbs=v(i);
```

```
Abs=A(i);
[entrbs, enrgbs, momtbs, robs, vbs] = funcs(hysolver, strInlet, Tbs, Pbs, Abs, mDot);
mDot_as= hySS.Cell('A7').CellValue;
Aas=Abs;

% Properties ownstream of the shockwave
[Tas,Pas ,machNumas, vas, converged, exception] = tpDistr(Tbs, Pbs, Abs,T(1)
,P(1),Abs,mDot_as);

 [entras, enrgas, momtas, roas, vas] = funcs(hysolver, strNatgas, Tas, Pas, Aas, mDot_as);

pas=L_c+(L_bs);
i=i+1;
p(i)= pas;
A(i)=Aas;
T(i)= Tas;
P(i)= Pas;
machNum(i)= machNumas;
v(i)=vas;
entr(i) = entras;
enrg(i)=enrgas;
momt(i) = momtas;
ro(i)=roas;

%Properties distribution after the shockwave location
hySS.Cell('B1').CellValue=dL_as;
for h=Shock+dL_as:dL_as:L
   i=i+1;
   p(i)=h
   R=(p(i)-L_c)*tan(alphaRad_d);
   A(i)= ((R+rt)^2) *pi;
   [T(i), P(i), machNum(i), v(i), converged, exception] = tpDistr(T(i-1), P(i-1), A(i-
1),T(1) ,P(1),A(i),mDot_as);
   [entr(i), enrg(i), momt(i), ro(i), v(i)] = funcs(hysolver, strNatgas, T(i), P(i), A(i),
mDot_as);

   end

Pex=P(i);
if Pex>Pexit
   display ('choose bigger shock')
else if Pex<Pexit
```

```
    display('choose lower shock')
  else display ('shocklocation is right');


end
end
```

A.2.5 FUNCTIONS

A.2.5.1 TPDISTR_AS

```
% % % % % % % % % % %

% tpDistr_as - computes stream properties along the nozzle
%
% Input:
%  T1 - current temperature
%  P1 - current  pressure
%  A1 - current  size
%  T2i - next xsection temperature initial guess
%  P2i - next xsection pressure initial guess
%  A2 - next xsection size
%  mDot - flow rate
% Output:
%  T2 - next xsection temperature
%  P2 - next xsection pressure
%  v - next xsection velocity
%  vFrac - next xsection vapour fraction
%  converged - NR convergence flag
%  exception - erroneous parameter flag


function [T2,P2, machNum, v, vFrac, converged, exception] = tpDistr_as(T1, P1,
A1,T2i,P2i, A2, mDot)

% linking with hysys
hyApp    = feval('actxserver', 'Hysys.Application');
hysolver = hyApp.ActiveDocument.Solver;
solver.CanSolve = 1; %Start solver
hysolver.CanSolve = 0;
```

```
strInlet  = hyApp.ActiveDocument.Flowsheet.MaterialStreams.Item('inlet');
hySS      = hyApp.ActiveDocument.Flowsheet.Operations.Item('SPRDSHT-1');

% Newton-Raphson
[entr1, enrg1,momt1,ro1,v1] = funcs(hysolver, strInlet, T1, P1, A1, mDot);

tol = 0.005; % tolerance for error
kmax = 100;   % maximum number of iterations

% set initial guess
T2 =T2i;% (C)
P2 = P2i;
k = 0;
tres = tol + 1.;
pres = tol + 1.;
entr2=entr1-20;
exception = false;
while (exception == false) && (tres >= tol|| pres >= tol) && k <= kmax


   err = errorEval_as(hysolver, strInlet,T1,P1,A1,T2,P2,A2,mDot);
   P2 = P2 + err(2, 1);
   T2 = T2 + err(1, 1);
   if  T2 < -150  || P2 < 0
      exception = true;

  else
      tres = abs( err(1,1) );
     pres = abs( err(2,1) );
      k = k + 1;
   end

end

 [entr2, enrg2, momt2, ro2, v2,nu2,D2,Mw] = funcs(hysolver, strInlet, T2, P2, A2,
mDot);
converged = false;
machNum = 0;
v = 0;
vFrac = 0;
if exception == false
   if k > kmax
```

```
        converged = false;
      else
        converged = true;
        [machNum, v] = mach(T2, P2, A2, mDot);
      end
    end
```

4.2.5.2 ERRORVAL_AS

```
    % % % % % % % % % % %
    % errorEval_as - computes stream properties in next xsection
    %
    % Input:
    %  T1 - current  temperature
    %  P1 - current pressure
    %  A1 - current xsection size
    %  T2 - next  temperature initial guess
    %  P2 - next  pressure initial guess
    %  A2 - next xsection size
    %  mDot - flow rate
    % Output:
    %  err-error in current neton-Raphson iteration

    function [err] = errorEval_as(solver, stream,T1,P1,A1,T2,P2,A2,mDot)

    dT = 0.1;
    dP = 0.1;
    hyApp   = feval('actxserver', 'Hysys.Application');
    hysolver = hyApp.ActiveDocument.Solver;
    solver.CanSolve = 1; %Start solver
    hysolver.CanSolve = 0;

    strInlet  = hyApp.ActiveDocument.Flowsheet.MaterialStreams.Item('inlet');

    strNatgas = hyApp.ActiveDocument.Flowsheet.MaterialStreams.Item('natgas');

    hySS     = hyApp.ActiveDocument.Flowsheet.Operations.Item('SPRDSHT-1');
    [entr1, enrg1, momt1, ro1, v1,nu1,D1,Mw,h1] = funcs(solver, stream, T1, P1, A1,
mDot);
    [entr2, enrg2, momt2, ro2, v2,nu2,D2,Mw,h2] = funcs(solver, stream, T2, P2, A2,
mDot);
```

```
roav=(ro1+ro2)/2;
Dav=(D1+D2)/2;
Tav=((T1+273.15)+(T2+273.15))/2;
Aav=(A1+A2)/2;
Vav=(v1+v2)/2;
nuav=(nu1+nu2)/2;
K=hySS.Cell('A6').CellValue; % pipe roughness
m=hySS.Cell('B5').CellValue; % mass flow rate (kg/h)

[Rx,PHi,f]=frictionfactor(hysolver,stream,ro1,nu1,D1,T1,v1,P1,A1,ro2,nu2,D2,T
2,v2,P2,A2,mDot); % finding the frictionfactor,energy loss term and thrust
L_segment=hySS.Cell('B1').CellValue;



f1 = enrg2 - enrg1+PHi;
f2 =  momt2 -momt1+Rx-((P1+P2)*500*(A2-A1));


[entr_Tinc,
enrg_Tinc,momt_Tinc,ro_Tinc,v_Tinc,nu_Tinc,D_Tinc,Mw_Tinc,h_Tinc]          =
funcs(solver,stream, T2 + dT/2, P2, A2, mDot);

[Rx_Tinc,PHi_Tinc,f_Tinc]=frictionfactor(hysolver,stream,ro1,nu1,D1,T1,v1,P1,
A1,ro_Tinc,nu_Tinc,D_Tinc,T2+dT/2,v_Tinc,P2,A2,mDot);

[entr_Tdec,
enrg_Tdec,momt_Tdec,ro_Tdec,v_Tdec,nu_Tdec,D_Tdec,Mw_Tdec,h_Tdec]          =
funcs(solver, stream, T2 - dT/2, P2, A2, mDot);

[Rx_Tdec,PHi_Tdec,f_Tdec]=frictionfactor(hysolver,stream,ro1,nu1,D1,T1,v1,P1
,A1,ro_Tdec,nu_Tdec,D_Tdec,T2-dT/2,v_Tdec,P2,A2,mDot);

[entr_Pinc,
enrg_Pinc,momt_Pinc,ro_Pinc,v_Pinc,nu_Pinc,D_Pinc,Mw_Pinc,h_Pinc]          =
funcs(solver,stream, T2 , P2+dP/2, A2, mDot);


[Rx_Pinc,PHi_Pinc,f_Pinc]=frictionfactor(hysolver,stream,ro1,nu1,D1,T1,v1,P1,
A1,ro_Pinc,nu_Pinc,D_Pinc,T2,v_Pinc,P2+dP/2,A2,mDot);

[entr_Pdec,
```

```
enrg_Pdec,momt_Pdec,ro_Pdec,v_Pdec,nu_Pdec,D_Pdec,Mw_P2dec,h_Pdec]          =
funcs(solver, stream, T2 , P2- dP/2, A2, mDot);


        [Rx_Pdec,PHi_Pdec,f_Pdec]=frictionfactor(hysolver,stream,ro1,nu1,D1,T1,v1,P1
,A1,ro_Pdec,nu_Pdec,D_Pdec,T2,v_Pdec,P2-dP/2,A2,mDot);

        F_dT=(pi*L_segment*Dav/2)*          ((f*Vav^2*(ro_Tinc-ro_Tdec))+(f*roav*((
v_Tinc-v_Tdec))^2)+ (roav*Vav^2*(f_Tinc-f_Tdec)));
        F_dP=(pi*L_segment*Dav/2)*          ((f*Vav^2*(ro_Pinc-ro_Pdec))+(f*roav*((
v_Pinc-v_Pdec))^2)+ (roav*Vav^2*(f_Pinc-f_Pdec)));
        Q_dT= (F_dT*Vav+ (v_Tinc-v_Tdec)*Rx)/(m/3600);
        Q_dP=(F_dP*Vav+ (v_Pinc-v_Pdec)*Rx)/(m/3600);

        df2_dT=((momt_Tinc -momt_Tdec)+ (Rx_Tinc-Rx_Tdec))/ dT;
        df1_dT = ((enrg_Tinc-enrg_Tdec)+(PHi_Tinc-PHi_Tdec)) / dT
        df1_dP = ((enrg_Pinc-enrg_Pdec) +(PHi_Pinc-PHi_Pdec)) / dP;
        df2_dP = (((momt_Pinc -momt_Pdec)+(Rx_Pinc-Rx_Pdec))/ dP)-((A2-A1)*500);


        jacobean = [df1_dT df1_dP; df2_dT df2_dP];

        err = -inv(jacobean)*[f1; f2]; % 2x1 matrix
```

4.2.5.3 FRCITIONFACTOR

```
        % % % % % % % % % % %
        % frictionfactor - computes the frictionfactor,energy loss term and thrust
        %
        % Input:
        %  ro1 - current  density (kg/m^3)
        %  nu1-  currnet kinematic viscosity (cSt)
        %  D1-   current xsection diameter(m)
        %  T1-   current temperature (C )
        %  v1-   current velocity( m/s)
        %  P1 - current pressure  (kPa)
        %  A1 - current xsection size (m^2)
        %  ro2 - next  density (kg/m^3)
        %  nu2-  next kinematic viscosity (cSt)
        %  D2-   next xsection diameter(m)
```

```
% T2- next temperature (C )
% v2- next velocity (m/s)
% P2 - current pressure (kPa)
% A2 - current xsection size (m^2)
% mDot - flow rate
% Output:
% Rx-Thrust
% PHi- energy loss term
% f- friction factor


function[Rx,PHi,f]=frictionfactor(solver,stream,ro1,nu1,D1,T1,v1,P1,A1,ro2,nu2,
D2,T2,v2,P2,A2,mDot)

hyApp    = feval('actxserver', 'Hysys.Application');
hysolver = hyApp.ActiveDocument.Solver;
solver.CanSolve = 1; %Start solver
hysolver.CanSolve = 0;

strInlet  = hyApp.ActiveDocument.Flowsheet.MaterialStreams.Item('inlet');
hySS      = hyApp.ActiveDocument.Flowsheet.Operations.Item('SPRDSHT-1');

% computing average properties
roav=(ro1+ro2)/2;
Dav=(D1+D2)/2;
Tav=((T1+273.15)+(T2+273.15))/2;
Aav=(A1+A2)/2;
Vav=(v1+v2)/2;
nuav=(nu1+nu2)/2;


K=hySS.Cell('A6').CellValue;  % kinematic viscosity (cSt)
m=hySS.Cell('B5').CellValue;   %mass flow rate (kg'h)
Re=Vav*Dav/nuav;              % caculating Reynolds number
  f=(1/((-3.6*log((  K/(3.7*Dav))^1.11)+(6.9/(Re)))))^2;    % calculating friction
factor

L_segment=hySS.Cell('B1').CellValue;
Rx= f*roav*((Vav^2)/2)*pi*L_segment*(Dav);      % calculating thrust term

PHi= Rx* Vav/(m/3600);                    % calculating energy loss term
```

4.2.5.4MACH

Machdrygas has the same procedure to calculate the Mach number for the nozzle after the shockwave.

```
% % % % % % % % % % %
% machNum - computes mach number & velocity
%
% Input:
%   T - temperature
%   P - pressure
%   A - xsection
%   mDot - flow rate
% Output:
%   machNum - mach number
%   v - velocity
function [machNum,v] = mach(T, P, A, mDot)

hyApp    = feval('actxserver', 'Hysys.Application');
hysolver = hyApp.ActiveDocument.Solver;
solver.CanSolve = 1;
hysolver.CanSolve = 0;
strInlet= hyApp.ActiveDocument.Flowsheet.MaterialStreams.Item('inlet');

dT = 0.1;
[entr1, enrg1,momt1,ro1,v1] = funcs(hysolver,strInlet, T, P, A, mDot);

tol = 0.005; % tolerance for error
kmax = 200;   % maximum number of iterations
P2_inc=P;
k = 0;
pres = tol + 1.;
exception = false;
while (exception == false) &&  (pres >= tol) && k <= kmax
  err = errorEval_mach(hysolver, strInlet,T+dT/2, P2_inc, A, mDot,entr1);
    P2_inc = P2_inc + err;
   if P2_inc< 0
      exception = true;
   else
```

```
        pres = abs( err );
        k = k + 1;
      end
    end

    [entr, enrg,momt,ro_inc,v_inc] = funcs(hysolver,strInlet, T+dT/2, P2_inc, A,
mDot);

     P2_dec=P;
    k = 0;
    pres = tol + 1.;
    exception = false;
    while (exception == false) && (pres >= tol) && k <= kmax
      err = errorEval_mach(hysolver, strInlet,  T-dT/2, P2_dec, A, mDot,entr1);

      P2_dec = P2_dec + err;
      if P2_dec < 0
        exception = true;
      else
        pres = abs( err );
        k = k + 1;
      end
    end

    [entr, enrg,momt,ro_dec,v_dec] = funcs(hysolver,strInlet, T-dT/2, P2_dec, A,
mDot);

    c = sqrt( abs( (P2_inc-P2_dec)*1000/(ro_inc - ro_dec) ) ); % sepeed of sound
(m/s)

    [entr, enrg,momt,ro,v] = funcs(hysolver,strInlet, T, P, A, mDot);

    machNum = v / c;
```

4.2.5.5FUNCS

```
% % % % % % % % % % %
% funcs - computes stream properties
%
% Input:
%   solver - hysys solver
```

```
%  stream - stream name
%  T - temperature
%  P - pressure
%  a - xsection
%  mDot - flow rate
% Output:
%  entr - enthalpy
%  enrg - energy
%  momt - momentum
%  ro - density
%  v - velocity

function [entr, enrg, momt, ro,v,nu,D,Mw,h] = funcs(solver, stream, T, P, a,
mDot)

hyApp    = feval('actxserver', 'Hysys.Application');
hysolver = hyApp.ActiveDocument.Solver;
solver.CanSolve = 1; %Start solver
hysolver.CanSolve = 0;
hySS     = hyApp.ActiveDocument.Flowsheet.Operations.Item('SPRDSHT-1');

stream.Temperature.SetValue(T,'C')
stream.pressure.SetValue(P,'kPa')
stream.MolarFlow.SetValue(mDot,'kgmole/h')
solver.CanSolve = 1; %Start solver
solver.CanSolve = 0; %Stop solver

S  = stream.MassEntropyValue;        % (kJ / kg*C)
h  = stream.MassEnthalpyValue * 1000; % (J / kg)
ro = stream.MassDensityValue;        % (kg / m^3)
nu=hySS.Cell('A5').CellValue;
D=sqrt(4*a/pi);
% Z=hySS.Cell('A7').CellValue;

Mw = stream.MolecularWeightValue;
m = mDot*Mw; % (kg / hr)

v = (m/3600) / (ro*a); % (m / s)

entr = S;          % (kJ / kg*C)
enrg = h + (v^2)/2; % (m^2 / s^2)
 momt= ((P*1000)*a)+((m/3600)*v);
```

4.2.5.6 ERROREVAL_MACH

```
% % % % % % % % % % %
% errorEval_mach - computes error in one iteration of newton raphson to
cpmpute
% Machnumber
%
% Input:
%  solver - hysys solver
%  stream - stream name
%  T - temperature
%  P - pressure
%  a - xsection
%  mDot - flow rate
% entr1- entropy inlet
% Output:
%  err - error in current newton raphson iteration to compute Mach number
function [err] = errorEval_mach(solver, stream, T, P, A, mDot,entr1)

dP = 0.1;

[entr, enrg,momt,ro,v] = funcs(solver, stream, T, P, A, mDot);
f1 = entr - entr1;

[entr_Pinc, enrg_Pinc,momt_Pinc,ro,v] = funcs(solver, stream, T, P + dP/2, A,
mDot);
[entr_Pdec, enrg_Pdec,momt_Pdec,ro,v] = funcs(solver, stream, T, P - dP/2, A,
mDot);

df1_dP = (entr_Pinc - entr_Pdec) / dP;

err = -f1/df1_dP; % 2x1 matrix
```

4.2.5.7ERROREVAL

```
% % % % % % % % % % %
% errorEval_as - computes stream properties downstream the shockwave
%
% Input:
%  T1 - current  temperature
%  P1 - current pressure
```

```
% A1 - current xsection size
% T2 - next temperature initial guess
% P2 - next pressure initial guess
% A2 - next xsection size
% mDot - flow rate
% Output:
% err-error in current neton-Raphson iteration

function [err] = errorEval(solver, stream, momt1, enrg1, T, P, a, mDot)

dT = 0.1;
dP = 0.1;

[entr, enrg,momt,ro,v] = funcs(solver, stream, T, P, a, mDot);
f1 = momt - momt1;
f2 = enrg - enrg1;

[entr_Tinc, enrg_Tinc,momt_Tinc,ro,v] = funcs(solver, stream, T + dT/2, P, a,
mDot);
[entr_Tdec, enrg_Tdec,momt_Tdec,ro,v] = funcs(solver, stream, T - dT/2, P, a,
mDot);
[entr_Pinc, enrg_Pinc,momt_Pinc,ro,v] = funcs(solver, stream, T, P + dP/2, a,
mDot);
[entr_Pdec, enrg_Pdec,momt_Pdec,ro,v] = funcs(solver, stream, T, P - dP/2, a,
mDot);

df1_dT = (momt_Tinc - momt_Tdec) / dT;
df2_dT = (enrg_Tinc - enrg_Tdec) / dT;
df1_dP = (momt_Pinc - momt_Pdec) / dP;
df2_dP = (enrg_Pinc - enrg_Pdec) / dP;

jacobean = [df1_dT df1_dP; df2_dT df2_dP];
err = -inv(jacobean)*[f1; f2]; % 2x1 matrix
```

4.2.5.8 tpDistr

```
% % % % % % % % % % %
% tpDistr - computes stream properties in shockwave downstream
%
% Input:
% T1 - current xsection temperature
% P1 - current xsection pressure
```

```
%  A1 - current xsection size
%  T2i - next xsection temperature initial guess
%  P2i - next xsection pressure initial guess
%  A2 - next xsection size
%  mDot - flow rate
% Output:
%  T2 - next xsection temperature
%  P2 - next xsection pressure
%  v - next xsection velocity
%  vFrac - next xsection vapour fraction
%  converged - NR convergence flag
%  exception - erroneous parameter flag


function [T2, P2, machNum, v, vFrac, converged, exception] = tpDistr(T1, P1,
A1, T2i, P2i, A2, mDot)

% linking with hysys
hyApp    = feval('actxserver', 'Hysys.Application');
hysolver = hyApp.ActiveDocument.Solver;
solver.CanSolve = 1; %Start solver
hysolver.CanSolve = 0;

strInlet  = hyApp.ActiveDocument.Flowsheet.MaterialStreams.Item('inlet');
 strNatgas = hyApp.ActiveDocument.Flowsheet.MaterialStreams.Item('natgas');
hySS     = hyApp.ActiveDocument.Flowsheet.Operations.Item('SPRDSHT-1');

% Newton-Raphson
[entr1, enrg1, momt1, ro1, v1] = funcs(hysolver, strInlet, T1, P1, A1, mDot);

tol = 0.005; % tolerance for error
kmax = 200;   % maximum number of iterations

% set initial guess
T2 = T2i;  % (C)
P2 = P2i; % (kPa)

k = 0;
pres = tol + 1.;
tres = tol + 1.;
exception = false;
while (exception == false) && (tres >= tol || pres >= tol) && k <= kmax
```

```
    err = errorEval_as(hysolver, strNatgas, T1,P1,A1, T2, P2, A2, mDot);
    T2 = T2 + err(1, 1);
    P2 = P2 + err(2, 1);
    if P2 < 0 || T2 < -273
        exception = true;
    else
        tres = abs( err(1,1) );
        pres = abs( err(2,1) );
        k = k + 1;
    end
end

converged = false;
machNum = 0;
v = 0;
vFrac = 0;
if exception == false
    if k > kmax
        converged = false;
    else
        converged = true;
        [machNum, v] = machdrygas(T2, P2, A2, mDot);
    end
end
```